1983

Petrology and Geochemistry of the Silver Plume-Age Plutons of the Southern and Central Wet Mountains, Colorado.

Russell Berryman Bender Jr
Louisiana State University and Agricultural & Mechanical College

Bender, Russell Berryman, Jr.

PETROLOGY AND GEOCHEMISTRY OF THE SILVER PLUME-AGE PLUTONS OF THE SOUTHERN AND CENTRAL WET MOUNTAINS, COLORADO

The Louisiana State University and Agricultural and Mechanical Col. PH.D. 1983

PETROLOGY AND GEOCHEMISTRY OF THE SILVER PLUME-AGE PLUTONS OF THE SOUTHERN AND CENTRAL WET MOUNTAINS, COLORADO

A Dissertation

Submitted to the Graduate Faculty of the
Louisiana State University and
Agricultural and Mechanical College
in partial fulfillment of the
requirements for the degree of
Doctor of Philosophy

in

The Department of Geology

by
Russell Berryman Bender, Jr.
B.S., Northeast State University, 1968
M.S., Northeast State University, 1971
May 1983

ACKNOWLEDGEMENTS

I would like to take this opportunity to express my appreciation to my major advisor, Dr. Gary Byerly of the Department of Geology for his assistance, guidance and critical review of this manuscript. Likewise, I would like to express my thanks to the other members of my graduate committee, Dr. Willem van den Bold, Dr. Donald Lowe, Dr. Jeffrey Hanor and Dr. Ajoy Baksi for their assistance and helpful suggestions during the final stages of this project. Special thanks to Dr. Charles Ray Givens and Mr. Hunter Raino of Nicholls State University for their aid in reviewing and proofreading this manuscript.

I would like to acknowledge my deepest appreciation to Dr. Marc Michael Murrary (1947-1975), who helped in the initial organization and planning of this project. His field supervision and laboratory assistance were invaluable. His caring and humanity will always be remembered.

To my family who stood by me for these eleven years, I extend a very special and profound thanks. My father and mother, Mr. Russell Bender, Sr. and Mary C. Bender, have served as an inspiration throughout my life. They have given me the values that I needed to complete this project (patience, determination and dedication). To my beloved wife, Catherine, who in the course of this study has been my photographer, draftsperson, typist, lab partner and field partner, there are no words that can adequately express my deepest appreciations and thanks for her long years of sacrifice. Also special thanks to Nicole, my daughter, who assisted in her own very special way. Finally, to He who helps us all in our hour of need.

TABLE OF CONTENTS

TABLE OF CONTENTS (CONT.)

TABLE OF CONTENTS (CONT.)

LIST OF TABLES

LIST OF TABLES (CONT.)

LIST OF TABLES (CONT.)

LIST OF FIGURES

LIST OF FIGURES (CONT.)

LIST OF FIGURES (CONT.)

LIST OF FIGURES (CONT.)

ABSTRACT

The 1.43 billion-year-old Silver Plume-age intrusive complex of the central and southern Wet Mountains, Colorado, is subdivided into six units. In inferred order of intrusion, these include: the San Isabel batholith, the granite of Cliff Creek, the granite of Williams Creek, the granite of Bear Creek, the Wixson Divide pluton, and the granite of the Mount Tyndall quadrangle. All rocks are metaluminus to mildly peraluminus, calc-alkaline, and modally range from melanocratic biotite- hornblende-rich granite to leucocratic alaskite. The biotite-rich granites are non-eutectic and crystallized at a temperature of 710^{o}C to 850^{o}C. The leucocratic granites are eutectic and crystallized between 650^{o}C and 700^{o}C. The depth of emplacement is mesozone to catazone, representing an emplacement depth less than 17 kilometers, with a load pressure of less than 4600 bars. The rocks have undergone pre-, syn-, and post-emplacement crystallization followed by late stage

recrystallization, mylonization, and potassium metasomatism.

Field, modal, and chemical characteristics of the Silver Plume granites, are not clearly indicative of any single model of granite formation. The granites closely resemble I-type or S-type granites. However, the plutons appear to have an anoroginic origin. This seemingly paradoxical situation may suggest that the magma produced during the anorogenic Silver Plume Disturbance-Thermal Event inherited much of its oroginic character from the melting of rocks generated during an earlier event.

INTRODUCTION

This study concerns itself with all of the six major Silver Plume-age intrusive plutons which crop out in the central and southern Wet Mountains. The objectives of this study are:

1) To prepare detailed and reconnaissance maps for those plutons that have not been previously mapped and to determine whether the larger plutons have a composite nature.

2) To determine the geologic structure and stratigraphy of the Silver Plume granites by examining the plutonic shapes, internal structures, and cross-cutting relationships.

3) To describe the texture, mineralogy, and major element composition of the plutons.

4) To discuss the mechanisms for the intrusion of the various plutons, their petrogenesis, and a tectonic model for Silver Plume-age igneous activity.

Precambrian Geology of the Colorado Front Range

The Precambrian rocks of the Colorado Front Range include medium- to high-grade metamorphic rocks and intrusive granites (Figure 1). The oldest units belong to the Idaho Springs Formation, a thick sequence of sedimentary and igneous rocks were deformed and regionally metamorphosed, 1,750 to 1,690 million years ago. The late stage of this orogeny, about 1,750 million years ago, involved intrusion of granite to quartz diorite plutons of the Boulder Creek magmatic series (Hutchinson, 1976).

A second period of plutonism, called the Silver Plume Disturbance-Thermal Event (Hutchinson, 1976) occurred 1.47 to 1.39 billion years ago. The main intrusive rocks are biotite-muscovite granites. Field relationships suggest these granites were not related to an orogenic event and were emplaced as upper catazonal to possibly middle mesozonal plutons (Hutchinson, 1976).

These Silver Plume granites are part of a trend of similar intrusive rocks extending from northern Minnesota, through Colorado, and into northwestern Mexico (Hedge, 1980). This trend of 1,470 to 1,390 million year-old granites is generally linear and, in Colorado, is about 300 kilometers wide.

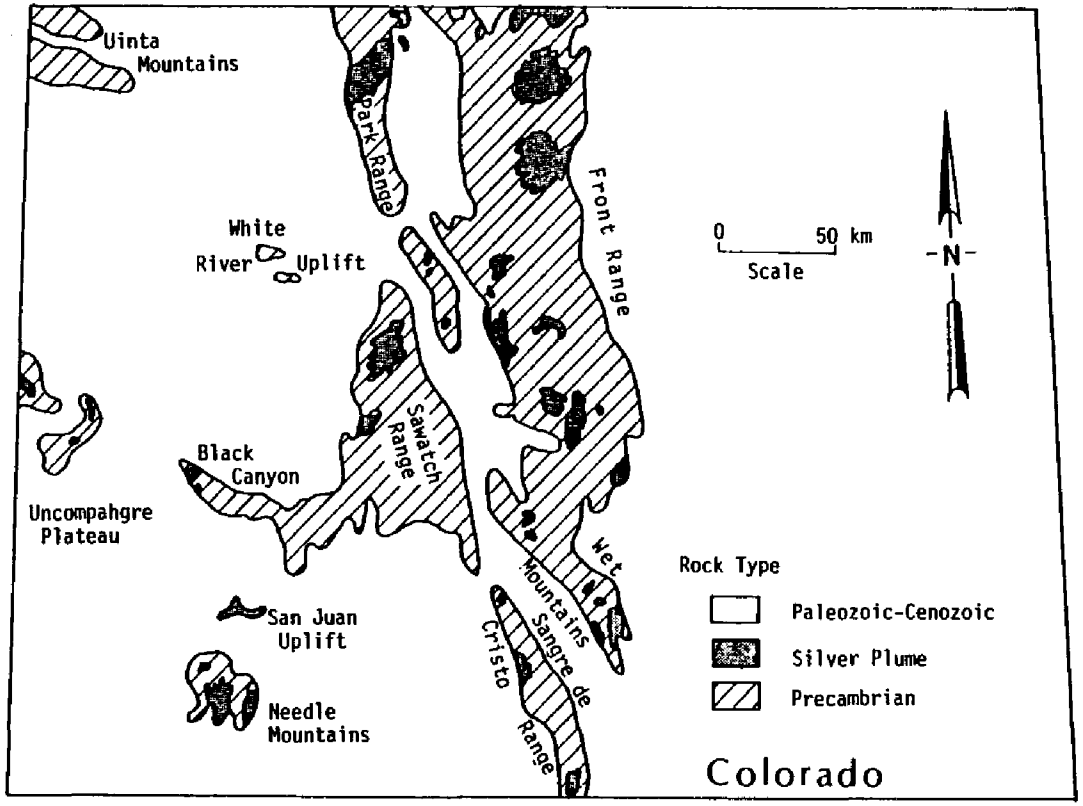

Figure 1. The general distribution of Precambrian and Silver Plume-age intrusive granites for the state of Colorado (Tweto, 1979)

Precambrian Geology of the Wet Mountains

The oldest rocks in the Wet Mountains (Figure 2) are 2.5 to 1.6 billion years old (Scott and Taylor, 1974). Metasedimentary and metavolcanic rocks (Brock and Singewald, 1968) correlate with the Idaho Springs Formation in the Front Range (Boyer, 1962). They represent a sequence of clastic sedimentary rock of non-volcanic origin interlayered with rhyodacitic and basaltic igneous intrusives, flows, and tuffs (Brock and Singewald, 1968). The sequence underwent isoclinal folding prior to metamorphism (Boyer, 1962). Metamorphic foliation in these rocks is ubiquitous and well developed.

The principal metamorphic rock types (Figure 3) of the Wet Mountains include layered feldspathic-biotite gneiss, quartz-plagioclase gneiss, *lit par lit* gneiss and migmatites that have been interpreted as reaching uppermost amphibolite facies during the principal period of regional metamorphism (Taylor, *et. al.*, 1975). Boyer (1962) recognized the same metamorphic grade in the southern portion of the range, while Brock and Singewald (1968) and Scott, *et. al.*, (1976a) found granulite grade metamorphic rocks in the central portion of the range. Foliation

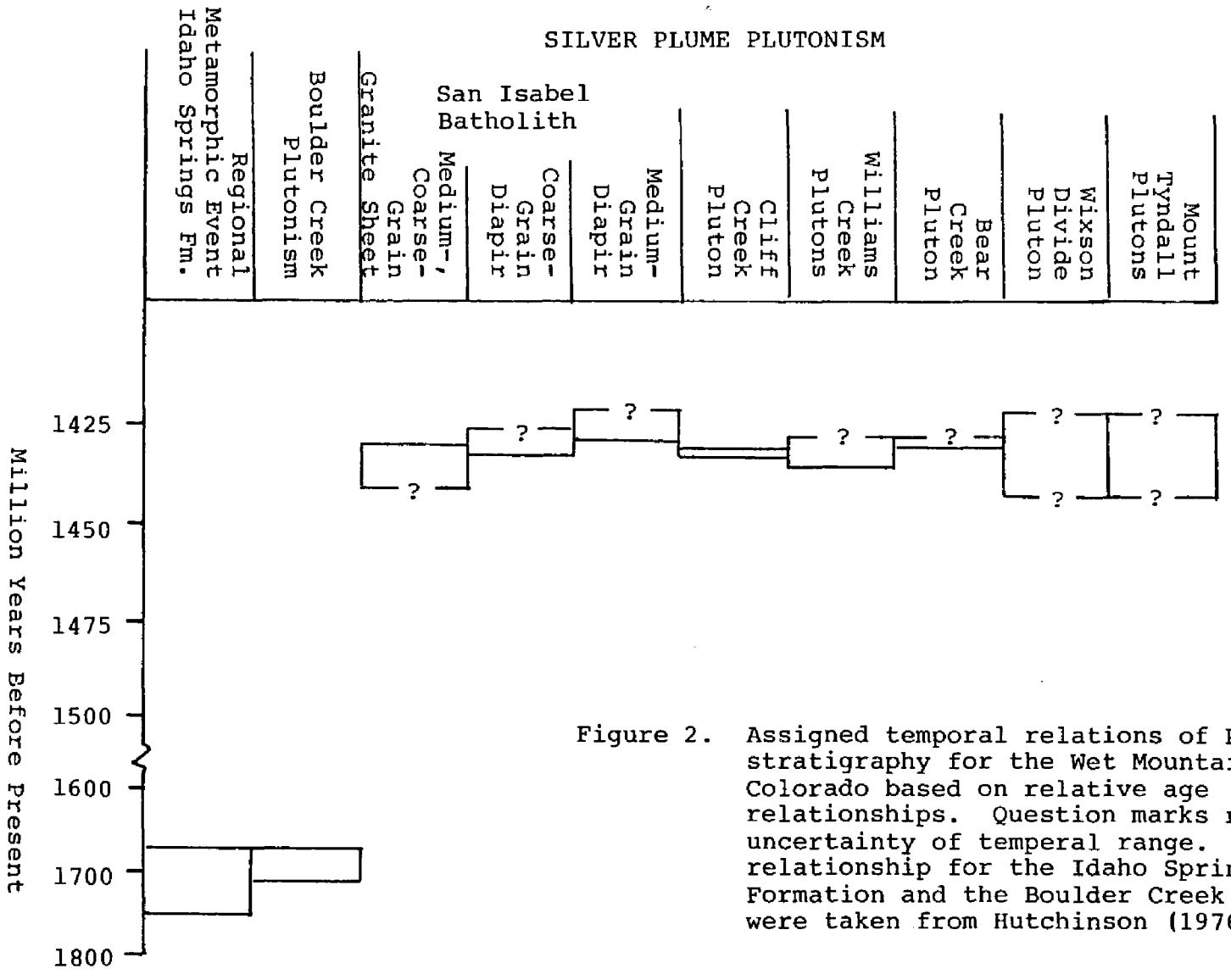

Figure 2. Assigned temporal relations of Precambrian stratigraphy for the Wet Mountains of Colorado based on relative age relationships. Question marks reflect uncertainty of temperal range. Age relationship for the Idaho Springs Formation and the Boulder Creek Batholith were taken from Hutchinson (1976).

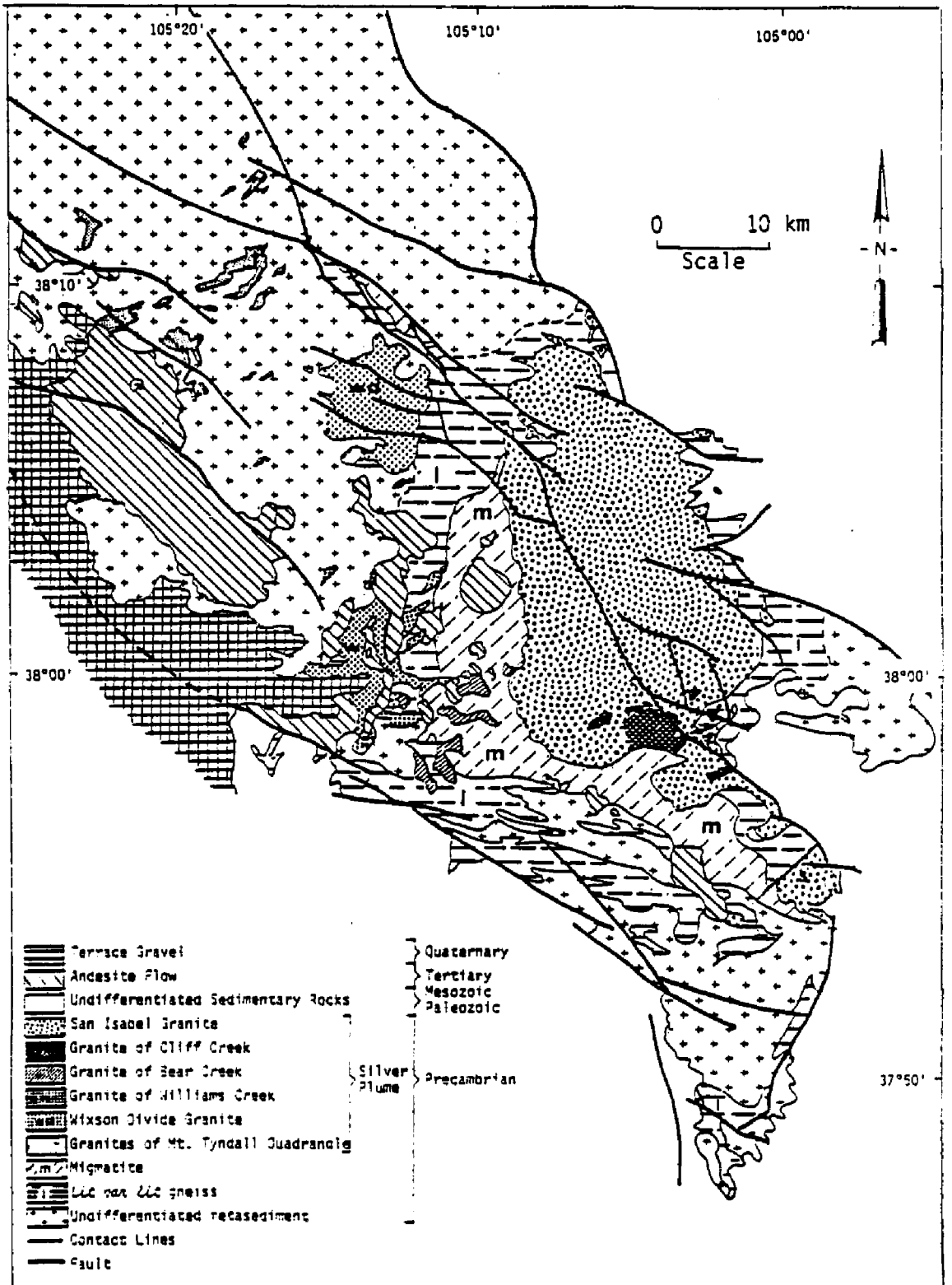

Figure 3. Geologic map of the central and southern Wet Mountains, Colorado (Boyer, 1962 and Scott, *et. al.*, 1976b).

of these rocks is ubiquitous and well developed with compositional layers generally paralleling foliation (Boyer, 1962).

Contacts between the principal metamorphic rock types are gradational. The granite-gneiss contacts are with few exceptions sharp, straight and lacking of an aphanitic chill margin.

The Wet Mountains contain granitic rock that are related to two separate plutonic events. The late syntectonic Boulder Creek-age plutons are dated at 1,720 million years (Taylor, *et. al.*, 1975), and the post-tectonic Silver Plume-age plutons (Boyer, 1962; Murray, 1970; and Brock and Singewald, 1968) are dated at 1,430 $\pm$ 200 million years (Boyer, 1962) and 1,450 million years (Taylor, *et. al.*, 1975). Recent unpublished data for the San Isabel batholith gives an apparent Rb/Sr age of 1,430 $\pm$ 10 million years (Hedge, 1980). Hedge established the initial $^{87}Sr/^{86}Sr$ ratio for the batholith at 0.7034. The regional plutonic relationship to the metamorphic rocks is that of mainly concordant emplacement for the Boulder Creek plutons and strongly discordant emplacement for the Silver Plume plutons.

STRUCTURE AND STRATIGRAPHY OF THE SILVER PLUME-AGE PLUTONS OF THE CENTRAL AND SOUTHERN WET MOUNTAINS

The Wet Mountains are a southeast trending range that forms an en echelon pattern with the Front Range to the northeast and the Sangre de Cristo to the west and southwest (Figure 4). The Wet Mountains and the rest of the Front Range are separated by the Canon City structural embayment. To the west, the Wet Mountain Valley syncline separates the Sangre de Cristo Range from the Wet Mountains. To the south and east, Huerfano Park Basin, Tioga Basin, and Raton Basin merge with the Denver-Julesburg Basin (Boyer, 1962).

The Precambrian core of the Wet Mountains is exposed in a north-south trending anticline which bifurcates to the south of the study area (Figure 4). The range is bounded on the east by the Laramide Frontal Thrust Fault, locally known as the Wet Mountains Fault, and on the west by the Westcliff Fault. The Ilse Fault is the only major fault within the range. All three faults strike generally north-northwest. The Laramide Frontal Thrust Fault and

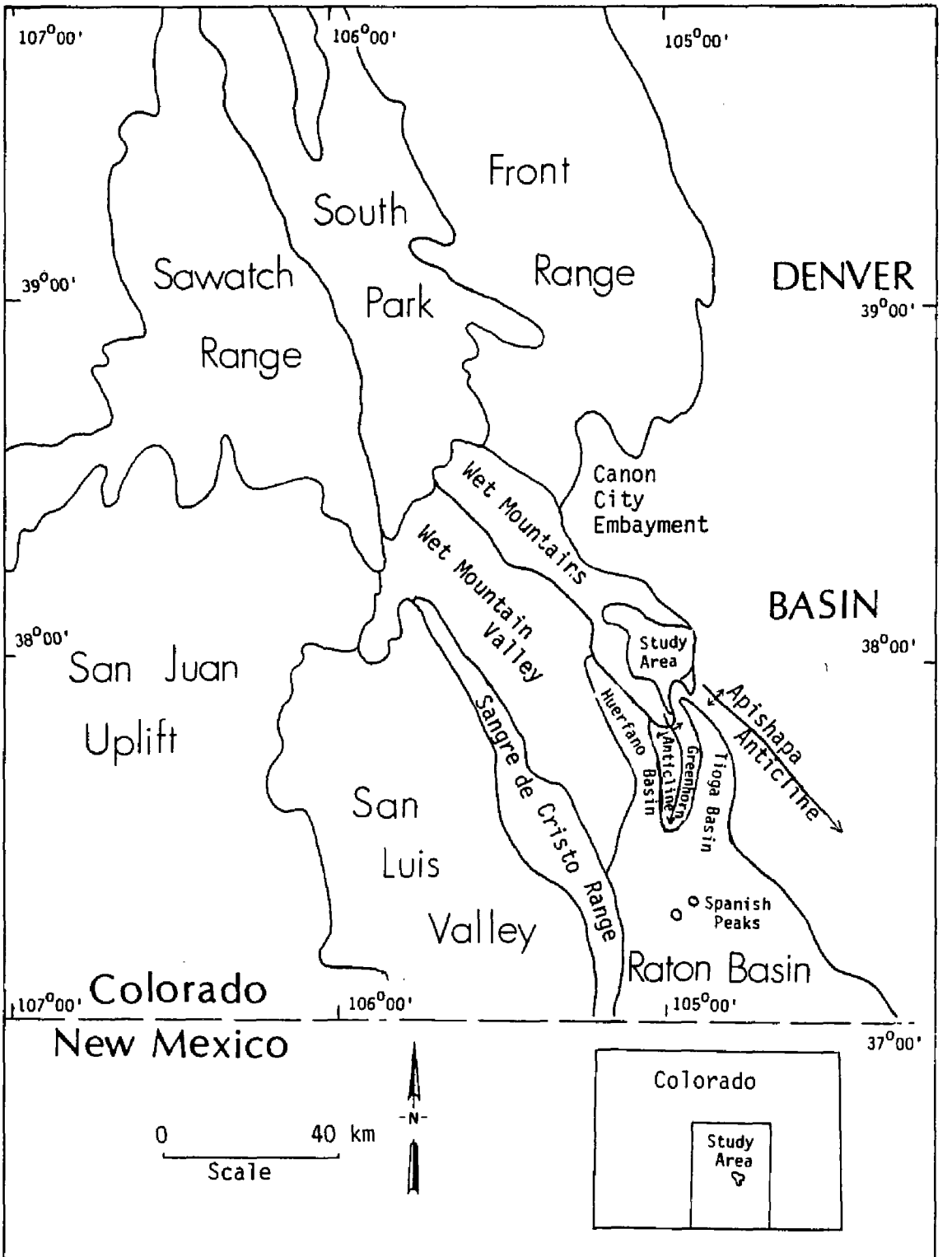

Figure 4. Index map showing the regional physiography for south-central Colorado (Murray, 1970) and showing the location of the study area

the Westcliff Fault are related to the Laramide Tectonic event (Boyer, 1962). The Ilse Fault, while exhibiting some Laramide movement (Boyer, 1962), exhibits pre-, syn-, and post-Silver Plume movements (Singewald, 1966; Murray, 1970; Harper, 1975). The majority of the Silver Plume plutonism occurs along the Ilse Fault zone (Scott, *et. al.*, 1976a).

Structure and Stratigraphy of the San Isabel Batholith

The San Isabel batholith has been subdivided into three textural facies (Figure 5). The facies (coarse-grain, medium-grain, and porphyritic) aid in understanding the internal structure of the batholith. Contacts between the various facies are generally gradational and vary in width from a few tens of meters to a kilometer. Foliations within the gradational contacts are generally poorly developed and are subparallel to the contact. There also tend to be few or no mineralogical changes across the gradational boundaries.

Sharp contacts between facies are also common but are restricted to a narrow zone along the Ilse Fault. These contacts are associated with elongate zones of fine-grain granite, which represents mylonitized and recrystallized granite. Sharp contacts not fault related are rare. They are invariably found

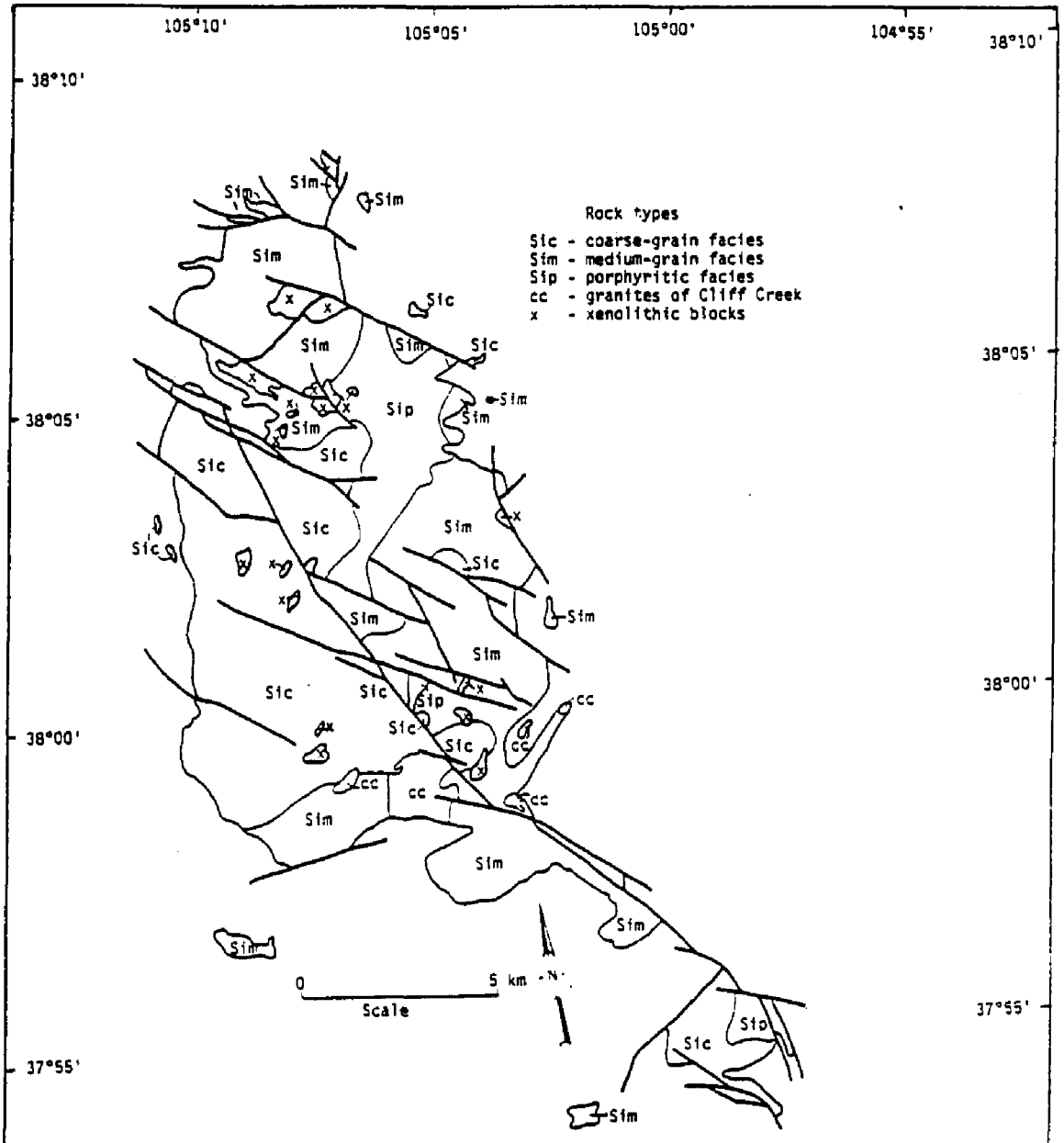

Figure 5. Geologic and structural map of the San Isabel batholith of the southern Wet Mountains, Colorado (Murray, 1970; Boyer, 1962; and Scott, *et. al.*, 1976b).

separating the coarse-grain facies from the medium-grain or porphyritic facies.

Three extensive areas containing massive, relatively xenolith-free granite exist within the coarse- and medium-grain facies. Encircling the massive granites are elliptical zones of increasingly abundant xenoliths and increasingly intense foliations (Figure 6). The foliations of the elliptical zones dip steeply in toward the center of the massive granites, and give the appearance of a cone-shaped structure with its apex still at some depth below the earth's surface.

The San Isabel batholith is structurally and stratigraphically the most complex pluton in the Wet Mountains (Figure 5). Multiple intrusions as a possible explanation for the internal complexity was first suggested by Boyer and King (1964). Whitten and Boyer (1964) with a series of two and three dimensional mineralogical isoplethic maps added support to the concept of a composite batholith. Murray (1970) with the aid of 680 specimens and plotting most of the mineralogical data on isopleth maps, found the pluton's interior to be much more complex. He noted that many of the mineral concentrations and abnormalities of his isopleth maps showed a curious alignment to the Ilse fault and concluded that the

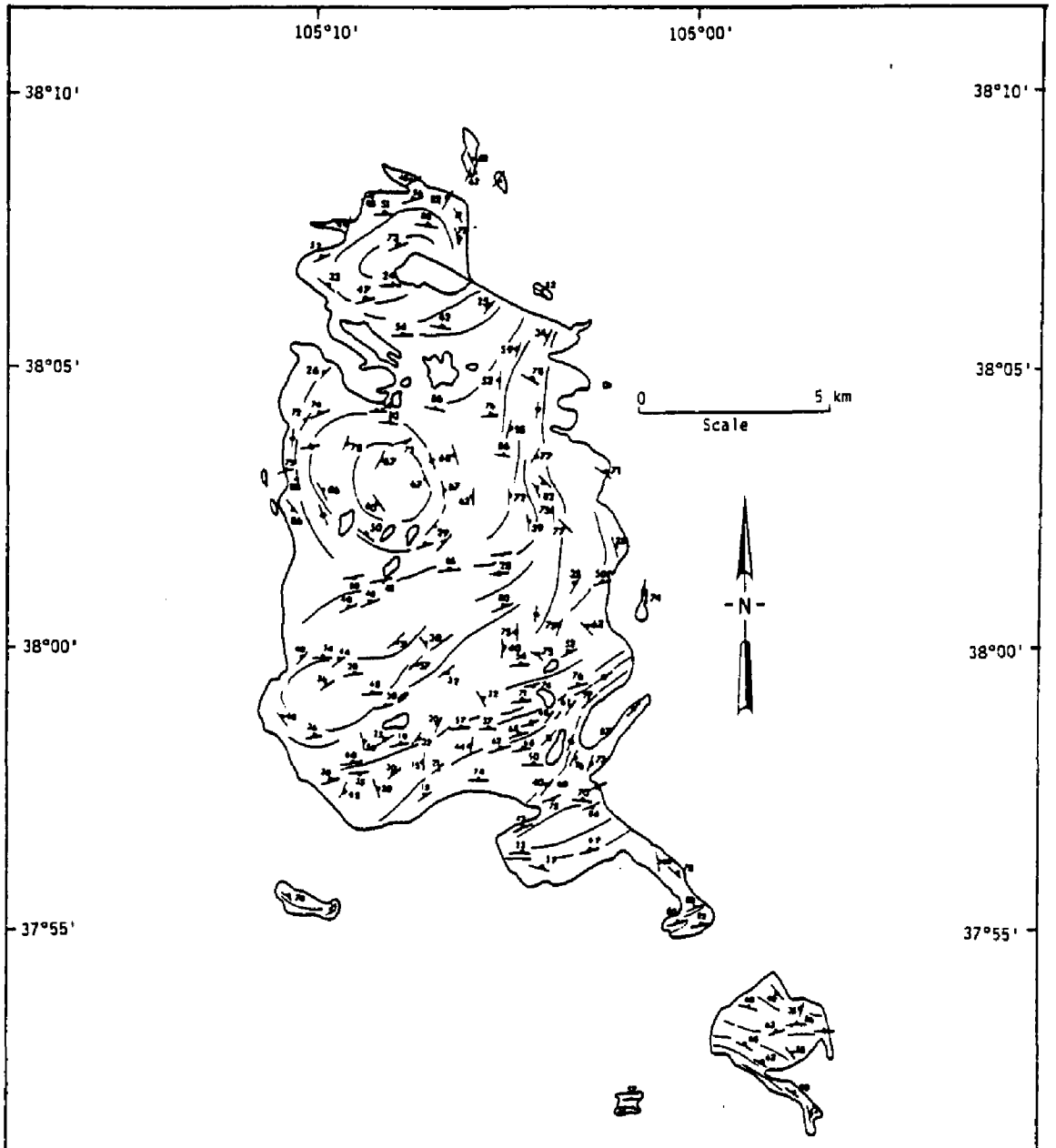

Figure 6. Flow foliations in the San Isabel batholith of the southern Wet Mountains, Colorado

batholith's complex nature is a product of a single intrusion which differentiated and was subsequently faulted.

Presently gathered field evidence, as well as mineralogical and petrological evidence, casts doubt on the view that the San Isabel batholith was a product of a single intrusion. The data suggests that the batholith is composed of three discrete granitic rock masses. Two small diapirs of approximately 10 kilometers in diameter and located in the northwestern portion of the batholith and are easily seen because of their concentric foliations (Figure 6). Cross-cutting relationships among the three masses make it evident that the intrusive sequence is: first, the intrusion of a thick granitic sheet followed by intrusion of two smaller diapiric granite bodies (Figure 6). The age relationship between the two younger diapirs could not be determined because of the lack of structural and spatial relationships. Based on field observations (Figure 6), the southern two conduits seem to have similar points of origin. However, the northern-most diapir seems to have its origin to the north, rather than to the northwest (Figure 6).

The granite-granite contact which exists between the southern-most diapiric granite and the sheet

granite is rarely observed because of the lack of color, modal, and textural contrasts between the two granites and because of vegetative, colluvial, and alluvial cover. The contacts when observed are sharp and straight. The physical and mineralogical changes which occur across one of these contacts is best seen within the Little Charles River Valley (Figure 7). Just west of the contact within the younger diapir, flow foliations are quite intense. Granitic foliation trends are always parallel to the contact and die out progressively toward the diapir's core. Foliations in the "marginal zone" of the diapir show not only mineral alignment but also preferred xenolithic alignment with the xenoliths' long axes parallel to the diapirs' marginal fabric. Dip direction plunges steeply toward the diapiric core (Figure 6). Feldspar lineation, though rare, shows the same structural feature. As the contact is approached from the diapir's core, mafic clots become progressively more aligned and flattened. At the contacts these same clots are stretched into elongate discs or plates. Metasedimentary xenoliths which are found along the granite-granite contact are compositionally dissimilar to the diapir's wall rock which is a distinctly different granite facies. The xenoliths, in fact, are dissimilar even to the nearest

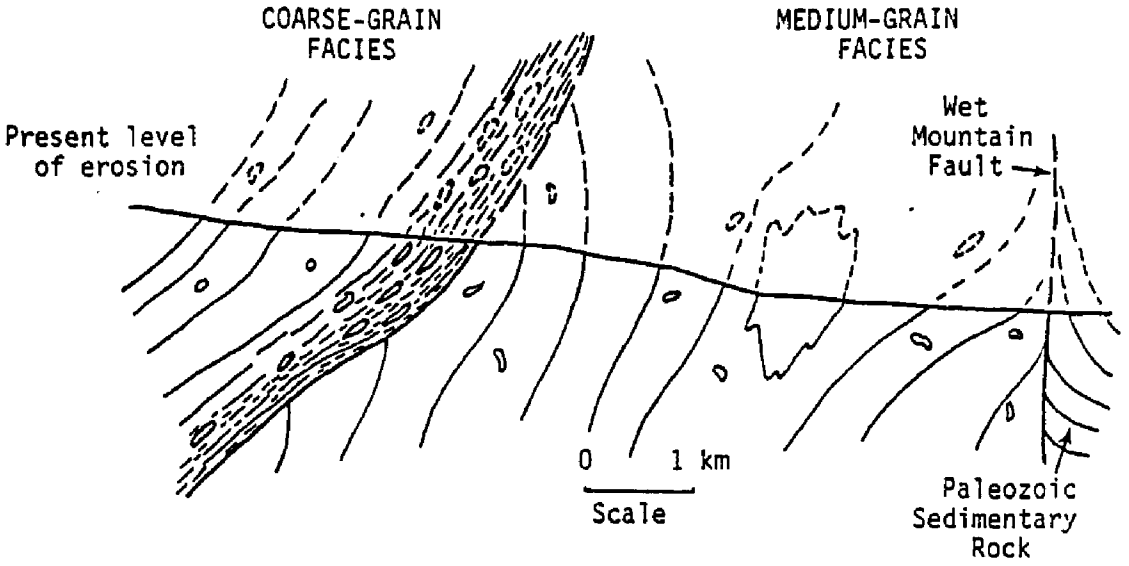

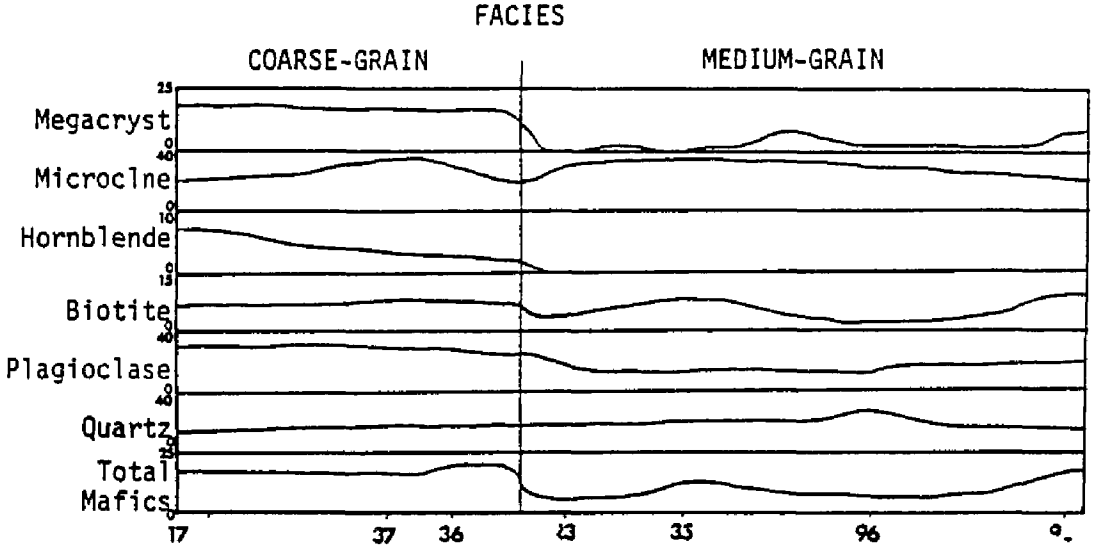

Figure 7. East-west cross-section across the central portion of the San Isabel batholith along Little Charles River. Relative changes in modal composition and textural character of the granites across the coarse-grain and medium-grain contact are shown. Mineral percentages are given along the verticle axis in the lower diagram.

wall rock of metamorphic origin. At this level of erosion the nearest metamorphic wall rock is some 8 kilometers east or 10 kilometers west of their present location. Most xenoliths are of a biotite and biotite-hornblende gneissic composition, and only a few xenoliths are composed of *lit par lit* gneisses and migmatites, the composition of the nearest wall rock.

To the east of the granite-granite contacts granitic flow foliation tends to be poorly developed; xenoliths are randomly oriented; and many areas are structureless. The diapir has had relatively little structural effect on the granite in which it intruded. Granites found just north of the Saint Charles River and east of the granite-granite contact show granitic flow foliation with foliations isoclinally folded. This suggests, along with the sharp, straight contacts, that the diapirs intruded at a time after the intrusion of the main mass of the San Isabel batholith and probably just after complete consolidation of the granite magma (Figure 7).

Structure and Stratigraphy of the Wixson Divide Pluton

The Wixson Divide pluton is not as internally complex as the San Isabel batholith. This is due in part to the pluton being a product of a single magmatic intrusion and in part to subsequent faulting being not

as intense (Figure 8).

The contact between the pluton at its enveloping metasedimentary wall rock is sharp and straight. Contacts are locally discordant and regionally concordant with the metamorphic foliation. Dips within the metasediment is generally to the northwest and tend to become steeper as the pluton is approached. Internal granite-granite contacts are both sharp and gradational. Sharp and irregular contacts exist between the fine-grain facies and other facies, while medium- and coarse-grain contacts are gradational and straight (Figure 8).

Mineral alignment is a common feature of the Wixson Divide pluton (Figure 9) but it varies widely in intensity. The alignment is produced by a planar orientation of biotite and, in the fine-grain facies, stretched and slivered quartz, along with micorcline augen. The area with maximum intensity of mineral alignment is at the pluton's granite-gneiss contact. There the mineral alignment parallels the contact and, in general, passes gradually inward to a typically massive granite. Plutonic contacts are generally discordant to and at times normal to the mineral alignment.

Foliation intensities vary according to the

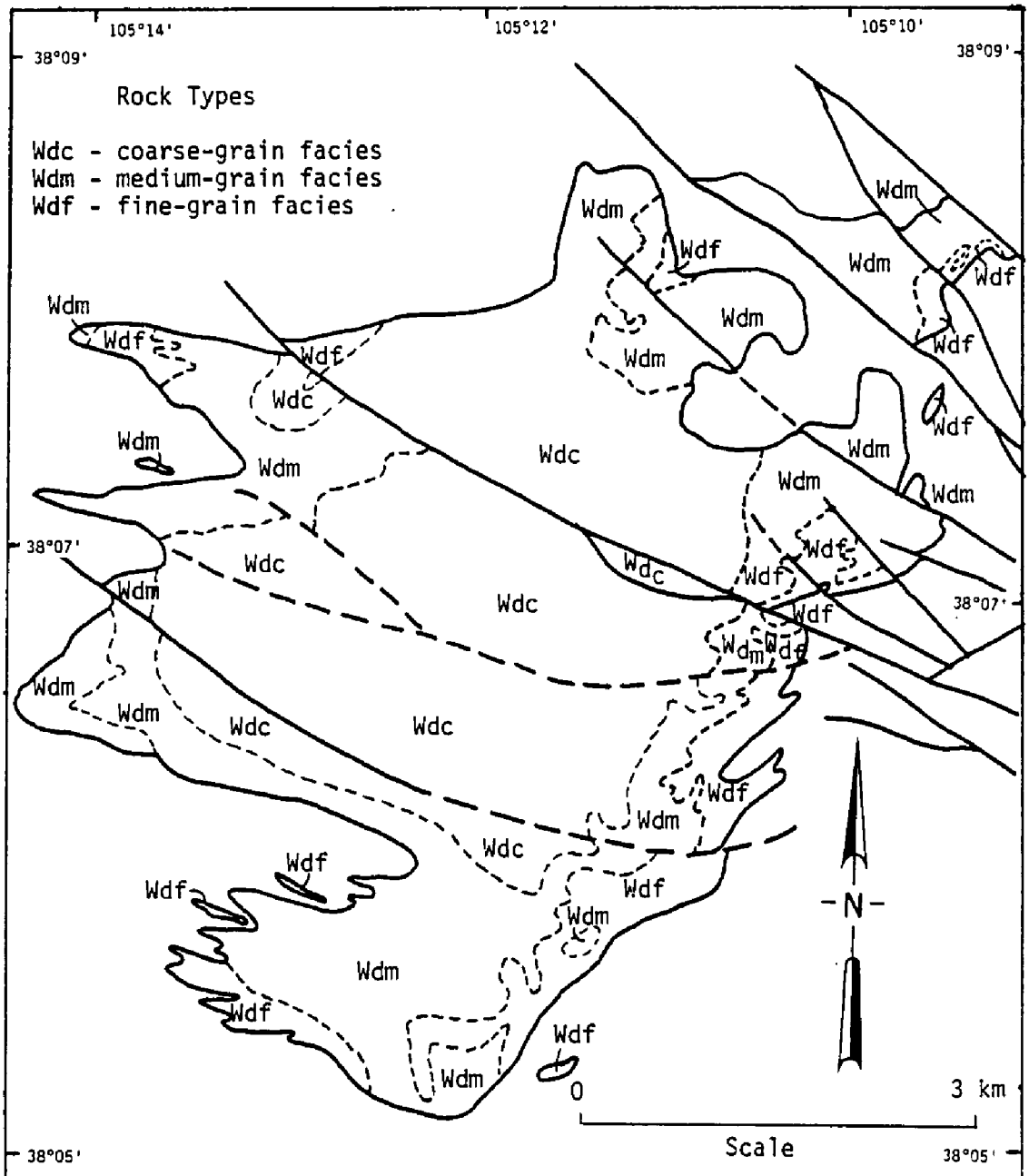

Figure 8. Geolcgic and structural map of the Wixson Divide pluton of the central Wet Mountains, Colorado

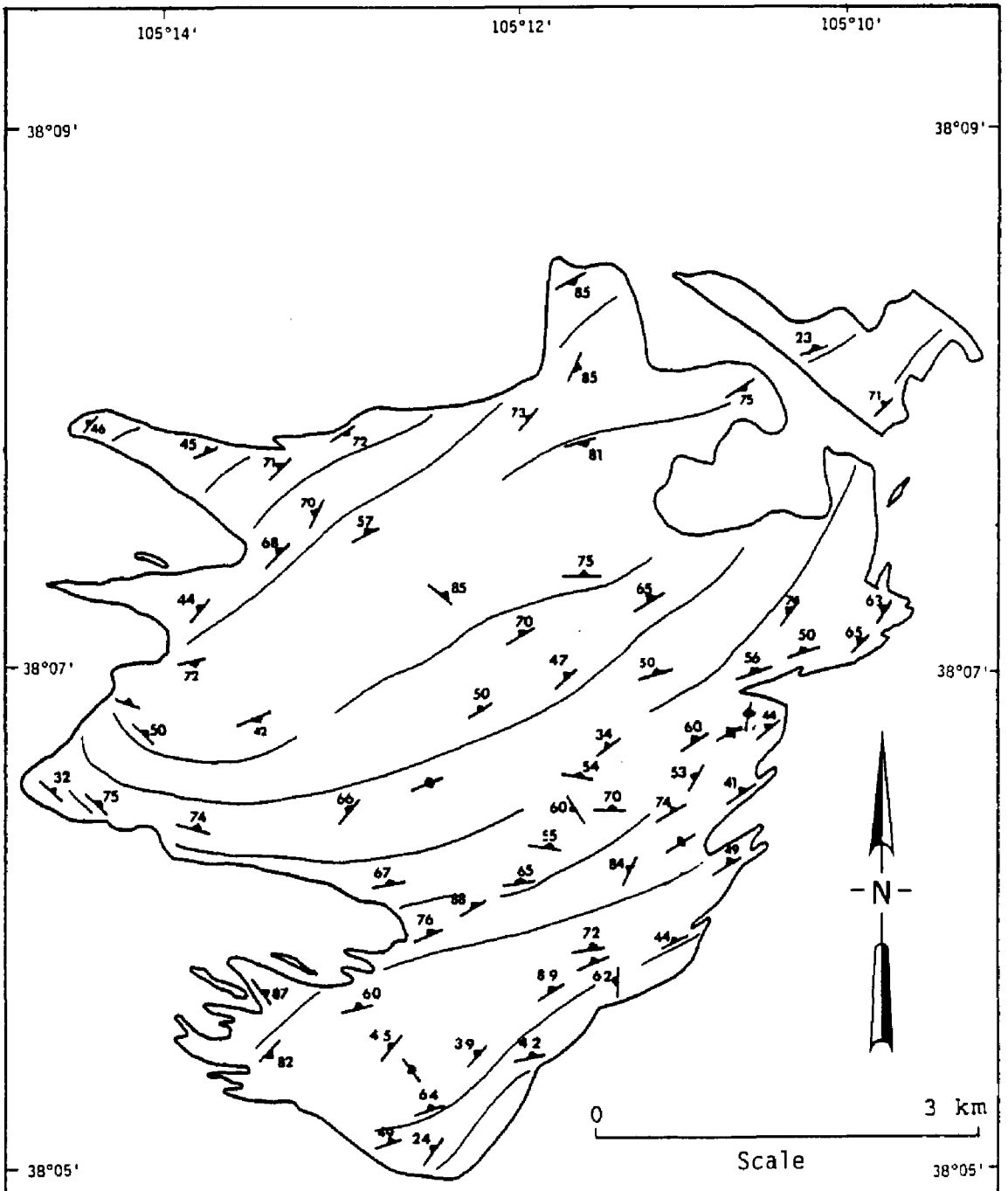

Figure 9. Structural map of the Wixson Divide pluton of the central Wet Mountains, Colorado

direction from which the center of the pluton is approached. From the south, across the fine-grain border facies, foliation intensities vary widely. The border fine-grain facies is well foliated at the granite-gneiss contact but the foliations "die out" as the medium-fine grain contact is approached. Once across the contact, the medium-grain facies' foliations are significantly more intense but then give way to a massive plutonic core. If the pluton is traversed from the north, the intensity of foliation is greatest along the granite-granite contact and gradually gives way to a massive granite at the pluton's core.

The possible genesis of the pluton's mineral alignment is two-fold. In the pluton's fine-grain margin mineral alignment is a result of post-consolidation shearing, which produces a cataclastic foliation. This in turn suggests that the fine-grain facies crystallized prior to final consolidation of the pluton, and the cataclastic texture is a product of shear created by a still mobile magmatic interior. After the cessation of movement in the marginal facies, the still molten medium-grain facies continued to flow creating a second zone of mineral alignment.

Xenoliths are common throughout the pluton but are concentrated most often in the zone of greatest mineral alignment. Xenolithic concentrations are greatest along the granite-gneiss contact, on the medium-grain side of the medium-fine-grain contact and along the linear branches of the Ilse fault. Within the fault zones xenolith to granite volumetric ratio is at its highest about 9:1. Xenoliths in these areas grade from large angular blocks to small pebble-size enclaves of granite gneiss and migmatite. This supports Murray's (1970) hypothesis that some movements along the Ilse fault are possible syn- Silver Plume in age.

Structure and Stratigraphy of the Minor Plutons

In number, and diversity of plutonic size and character, the Mount Tyndall granites are unmatched by any of the Silver Plume-age intrusives of the Wet Mountains. These granites are widely scattered over a large area and crop out as laccoliths, phacoliths, sills, dikes, and a small stock.

The mineral alignment in these plutons is generally quite poorly developed. However, in some dikes, sills, and small phacoliths, a planar orientation of biotite exists. In the larger granitic plutons very faint subparallel biotite alignments are found parallel to subparallel to the granite-gneiss contact. Generally,

the dip direction of these faint foliations is to the north and northwest.

Xenoliths are also not commonly observed in any of the granitic intrusive bodies. Those xenoliths that do exist vary in size but do not exceed one meter. Most xenoliths are quite small -- 0.5 to 5.0 cm in length. In shape, there is trimodal distribution. The larger xenoliths are irregular in shape and are compositionally similar to adjacent metasedimentary country rock. The intermediate size xenoliths are composed of elongate to lenticular wisps of black biotite. Biotite clusters and clots comprise the smallest group of xenoliths. All xenoliths align themselves parallel to subparallel to the faint foliations of the granite.

The granites of the Mount Tyndall quadrangle are subdivided into easily recognizable facies by Brock and Singewald (1968) - the "r" granite (radioactive granite) and "d" granite (porphyritic granite). Internal contacts between the two facies are rare. Contacts were observed at two localities, and at both localities they are sharp and straight. Foliations in the "r" granite parallel the facies, while the faint foliations of the "d" granite are cut by the contact. This suggests that the "r" granite facies has an intrusive

nature with respect to the "d" granite facies.

The granites of Williams Creek and the granites of Bear Creek comprise numerous small plutons which crop out primarily along creeks of their namesake on the western slopes of the Wet Mountains (Figure 10). These plutons are the only plutons of Silver Plume age not in direct contact with the Ilse Fault zone. The plutons exhibit a strongly intrusive nature with local wall rock foliations being plastically deformed into symmetrical, asymmetrical and isoclinal folds (Boyer, 1962, and this author).

The plutons display both granite-granite and granite-gneiss contacts. The granite-gneiss contacts are all sharp and straight. The granite-granite contacts between Williams Creek and Bear Creek granites are gradational over approximately 50 meters (Boyer, 1962, and this author). A transitional granite intermediate between the two major granite rock types exists at these boundaries. Across the contact zone there is not only a change in grain size but an overall change in mineralogy. The Williams Creek granite is coarser-grained and contains more biotite and hornblende, as well as microcline phenocrysts, than the typical Bear Creek granite. In most cases where the Bear Creek granite was found in contact with the

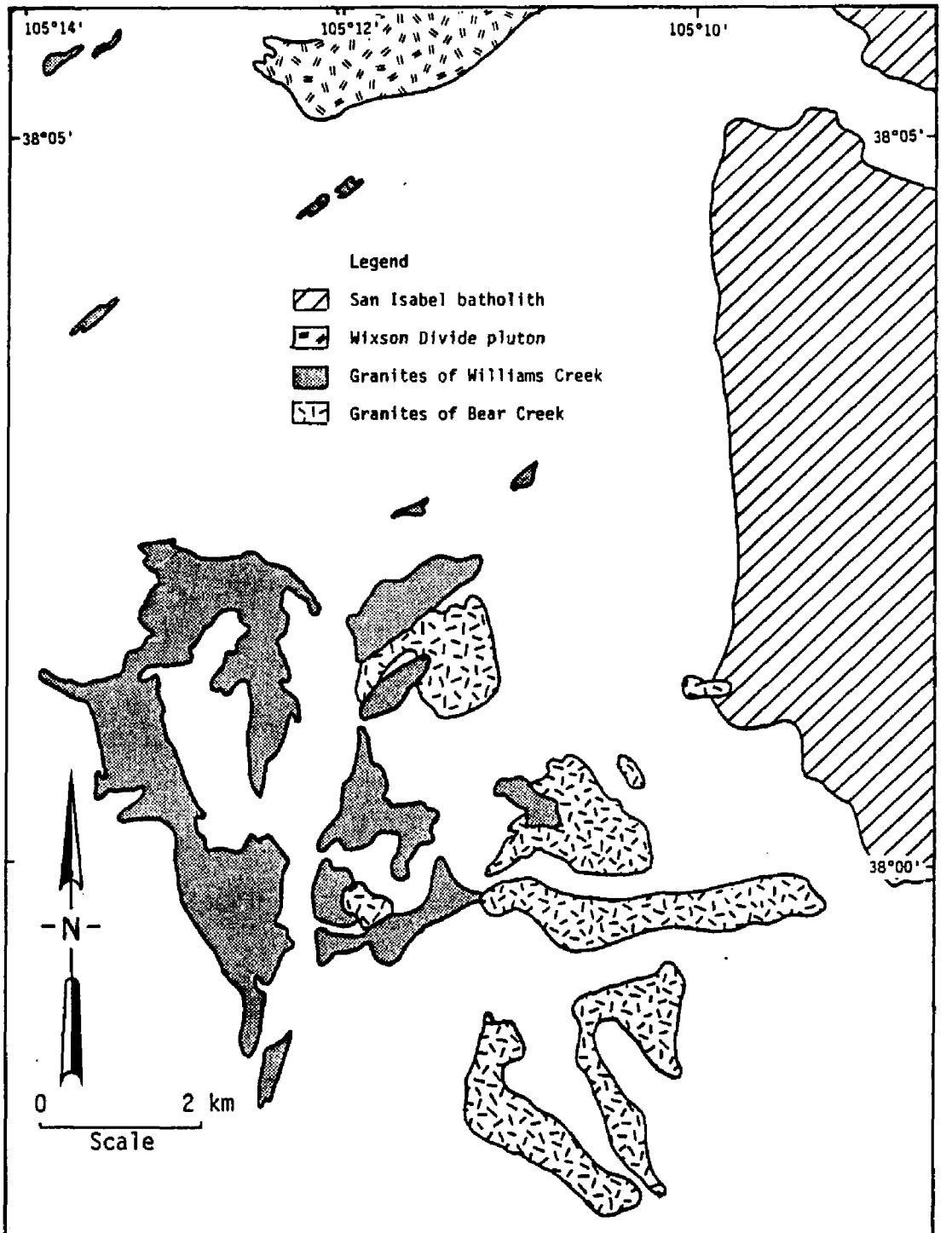

Figure 10. Geologic map of the intrusive plutons of the southwestern portion of the Wet Mountains, Colorado (modified after Boyer, 1962 and Scott, *et. al.*, 1976b)

Williams Creek granite, the Bear Creek granite was topographically higher. A granite-granite contact between one of the Bear Creek plutons and the San Isabel batholith was originally mapped by Boyer (1962). Unfortunately, the contact relations cannot be located precisely in the field but only can be approximated within 30 meters. Contact lines, even though they are subjective, are consistent with a discordant relationship between the Bear Creek and San Isabel plutons with no evidence of gradational boundaries and suggest that the San Isabel granite was in a high degree of consolidation at the time of the Bear Creek intrusive event.

Granitic foliations exist only within the Williams Creek granites. They are generally parallel to the granite-gneiss contact. Foliations die out as the plutonic center is approached. Dips in all plutons are moderate to steep and all are toward the northwest (Figure 11).

Xenoliths within the Williams Creek plutons are small and parallel to subparallel to the granitic flow foliations. Xenoliths are normally found within a few meters of the pluton's border. In the plutons' center, schlieren and wisps of biotite are also found. A few areas of xenolithic concentrations were found in the

Figure 11. Flow foliations in the Williams Creek and Bear Creek plutons of the southwestern portion of the Wet Mountains, Colorado

upper portions of several plutons and probably represent areas of stoping. Near the basal sections of other plutons are areas with extremely high concentrations of biotite. This may represent a zone of crystal settling or a zone of complete xenolithic dismemberment.

Xenoliths of the Bear Creek plutons are quite uncommon. Only the rare stretched mafic xenoliths and small biotite clots are observed. When gneissic xenoliths are observed in the granites, they normally appear blocky and tend to be located near the granite-gneiss contact.

The granites of Cliff Creek (Boyer, 1962) are texturally heterogeneous through their area of exposure. Plutons are composed of two textural rock types -- a medium- and a fine-grain facies (Figure 12). Each pluton, on the other hand, is homogeneous. No internal or external contacts were observed either between the two textural facies or between the Cliff Creek and San Isabel granites. Contacts between the two facies and the San Isabel granitic wall rock seem to be gradational and are about 50 meters in width. Cliff Creek granites are massive with only peripheral areas of the plutons exhibiting any foliation. In these areas foliation tends to parallel the foliation within the San Isabel batholith.

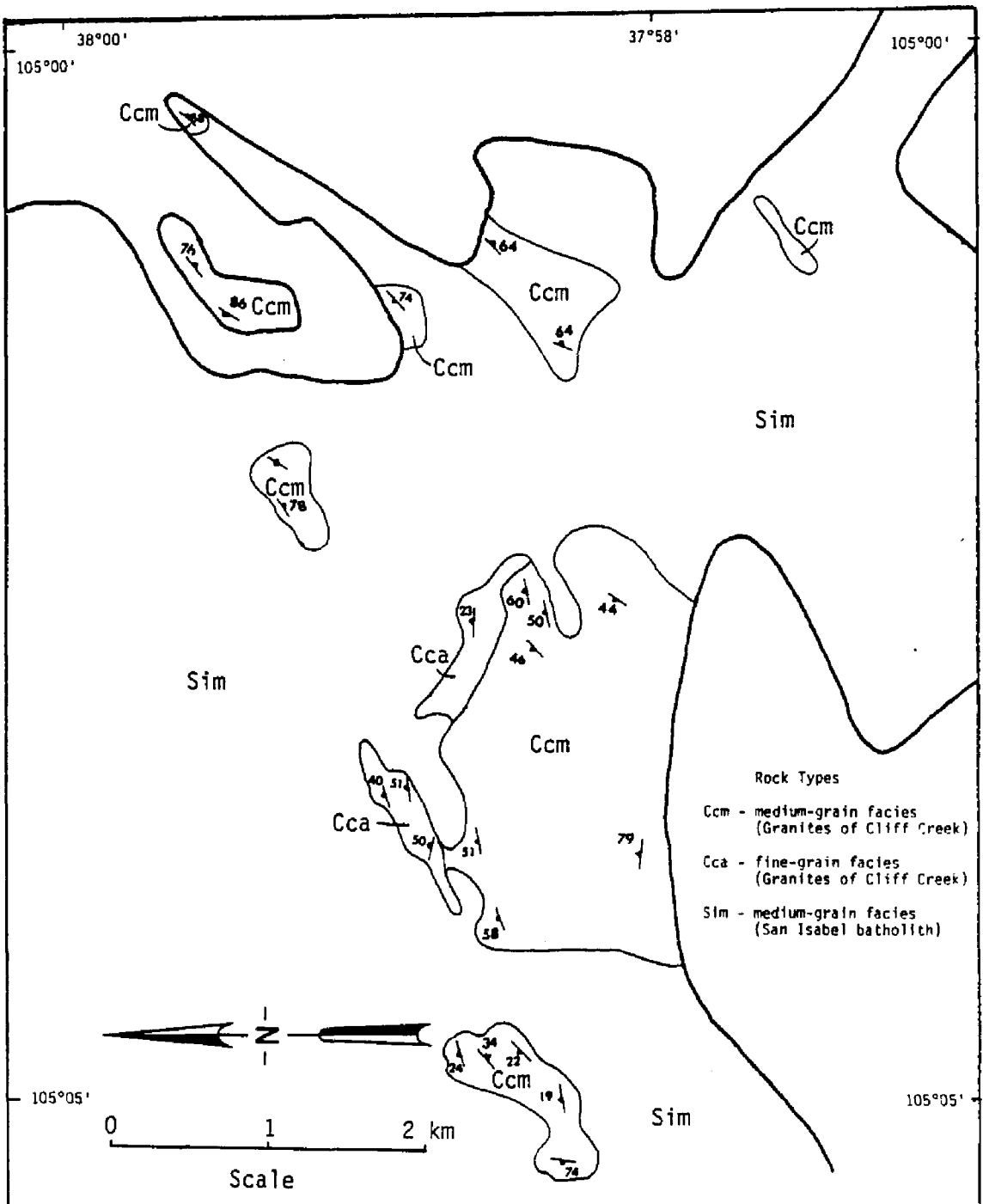

Figure 12. Geologic and structural map of the granites of Cliff Creek in the southern Wet Mountains, Colorado (modified from Boyer, 1962)

PETROGRAPHY OF THE SILVER PLUME PLUTONS

The Silver Plume plutons of the central and southern Wet Mountains consist of two major lithologic varieties: biotite-rich and leucocratic granites. The biotite-rich granites are the most common plutonic rock type in the range and include the San Isabel batholith, Wixson Divide pluton, granites of the Mount Tyndall quadrangle, and the granites of the Williams Creek. The granites of Bear Creek and Cliff Creek are leucocratic. All granites are muscovite-bearing with secondary muscovite found in every pluton and primary-looking muscovite found in only the two northernmost plutons.

The granites of the San Isabel batholith were originally described by Boyer (1962) and Murray (1970). They established four textural facies, coarse-grain, medium-grain, fine-grain and porphyritic. The same facies classifications were used by this writer during the mapping of the other plutons with the exception of the granites of the Mount Tyndall

quadrangle. The facies of the Mount Tyndall granites had already been named, the "r" granite and "d" granite, by Brock and Singewald (1968) prior to this study.

Petrography of the San Isabel Batholith

The texture of the San Isabel batholith is typically granitic, ranging from xenomorphic- to hypantomorphic- granular and porphyritic. Seriate textures have developed along and around some of the larger microcline megacrysts. Cataclastic textures have developed along fault zones. The foliate texture is best developed along the batholith's margins.

Microcline megacrysts are common in all facies but volumetrically dominate the coarse-grain and porphyritic facies. Megacrysts are rarely euhedral but are most commonly subhedral with rounded corners. They exhibit albite-pericline twin planes. Carlsbad twins are occasionally observed. Both macro- and micro-perthite are common. Perthite appears as films, rods, strings, veins, and patches. The percent of albite within the microcline host ranges up to 30 percent. Megacrysts are relatively free of inclusions. Of those inclusions observed, round or bead quartz is most common. Other less common inclusions are subhedral to euhedral hornblende and sphene which

exhibit no alterations and are located more to the center of the crystals. A few megacrysts in the medium- and coarse-grain facies and a majority of the megacrysts of the porphyritic facies are liberally sprinkled with aligned plagioclase inclusions and patchy perthite. These grains invariably include small very irregular unstrained quartz inclusions. Adjacent to some of these microcline megacrysts are partially replaced plagioclase that have the same optic orientation as the plagioclase inclusions. The smaller interstitial microcline is anhedral with strong grid twins and rarely contains perthite or inclusions.

Plagioclase, most commonly calcium oligoclase to sodium andesine (An_{23} to An_{34}), is the second most common mineral in the batholith. Four types of plagioclase are present. Large magmatic plagioclase crystals are euhedral to subhedral. The subhedral crystals have mechanically rounded corners. The interstitial plagioclase is anhedral. Myrmekitic plagioclase is common and has developed along microcline-microcline and microcline-plagioclase crystal boundaries. Myrmekite appears as large irregular masses and as well developed vermiform-rich mushrooms. Perthitic plagioclase occurs frequently.

In the northwest and central portion of the batholith plagioclase aggregates (An content unknown) are dominantly monomineralic with only minute amounts of irregularly-shaped interstitial quartz. Generally, the aggregates are partially replaced by microcline. Microcline nucleates at the triple junctions and if unimpeded would probably replace the aggregate.

Both types of polysynthetic twins are present in the plagioclase. Albite twins are thin and ubiquitous. Pericline twins are formed from secondary deformation and are rare. Carlsbad twins are common. Other types of twins observed are growth (nucleated and synnosis), penetration, and complex. Normal zonation of plagioclase is frequent. Aggregates are also zoned with the albite-rich rim crossing individual plagioclase boundaries. Incomplete or albite rims have also developed on some plagioclase crystals.

Plagioclase crystals contain few inclusions. However, a substantial majority of plagioclase crystals have undergone complete or partial alteration to a fine-grain white mica (sericite), clay minerals, and epidote. Those grains that are only partially altered have their alteration products concentrated in the crystals' core.

Quartz is an anhedral interstitial mineral that

exhibits both deformation and recrystallization textures. These textures include: 1) crystals with deformation lamellae, expressed by undulatory extinction, 2) quartz slivers and stretched grains with strong undulatory extinction, and 3) strain-free mosaic of sutured quartz with well developed triple-point junctions. Inclusions are rare and only include euhedral apatite, acicular rutile, and aligned liquid inclusions.

Biotite is always found associated with other accessory minerals in either small round to strongly elliptical masses of 10 to 15 mm or as individual anhedral flakes of at least 1 mm. The elliptical masses or mafic clots are common in the north-central portion of the pluton and especially in the coarse-grain facies. Biotite is strongly pleochroic and varies in color from light greenish brown to dark olive green or from a light to dark brown. Two types of biotite exist in the batholith -- inclusion-rich biotite, which appears to be a by-product of hornblende alteration, and inclusion-free biotite, which is probably a product of magmatic crystallization or is unmelted residual material.

Hornblende is often partially corroded, embayed, and altered. Hornblende is anhedral and is almost

exclusively confined to the elliptical mafic clots of the north-central portion of the batholith. Deep blue-green to dark green pleochroism is common.

Sphene is found throughout the batholith but is most common in the mafic clots. The crystals are anhedral and are broken, fractured, and rounded. They are partially altered to leucoxene. Other accessories include: rounded and occasionally zoned zircon, when included in biotite form rather large radioactive haloes; anhedral magmetite; euhedral apatite; epidote; allenite; and rutile.

The average modal analysis listed in Table 1 is a summary of 150 samples collected from the San Isabel batholith and its satellites (appendix Figure B.1). Detailed modal analyses are given in appendix Table B.2. As the extremes and standard deviations show, the variation about the mean composition is large. Trigonal plots (appendix Figure B.3.) show the rocks of the pluton to be plagioclase-rich granites. Modal differences between the medium-grain and porphyritic facies are remarkably slight, while the coarse-grain facies is more plagioclase- and mafic-rich. The medium-grain facies also contains modal differences depending on sample localities. Those samples collected north of the porphyritic facies are modally more like

Table 1. Average Modal Composition in Volume Percent and Major Element Composition in Weight Percent of the San Isabel Batholith Based on 150 Modal and 36 Chemical Analyses

	Mean	Standard Deviation	Extremes
Kspar	30.56	7.39	49.0-12.5
Plagioclase	29.87	5.71	48.1-14.1
Quartz	21.51	4.52	41.3-11.1
Biotite	8.13	3.69	18.8- 0.0
Magnetite	2.55	1.40	7.0- 0.0
Sphene	2.13	1.41	7.7- 0.0
Hornblende	1.15	2.16	19.7- 0.0
Accessory minerals	4.08	2.97	16.1- 0.0
SiO_2	67.93	4.72	75.55-56.16
Al_2O_3	15.52	1.25	18.08-12.47
Fe_2O_3	1.77	0.92	3.81- 0.32
FeO	2.06	1.28	5.29- 0.27
MnO	0.08	0.05	0.16- 0.01
MgO	1.10	0.69	2.49- 0.05
CaO	2.35	1.13	7.28- 0.64
Na_2O	3.26	0.31	4.00- 2.56
K_2O	4.27	0.68	5.36- 2.53
TiO_2	0.77	0.39	1.51- 0.14

Wixson Divide granite than San Isabel medium-grain granite (appendix Table B.2).

Chemical analysis and CIPW norms of the samples collected in the San Isabel batholith are shown in appendix Table B.4. The chemical data are summarized in variation diagrams (appendix Figure B.5).

Petrography of the Wixson Divide Pluton

The petrographic textures of the pluton's rocks are dominantly xenomorphic-granular. Foliate texture is common near the granite-gneiss and fine-medium grain facies contacts. In the fine-grain facies quartz appears sutured, mosaic, and somewhat granular. Mica flakes at times are bent, kinked, and contain microfaults, while feldspar crystals appear rounded or broken. All observations demonstrate the cataclastic nature of the border facies.

Microcline is the most abundant mineral in the pluton. Unlike the microcline of the San Isabel batholith no megacrysts are present. Microcline is euhedral to subhedral in the coarse- and medium-grain facies and anhedral (rounded and fractured) in the fine-grain facies. Rounding and fracturing appear to be a product of crystals rolling within a completely solidified but very plastic granite. All microcline is either twinned or perthitic. Some crystals exhibit a

combination of both features. Twinning follows the albite-pericline twin laws. Carlsbad twins are rare. Perthite is microperthitic only. Types of perthite include (in order of abundance) string, film, stringlet, vein, flame, rod, and patches. Inclusions, biotite, and bead quartz are common within the larger crystals. The oriented plagioclase inclusions, common in the San Isabel's megacrysts, are not found in this pluton.

The anorthite content for plagioclase ranges from An_{22} to An_{28}. Anorthite contents were difficult to determine because of the overall lack of and indistinctness of the polysynthetic twins. Carlsbad, Carlsbad-albite, growth, and penetration twins are also observed in the pluton but are rare. Cataclastic textures which include mechanical and glide twins, microfaulting and dislocations are observed in the plagioclase crystals of the fine-grain facies and of fault zones. Simple zonation of plagioclase is common. Albite or incomplete rim development is rare. Plagioclase is generally inclusion-free. Myrmikite is abundant, with some well-developed plagioclase warts. Alteration of plagioclase is common. In fact, plagioclase is easy to differentiate from microcline because of its higher degree of alteration. Plagioclase crystals vary in the magnitude of alteration from a

light dusting to a very heavy concentration of sericite, clay minerals, and epidote. The heaviest concentration of alteration products is in the cores of zoned plagioclase crystals.

Quartz is equivalent in size to both plagioclase and microcline within the pluton. The majority of the quartz is either deformed or recrystallized. Common textures include glide planes, deformation lamellae, and undulatory extinction. Textures only seen in the fine-grain facies include quartz slivers, stretched crystals, recrystallized mosaics, and well-developed sutures. Inclusions in quartz are common and include biotite, rutile, apatite, hematite, "bubble trains," and muscovite.

Anhedral plates and books of brown to green pleochroic biotite are present in all facies of the pluton. In the fine-grain facies the biotite is tattered, broken, bent, or split along the generally well-developed cleavage planes. The biotite-rich mafic clots of the San Isabel batholith are not present in this pluton.

Dark bluish-green pleochroic hornblende is observed in a few thin sections. These thin sections are taken from rocks collected from the deepest part of the pluton -- the northwestern part. These grains are

highly altered and in part replaced by biotite. Crystals are embayed and corroded. Muscovite appears to have both a primary and secondary origin. Primary muscovite is subhedral, ragged, strained, and contains some microfaults. Quartz inclusions are rather common, and the mineral is generally found in association with biotite, magnetite, and quartz. Secondary muscovite is formed from sericite at the expense of plagioclase and has formed at the expense of some hydrothermally altered biotite. Other accessory minerals include broken to rounded wedges of sphene; anhedral to euhedral magnetite; zircon; apatite; rutile; and alteration products that include hematite, epidote, limonite-geothite, pyrolucite, leucoxene, and a variety of clay minerals.

Modal analysis of 79 samples (appendix Figure C.1) are summarized in Table 2. Modal variation (appendix Table C2) within the pluton is slight when compared with the San Isabel modes. The rocks of the pluton are granitic in composition (appendix Figure C.3).

Chemical analysis and CIPW norms of the samples collected in the Wixson Divide pluton are shown in appendix Table C.4. The chemical data for the pluton are summarized in variation diagrams (appendix Figure C.5).

Table 2. Average Modal in Volume Percent and Major Element Composition in Weight Percent of the Wixson Divide Pluton Based on 87 Modal and 24 Chemical Analyses

	Mean	Standard Deviation	Extremes
Kspar	36.62	7.39	63.7-19.4
Plagioclase	25.87	6.01	37.9-10.7
Quartz	26.00	4.67	39.4-12.3
Biotite	6.52	3.21	14.7- 0.0
Magnetite	1.50	0.79	3.4- 0.0
Sphene	0.92	0.96	3.9- 0.0
Accessory Minerals	1.86	1.25	4.9- 0.0
SiO_2	71.08	2.96	75.67-64.81
Al_2O_3	14.88	1.21	16.74-12.89
Fe_2O_3	1.32	0.61	2.69- 0.46
FeO	1.69	0.82	3.60- 0.20
MnO	0.06	0.04	0.12- 0.00
MgO	0.79	0.34	1.59- 0.32
CaO	1.45	0.91	3.57- 0.10
Na_2O	3.23	0.31	3.85- 2.64
K_2O	4.66	0.65	6.69- 3.81
TiO_2	0.52	0.34	1.43- 0.04

Petrography of the Granites of the Mount Tyndall Quadrangle

The granite plutons of the Mount Tyndall quadrangle are categorized as being composed of two types of granites, "r" variety and "d" variety of Brock and Singewald (1968). The rock texture of the "r" granite facies is xenomorphic-granular. The "d" granite facies on the other hand, has a porphyritic texture. Its groundmass texture is similar to that of the "r" granite. The "d" granite is also at times sucroidal to granoblastic. Cataclastic textures are prevalent to both facies.

Microcline, plagioclase, and quartz alternate with one another as the most abundant minerals in various rock samples. Microcline is often the most common mineral. All crystals tend to be anhedral to serrated. Twinning is common in all microcline. The most common twin type is albite-pericline. Perthite is uncommon. Two varieties of perthite were observed -- film and stringlet.

Zonation of microcline was not observed. On the other hand, mantling of microcline on microcline was noted in the "r" granite facies. Crystals that exhibit this type of mantling normally display a narrow zone of

bead quartz or film perthite in a ring around the crystal's core. The larger crystals appear to have been tumbled and rolled. Inclusions and myrmekites are common in the "r" facies only. Microcline also appears to be relatively unaltered by either superficial weathering or hydrothermal processes.

Plagioclase, mostly calcium oligoclase An_{24} to An_{30} is bimodal in its size distribution. Single crystals include anhedral autocrysts, which exhibit a sercusate texture. Plagioclase aggregates (An content optically not possible to determine) are present in the "d" granite. Polysynthetic twinning within the "r" granite facies is clear and well developed. However, within the "d" granite facies twin planes are normally weakly developed. Simple zonation in some of the aggregates and in virtually all the plagioclase phenocrysts is crudely developed. No significant development of simple zonation was observed in the interstitial plagioclase. Inclusions are bead quartz, and in the larger phenocrysts, ragged biotite. Alteration products generally are quite intense. Plagioclase seems to be altering to a white mica (sericite), epidote, and clay minerals.

By far the majority of "phenocrysts" as described by Brock and Singewald (1968) are in reality

plagioclase aggregates, similar to those described in the San Isabel coarse-grain facies. These aggregates are dominantly monomineralic with only minute amounts of interstitial unstrained quartz and biotite. The aggregate's texture is allotrimorphic-granular with sutures and penetration twins common. Polysynthetic twinning in the aggregates is poorly developed. The zonation of the aggregates appears to cross individual crystal boundaries. Partial replacement features, which were commonplace in the San Isabel's coarse-grain facies, are not observed. Aggregates appear rounded and are part of the weak flow foliation of the granite.

Quartz, which is rather abundant in both facies, is irregularly shaped and interstitial. The smaller crystals are bead or dipyramidal quartz inclusions. Interstitial quartz contains deformation lamellae and glide planes. In cataclastic zones, quartz appears highly sutured, stretched, slivered, and in mosaics.

Biotite is the most abundant dark mineral. It appears as rounded books, well cleaved to irregular with broken crystals and crystal clots. Lens- to disc-shaped clots of biotite, ragged hornblende, apatite, quartz, magnetite, sphene, and zircon are found in both facies. When sphene or zircon is adjacent to biotite, a very pronounced pleochroic halo develops. Biotite itself is strongly pleochroic and

varies in color from a light to dark brown, "r" granite, and light green to dark olive green "d" granite. In the "d" granite facies biotite at times displays undulatory extinction, micro-faults, microfolds, and glide planes.

Magnetite and sphene are the most common accessory minerals in the two facies. Muscovite is much less common and physically resembles the muscovite of the Wixson Divide granites. Other accessory minerals include hornblende, zircon, rutile, and apatite.

Modal and chemical analysis of the Mount Tyndall granites are given in appendix Figures and Tables D.1 through D.5 and are summarized in Table 3. These rocks are modally all granites and chemically have a very narrow range of major cation variation.

Petrography of the Granites of Williams Creek

The microscopic character of the granites of Williams Creek is much like the description given the coarse-grain facies of the San Isabel batholith. Most samples are xenomorphic-granular. Gradational contact zones tend to be more porphyritic. The porphyritic texture is due primarily to a decrease in the size of phenocrysts. Phenocrysts are of two varieties: irregularly shaped microcline crystals and rounded plagioclase aggregates. Foliate texture is more

Table 3. Average Modal in Volume Percent and Major Element Composition in Weight Percent of the Granites of the Mount Tyndall Quadrangle Based on 16 Modal and 5 Chemical Analyses

	Mean	Standard Deviation	Extremes
Kspar	30.52	4.99	37.6-22.6
Plagioclase	31.48	4.41	40.9-23.0
Quartz	26.04	3.68	33.0-20.3
Biotite	7.71	3.95	18.7- 2.5
Magnetite	1.53	0.92	3.2- 0.2
Sphene	0.88	1.41	4.9- 0.0
Accessory Minerals	1.44	1.24	3.6- 0.0
SiO_2	70.21	1.33	72.22-69.00
Al_2O_3	15.47	0.68	16.31-14.63
Fe_2O_3	1.33	0.45	2.03- 0.92
FeO	1.43	0.48	1.89- 0.87
MnO	0.03	0.05	0.11- 0.00
MgO	0.41	0.48	1.12- 0.05
CaO	1.92	0.49	2.56- 1.19
Na_2O	2.84	0.30	3.13- 2.34
K_2O	4.90	0.36	5.39- 4.38
TiO_2	0.59	0.15	0.77- 0.37

dominant near the plutons' borders. The texture is due largely to the alignment of ferromagnesium minerals.

Microcline is found both as interstitial and as phenocrysts. All crystals possess well-formed twins following the albite-pericline twin laws. Carlsbad twins are much less common. Perthite is rare. Some film and stringlet perthites were observed. Inclusions are restricted primarily to the larger grains -- oriented to random plagioclase, bead quartz, biotite, and euhedral magnetite. Microcline tends to develop myrmekite when in contact with plagioclase. Alteration products on microcline are a rarity.

Plagioclase, An_{27} to An_{28}, occurs as anhedral to subhedral rounded phenocrysts and interstitial aggregates. All plagioclase is well twinned and exhibit albite, pericline, carlsbad, and complex carlsbad-albite. Zoning is normal. Some pre-consolidation deformation features such as bent or broken crystals and twin plane displacement are common. Interstitial grains do not exhibit zonation, deformation features or twinning. All plagioclase crystals are relatively clean of inclusions, and the crystals from samples collected east of Williams Creek are among the cleanest and less altered in the range.

West of Williams Creek plagioclase is highly altered and, in the plutons of Deer Peak and Rosita quadrangle, is composed of 90 to 100 percent white mica, epidote, and clay minerals.

Quartz is like that of any other pluton in the Wet Mountains. They are small and strongly deformed and recrystallized. Biotite and hornblende of these plutons resemble exactly the petrographic description of the same minerals in the coarse-grain facies of the San Isabel batholith, as do the accessory minerals. In fact, if it were not for the abundance of the ferromagnesium minerals and their generally smaller grain size, rocks of these plutons could very easily be mistaken for those of the San Isabel coarse-grain facies.

Twenty-two modes and seven chemical analyses (appendix Figures and Tables E.1 through E.5) are summarized in Table 4. Modally there is a considerable spread of major minerals as seen on appendix Figure E.3. Part of the spread is due to the compositional differences between the individual plutons. However, the major cause of the spread is due to the type of granite collected. Data points of the granite field represent the bulk composition of the plutons. The four quartz-poor plots, which include

Table 4. Average Modal in Volume Percent and Major Element Composition in Weight Percent of the Granites of Williams Creek Based on 22 Modal and 7 Chemical Analyses

	Mean	Standard Deviation	Extremes
Kspar	27.97	6.70	41.2-14.6
Plagioclase	34.13	5.24	47.5-26.3
Quartz	21.55	8.51	38.1- 4.0
Biotite	10.09	4.98	19.1- 2.6
Hornblende	2.01	4.58	7.5- 0.0
Magnetite	1.70	0.99	3.7- 0.1
Sphene	0.96	1.74	2.8- 0.0
Accessory Minerals	1.49	2.02	8.1- 0.0
SiO_2	65.05	5.80	73.94-55.14
Al_2O_3	16.45	1.85	19.67-13.85
Fe_2O_3	0.85	0.56	2.03- 6.40
FeO	2.53	1.48	4.60- 0.29
MnO	0.10	0.08	0.19- 0.00
MgO	1.13	1.08	2.91- 0.00
CaO	2.62	0.91	4.48- 1.87
Na_2O	3.29	0.46	3.71- 2.36
K_2O	4.58	0.72	5.28- 3.57
TiO_2	0.84	0.32	1.28- 0.35

the major portion of the modal spread, represent a biotite-rich zone generally found at the base of some plutons. These zones may represent local concentrations of partially digested xenoliths. Chemical data also support the idea of magmatic contamination within these plutons.

Petrography of the Granites of Bear Creek

The granites of the Bear Creek plutons are xenomorphic-granular. Biotite crystals that have developed a weak alignment along the plutons' margin display a subdued foliate texture. Specimens collected from the gradational granite-granite contact show a much less intense foliate texture. This is especially true nearest the Williams Creek end of the gradational zone. The granite becomes more massive, thus losing its foliate texture as well as its micaceous mineral content, as the Bear Creek end of the gradational zone is approached.

Microcline crystals are equigranular and anhedral with no obvious rounding. No phenocrysts are present. Almost all crystals exhibit well developed albite-pericline grid twins. No other twin types were observed. Perthite is rare, and zoning is not observed. Myrmekite, as large well developed "warts," occasionally developed along the microcline-plagioclase

boundary. Inclusions are infrequent, and microcline remains unaltered in all specimens.

Larger plagioclase crystals, An_{20} to An_{25}, have developed strong sets of albite twins. However, as the grain size diminishes, so does twin clarity, and many of the smaller crystals are relatively untwinned. Zoning is not present except for a small number of albite rims. Crystals tend to be inclusion free, and alterations are light to moderate.

Quartz appears as unstrained bead and graphic quartz, as anhedral intergranular quartz, which has developed weak to moderately strong glide planes and as larger crystals lightly sprinkled with rutile, apatite and "bubble trains." Some irregular penetrations and replacements of microcline and plagioclase are noted.

Biotite is observed as individual crystals, normally well-developed broken to bent books. Mafic clots are rare. All biotite-rich clots are found near the gradational contact zones. Fresh biotite displays a range of pleochroic colors from dark to light brown. Inclusions are quite common and tend to be primarily metallic oxide (probably magnetite), zircon with pleochroic halos, sphene, and quartz. Small amounts of albite and garnet are observed.

Of the accessory minerals, sphene and magnetite are most common. Sphene is anhedral -- rounded to

broken. Magnetite is anhedral and also normally rounded. Other accessory minerals and alteration products include: zircon, rutile, apatite, garnet, clay minerals, white mica, muscovite, epidote, hematite, leucoxene, and pyrolucite.

Modal and chemical data for the Bear Creek plutons (appendix Figures and Tables F.1 through F.5) are summarized in Table 5. The 15 modal analyses plot in the granite field of appendix Figure F.3. The plots show a relatively constant K-spar/quartz ratio with a varying plagioclase content. The trend established, herein, has modal points of the Bear Creek plutons plotting in the same area as those of the Williams Creek granites. In fact, most of the Bear Creek data points that plot in this area come from specimens collected from the gradational granite-granite contact. The pluton's rock specimens become modally more sialic as the gradational zone is departed. The skewing of the Bear Creek data points away from the Williams Creek field and is evidence of either extreme differentiation of some original magma or differential melting of possible different source rocks. In any case, their origin seems to be genetically related.

Petrography of the Granites of Cliff Creek

The texture for the Cliff Creek granites is

Table 5. Average Modal in Volume Percent and Major Element Composition in Weight Percent of the Granites of Bear Creek Based on 15 Modal and 5 Chemical Analyses

	Mean	Standard Deviation	Extremes
Kspar	37.23	5.20	43.8-29.1
Plagioclase	26.66	7.14	39.7- 9.5
Quartz	29.61	6.11	41.3-19.9
Biotite	4.34	3.80	12.0- 0.2
Magnetite	0.65	0.51	1.5- 0.0
Sphene	0.24	0.53	1.6- 0.0
Accessory Minerals	1.13	1.24	3.7- 0.0
SiO_2	74.90	1.32	76.49-73.22
Al_2O_3	13.65	0.84	14.75-12.81
Fe_2O_3	0.78	0.26	1.21- 0.53
FeO	0.64	0.33	1.20- 0.36
MnO	0.00	0.00	0.01- 0.00
MgO	0.10	0.16	0.38- 0.00
CaO	0.80	0.33	1.24- 0.33
Na_2O	2.55	0.15	2.65- 2.30
K_2O	5.34	0.23	5.67- 5.07
TiO_2	0.32	0.13	0.49- 0.21

xenomorphic-granular. Some samples transmit a vague ghost-like foliate texture in and near the gradational contacts with the San Isabel granite.

Microcline is anhedral and has developed well-formed grid twins on almost every crystal. Microcline contains little to no perthite, zonations, inclusions, or extensive myrmekite development. Myrmekite is much more common. Alteration products were not observed.

Quartz is the second most abundant mineral in the plutons. All crystals are anhedral and exhibit some degree of undulatory extinction. Glide planes are common. In some specimens quartz appears to have replaced parts of both plagioclase and microcline crystals. Inclusions are common, and are dominantly accicular rutile, euhedral apatite, ragged mica, rounded "islands" of microcline, and "bubble trains." Many "bubble trains" are abnormally large and contain liquid and solid inclusions. The solid inclusions appear to be isometric crystals and have the shape of perfect cubes (possibly halite). Because of the development of octahedral faces on one crystal some of the mineral inclusions may quite possibly be sylvite.

Plagioclase seems to be bimodal in its composition. It tends to be An_{20} to An_{24} in some

plutons and An_{10} to An_{15} in other plutons. Plagioclase is normally anhedral and albite twin planes are poorly developed. No carlsbad or pericline twins were observed. Zonation is only observed as albite rims. Alteration products as well as inclusions are uncommon.

Biotite, as single isolated crystals, is rare. It appears as broken, splintered, and irregular books of dark to medium brown pleochroic minerals. Among the alteration products are magnetite, muscovite, hematite, and leucoxene. Other accessory minerals are magnetite, rutile, and apatite.

Eight modal and two chemical analyses (appendix Figures G.1 and G.2 and appendix Table G.3) of the Cliff Creek granite specimens are summarized in Table 6. Appendix Figure G.3 demonstrates a considerable spread of major mineral components in what seems to be fairly homogeneous rock units. In fact, two samples, which were collected within the same pluton specimens 299 and 302), do plot relatively close to one another. Thus, individual plutons are probably, as they appear in the field, homogeneous, while the heterogeneity of the plots is due to the slight differences in chemical and mineral composition that exist between plutons. No geographic relationship seems to exist between plot locations and the field

Table 6. Average Modal in Volume Percent and Major Element Compositions in Weight Percent of the Granites of Cliff Creek Based on 8 Modal and 2 Chemical Analyses

	Mean	Standard Deviation	Extremes
Kspar	45.39	7.72	58.9-34.7
Plagioclase	17.51	7.83	23.5- 6.1
Quartz	34.44	7.61	47.2-23.0
Biotite	2.00	1.50	4.9- 0.6
Magnetite	0.90	0.81	2.2- 0.2
Sphene	0.10	0.18	0.5- 0.0
Accessory Minerals	0.59	1.51	4.3- 0.0
SiO_2	77.10	0.37	77.36-76.84
Al_2O_3	13.10	0.18	13.23-12.97
Fe_2O_3	0.19	0.01	0.20- 0.18
FeO	0.04	0.02	0.06- 0.02
MnO	0.00	0.00	0.00- 0.00
MgO	0.00	0.00	0.00- 0.00
CaO	0.76	0.29	0.96- 0.55
Na_2O	2.06	0.37	2.32- 1.79
K_2O	5.68	0.11	5.76- 5.60
TiO_2	0.20	0.12	0.28- 0.11

collection localities. The only relationship noted is that those specimens collected near or within the gradational contact zones are modally more San Isabel in character.

PETROGENESIS OF THE SILVER PLUME PLUTONS

The Silver Plume-age plutons of the Wet Mountains are a product of an intruding crystallizing melt. The magma's emplacement was by both the "shouldering" aside of the metasedimentary wall rock and by the stoping of the roof. The plutons appear to be mesozone to catazone in their level of emplacement by criteria established by Buddington (1959). The plutons that fit the mesozone criteria are those of the southern Wet Mountains. The Mount Tyndall and, in part, the Wixson Divide plutons of the central Wet Mountains seem to have a deeper emplacement character.

The origin of the different mineral species can be divided into three distinct periods of formation: pre- and syn-intrusive, post-intrusive, and post consolidation. The relationship to local flow foliations provides textural evidence in support of the time of mineral formation. Plagioclase, biotite, hornblende, sphene, and some accessory minerals crystallized or were in existence prior to or during

the granitic intrusion. They are aligned in a direction of least stress to flow and are a major part of the rock's foliate texture. Some crystals exhibit physical abrasion in the form of rounding. Microcline and quartz, on the other hand, are oriented discordantly to the granites' flow foliations and were formed at a time when the internal flow stresses ceased. This is consistent with a post-intrusive origin. A period of recrystallization would have ostensively occurred after the magma was completely crystallized (post-consolidation) and should have produced minerals that cross pre-existing mineral alignment. In the San Isabel batholith and in a few other smaller plutons microcline megacrysts not only cross these lines but also have caused recrystallization and deformation of adjacent mineral species. In fact, the megacrysts at times have promoted the development of secondary foliations in the groundmass.

In the Bear Creek and Cliff Creek granites the crystal size and shape, as well as the massive character of the plutons' interior, suggest that the three major mineral phases (microcline, plagioclase, and quartz) continued to crystallize until the entire magma was exhausted. The lack of foliation in these plutons also suggests that the minerals crystallized

in an environment of little or no flow stress.

Chemical data are in complete agreement with these petrographic observations. The order of crystallization of the major mineral phases for the Silver Plume-age plutons can be considered initially in terms of the An-Ab-Or-SiO_2-H_2O system (Winkler, 1976).

Selected normative data (Figure 13) taken from the plutons plot along the cotectic minimum between the plagioclase-alkali feldspar fields. The points that plot away from the cotectic minimum probably represent local contamination, which is common in these plutons. Figure 14 represents a plot of normative values from some representative specimens of the various Silver Plume magmas on Carmichael's (1963) An-Ab-Or-SiO_2-H_2O tetrahedron. The probable crystallization path is in the central portion of the tetrahedra. In the San Isabel, Wixson Divide, Mount Tyndall, and Williams Creek magmas plagioclase was the first crystal phase to form. As plagioclase continued to crystallize, the composition of the magma was driven toward the microcline field. Once the liquid composition reached the microcline field, both feldspars crystallized together. The liquid became more quartz-rich as the feldspar continued to

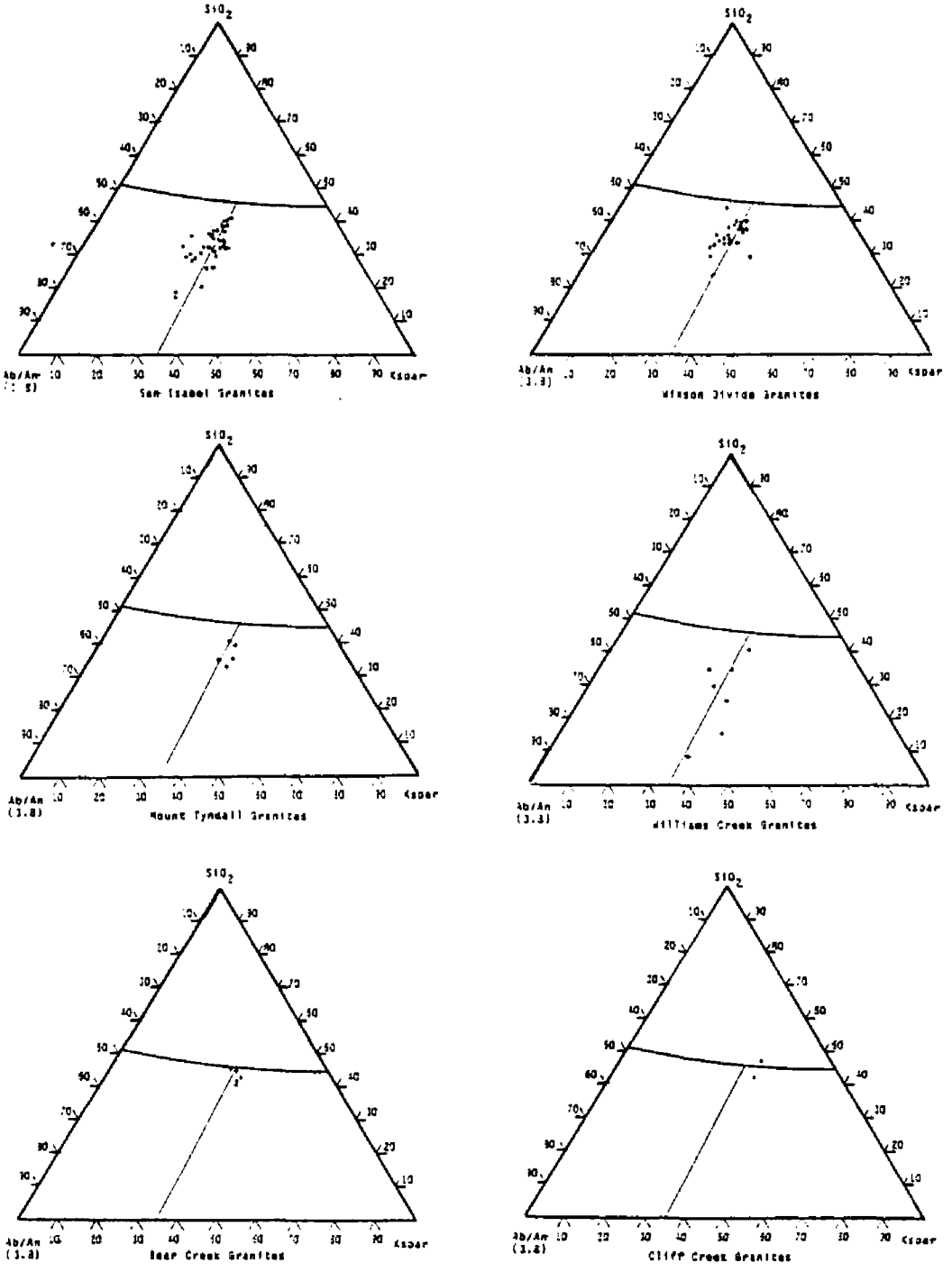

Figure 13. Normative plots from the various Silver Plume plutons, Wet Mountains, Colorado plotted on Ab-An-Or-SiO_2-H_2O diagram (von Platen, 1965 and Winkler, 1976).

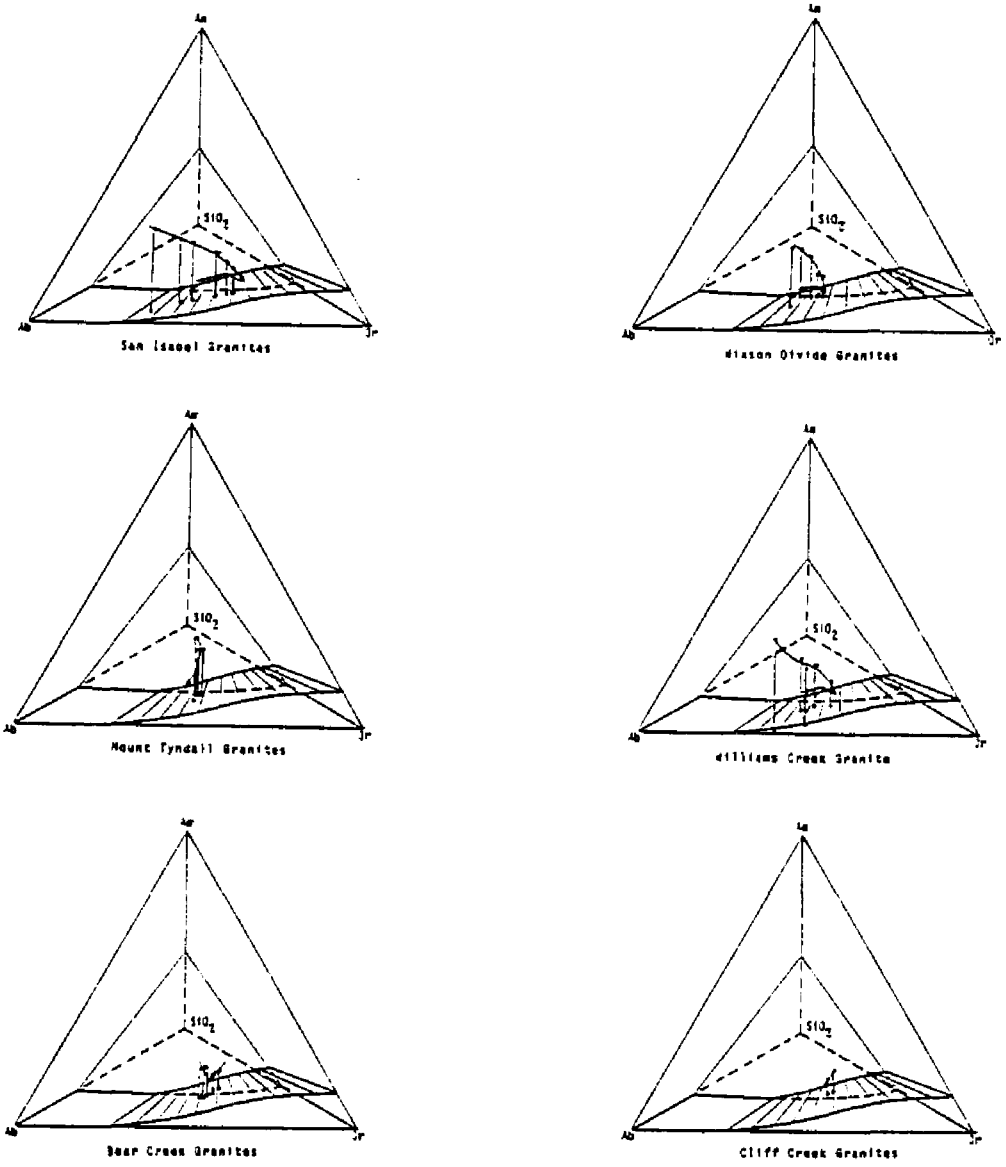

Figure 14. The probable crystallization path for the Silver Plume plutons of the Wet Mountains, Colorado, based on plots of compositions chosen as representative of the range of specimens reported in this study. The predicted phase relations in the system An-Ab-Or-SiO_2-H_2O are those of Carmichael, (1963)

crystallize until the cotectic was reached. At that point all three mineral phases crystallized until the liquid was exhausted. This order of crystallization is consistent with petrologic observations.

Chemical data for the Bear Creek and Cliff Creek granites are also in complete agreement with the petrographic observations in that the major mineral phases of the two plutons began to crystallize at approximately the same time. Figure 14 depicts a short and narrow range for the mineral crystallization paths. Plagioclase crystallized prior to quartz, and once the liquid reached the quartz compositional field, it continued only a short distance into the cotectic trough, where all three mineral phases crystallized until the liquid was exhausted.

Evidence of post-magmatic recrystallization in the various granitic plutons is seen in the development of recrystallized albite rims on the boundary of many plagioclase crystals. Myrmekite occurs on plagioclase-microcline boundaries and along microcline-microcline boundaries. Quartz occurs in the myrmekite and as a recrystallized mosaic. The quartz mosaic is most common in the fine-grain facies.

Pressure and Temperature Conditions of Crystallization

Criteria used by Murray (1970) to establish the

depth of emplacement for the San Isabel batholith are taken from Buddington (1959) and can be used for the other plutons of the southern Wet Mountains. Their level of emplacement, mesozone, represents a depth of approximately 12 kilometers and a confining pressure of 3.2 kilobars. The Wixson Divide plutons seem to be at a transitional level between mesozone and catazone. Mineralogically, the appearance of small amounts of primary muscovite (appendix Table C.2) is consistent with a slightly greater depth. The probable depth is no more than 12 to 14 kilometers with a confining pressure of 3.2 to 3.8 kilobars. Mount Tyndall plutons, which contain much more primary muscovite (Appendix Table D.2), can be characterized as being even deeper in its depth of intrusion. The plutons seem to be transitional between catazone and mesozone emplacement. This represents a depth between 23 and 17 kilometers with a load pressure of 3.6 to 4.8 kilobars (Buddington, 1959).

The appearance of primary muscovite suggests a probable deeper zone of emplacement for the rocks of the two northern most granites. Winkler and von Platen (1958) and Winkler (1976) suggest that in the presence of quartz or free silica, muscovite will convert to sillimanite before the beginning of melting, and that

muscovite can only be crystallized in a magma where water pressure is greater than 2000 bars during the time of crystallization. The minimum stability range according to Fyfe (1970) is between 3500 and 5000 bars at a temperature of 650° to 675°C. These pressures correspond closely to the pressures anticipated by Buddington's (1959) criteria for the catazone to mesozone level of emplacement.

The temperature of the various plutons at the time of their intrusion was determined to be between 650° to 750°C. The difference in mineralogy and chemistry of the biotite-rich granites (i.e., San Isabel, Wixson Divide, Mount Tyndall, and Williams Creek granites) and the leucocratic granites (i.e., Bear Creek and Cliff Creek granites) suggest a higher intrusive temperature for the biotite-rich granites. The average modal composition of the two granitic rock types (Winkler, 1976) suggests that the leucocratic granites, which are near Or = 34 percent, Ab = 23 percent, Q = 41 percent, and An = 2 percent, crystallized at or near the eutectic at approximately 685°C and 2000 bars. Modal data also suggest that the biotite-rich granites of Or = 26 percent, Ab = 28 percent, Q = 18 percent, and An = 28 percent are non-eutectic. Normative plots of the two rock types'

data points indicate the same general relationship. Kleeman's (1965) equilibrium diagram (Figure 15), which depicts the silica saturated surface of the Or-Ab-An-SiO_2 system at 5000 bars projected onto the Or-Ab-An face of the tetrahedron, shows essentially the same results. Biotite-rich granites plot between 700° to 750°C, while the leucocratic granites again set in the cotectic trough near the eutectic and at a temperature of 650° to 700°C. These observations are also supported by Murray (1970) who determined the intrusive temperature of the San Isabel batholith to be 725°C. Experimental work done by Piwinskii and Wyllie (1968) shows that mafic clots, which are quite common in many biotite-rich granites, are in equilibrium with a granite magma at temperatures between 740° and 850°C at 2000 bars, which is consistent with temperatures already proposed.

Chemical Nature of the Plutons

Chemical anlaysis and CIPW norms of 82 specimens from six Silver Plume-age plutons of the southern and central regions of the Wet Mountains, Colorado are reported in the appendices. Variation diagrams are employed to illustrate the relative similarities and differences of chemical trends of the six plutons. In many cases the plotted trends are so well defined

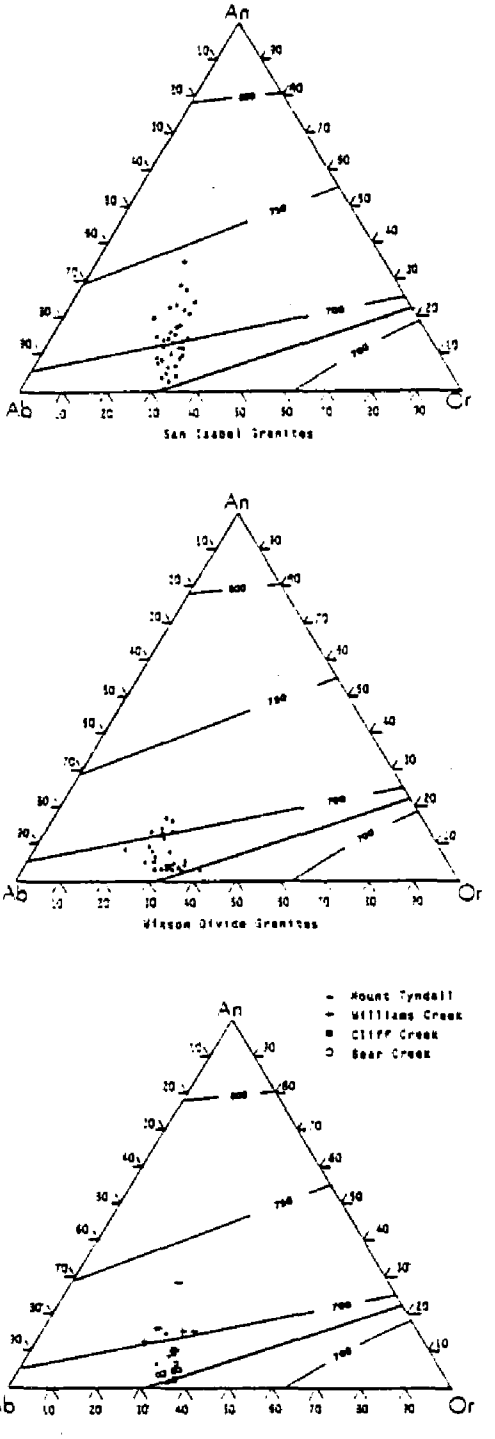

Figure 15. The SiO_2-saturated surface of the Or-Ab-An-SiO_2 system at 5000 bars P_{H_2O} projected onto the Or-Ab-An face of the tetrahedron (Kleeman, 1965)

that lines approximating least-square fits can be plotted by eye with a fair degree of confidence. In fact if the various pluton's silica variation diagrams (appendix) were presented as one diagram, a single trend would be produced. This suggests that these plutons have chemical trends distinctly similar, just as any other set of plutons would be if they were also related both spatially and temporally.

Peacock (1931) used a silica variation diagram (Figure 16) to classify various igneous rock suites. He notes that the point of intersection of the total alkali ($K_2O + Na_2O$) and lime (CaO) curves (Peacock index) was characteristic of igneous rock suites and can be used to distinguish one suite from another. The Peacock index for the granites of the central and southern Wet Mountains is 57.6% silica (power least-square trend line analysis used) and represents a rock suite that is calc-alkaline in character.

Trigonal plots showing the relationship between total iron oxides, total alkali, and magnesium oxide (AMF diagram); and potassium oxides, calcium oxide, and sodium oxide (KCN diagram) have been constructed and both show calc-alkaline trends (Figure 17 and 18). Figure 17 displays a relative concave trend in which there seem to be a slight total iron enrichment as

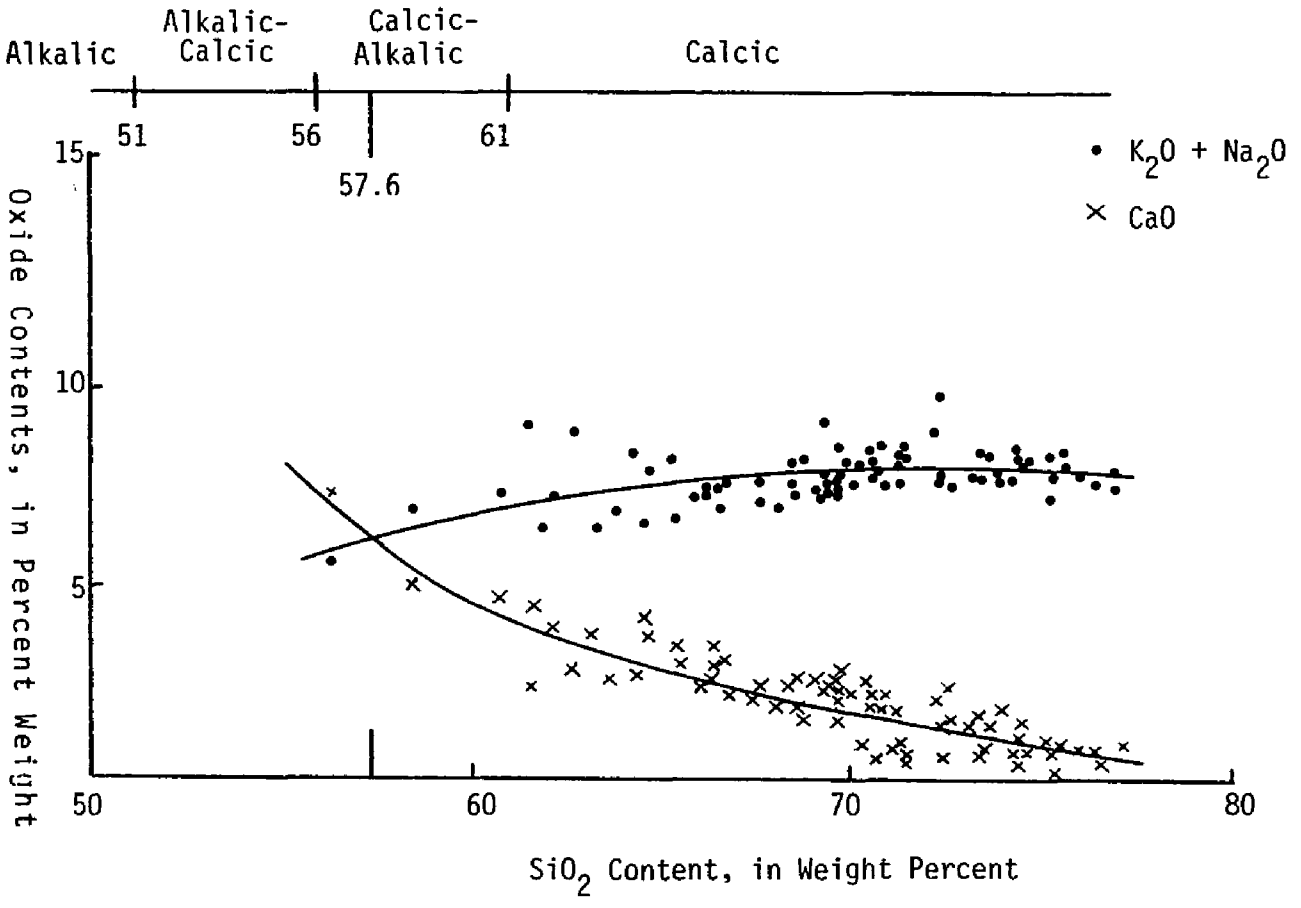

Figure 16. The Peacock Index of the Intrusive Silver Plume-Age Granitic Rocks of the Wet Mountains of Colorado

• San Isabel batholith

+ Wixson Divide pluton

× Granites of Mount Tyndall

• Granites of Williams Creek

■ Granite of Bear Creek

△ Granite of Cliff Creek

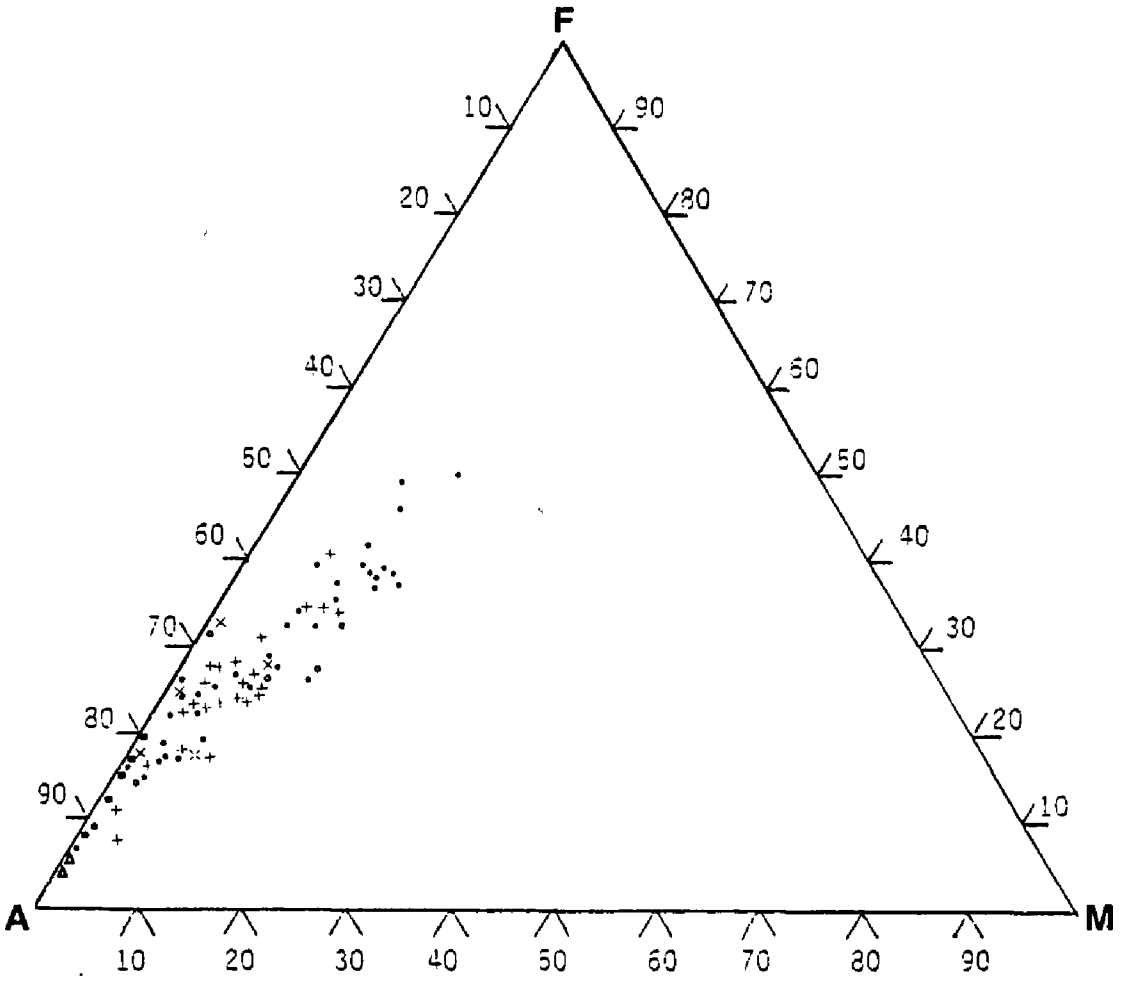

Figure 17. AMF diagram is a plot of the Silver Plume-age rocks of the southern and central sections of the Wet Mountains, Colorado. The diagram shows a strong calc-alkaline trend. The AMF diagram is a plot of A = K_2O + Na_2O, M = MgO, and F = Fe_2O_3 + FeO percentages

• San Isabel batholith

+ Wixson Divide pluton

× Granites of Mount Tyndall

∘ Granites of Williams Creek

■ Granite of Bear Creek

△ Granite of Cliff Creek

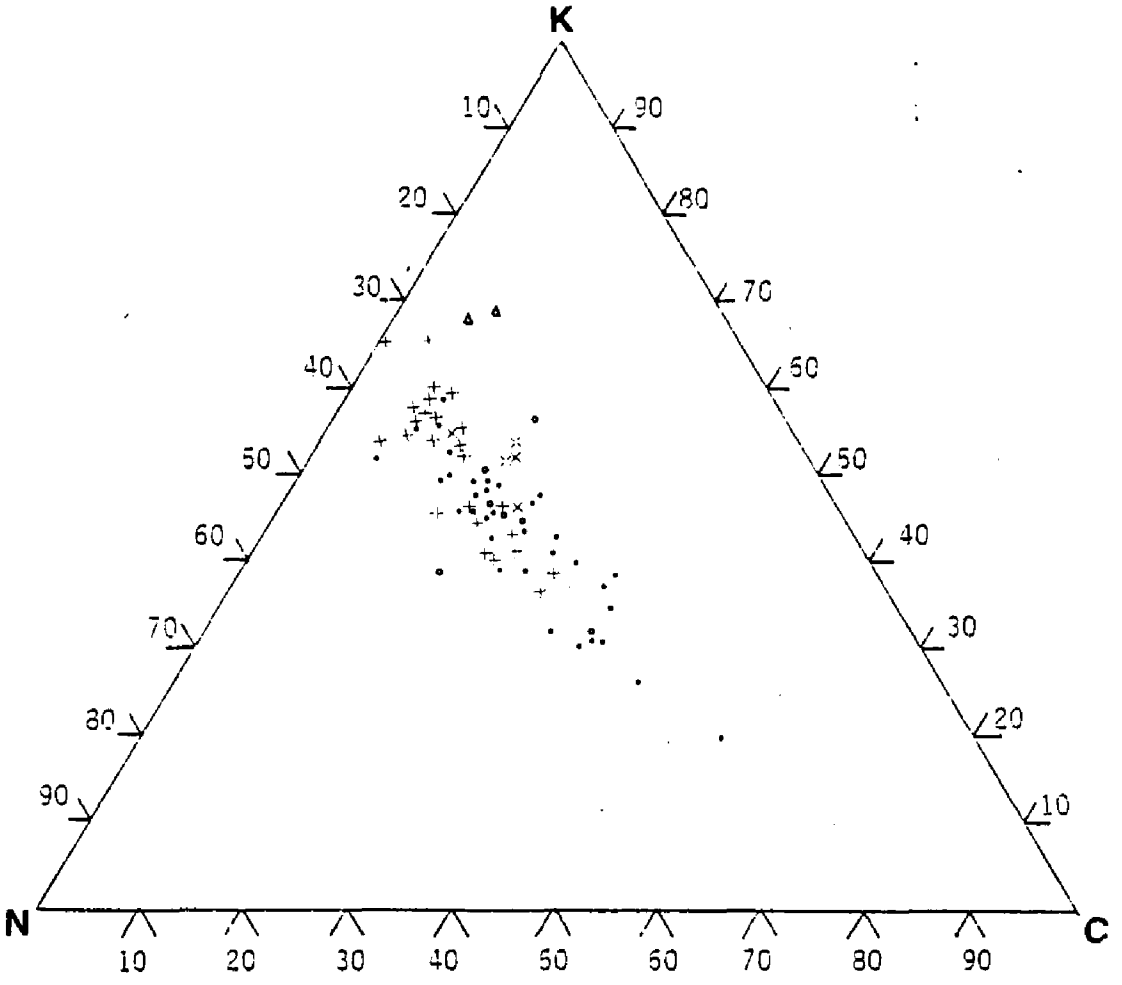

Figure 18. KCN diagram is a plot of the Silver Plume-age rocks of the southern and central sections of the Wet Mountians, Colorado. The diagram is a plot of K = K_2O, N = Na_2O, and C = CaO percentages.

total alkali decrease. The calc-alkaline trend for the Silver Plume-age granites is similar to that of the southern Sierra Nevada batholith and the Southern California batholith (Larsen, 1948), but with a very slight alkali tendency. The minor deviations and anomalous data points seen on these two figures are probably representations of local variations in magma content.

The An-Ab-Or diagram (Figure 19), which displays the average normative values of the six Silver Plume plutons, shows a basic difference between the biotite-rich and leucocratic granites. The normative data from the San Isabel batholith, Wixson Divide pluton, granites of Mount Tyndall quadrangle, and the granites of Williams Creek plot on the diagram away from the cotectic. Thier data points and, hence, their plutonic rock trends, compositionally are aligned almost perpendicular to the thermal trough near the diagram's eutectic. These rocks show varying degrees of differentiation and/or contamination during their time of creation, evolution, and emplacement (Kleeman, 1965). For the leucocratic granites the normative compositions (granites of Cliff Creek and Bear Creek) are entirely within the cotectic near the diagram's eutectic. Little evolution of these rocks seem to

• San Isabel batholith

+ Wixson Divide pluton

× Granites of Mount Tyndall

○ Granites of Williams Creek

■ Granite of Bear Creek

△ Granite of Cliff Creek

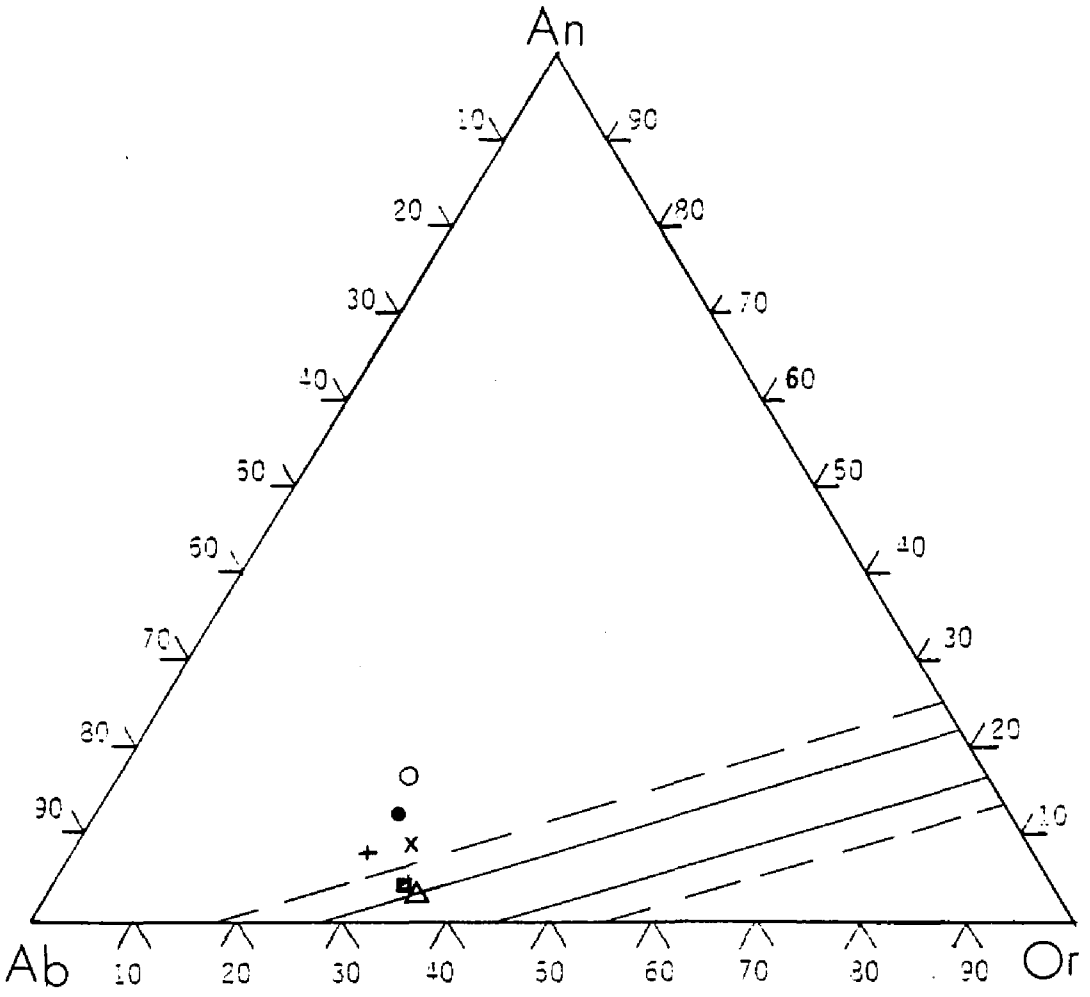

Figure 19. The average normative values for the Silver Plume-age granites of the southern and central portion of the Wet Mountains, Colorado is plotted on the SiO_2-saturated surface of the Or-Ab-An-SiO_2 system at 5000 bars P_{H_2O} projected on to the Or-Ab-An face of the tetrahedron (Kleeman, 1965). Solid lines represent the low temperature trough, while the dashed lines show the uncertainty due to possible analytical error.

have occurred, since none of their plots tend normal to or parallel to the cotectic trough (Kleeman, 1965). This suggests a relatively close relationship in terms of origin and evolution of the two leucocratic granites and a similarly close relationship for the four biotite-rich granites.

GENESIS OF THE SILVER PLUME-AGE GRANITIC MAGMA

The origin of granitic magmas traditionally follows one of two models. The first model originally proposed by Bowen (1928) and later refined by Kleeman (1965), Hamilton and Myers (1967), Hamilton (1969), Gilluly (1969), and Dickinson (1970) calls for the production of a residual liquid of granitic composition from a fractionating basaltic magma which may or may not have assimilated silceous rock. The second model involves the partial or complete melting of metasedimentary rock (Eskola, 1932; Tuttle and Bowen, 1958; Kleeman, 1965; Hyndman, 1969; and Bateman and Dodge, 1970).

Recent classification of granite magma types was presented by Chappell and White (1974). They established two genetic models for the production of granitic magmas: the I-type (a granitic magma produced from an igneous source) and the S-type (a granitic magma generated by the partial or complete melting from a sedimentary source). Direct

applications of the new granite classification on specific magmatic provinces and the relationship of the newly classified granites to various tectonic environments have been made by White, *et. al.* (1974) and White and Chappell (1977), and are summarized in Pitcher (1978) and Hyndman, *et. al.* (1980).

Two basic plate tectonic settings are commonly cited to explain the genesis of the two varieties of granitic magmas. The settings reflect a general relationship between magmatism and tectonism. The Andinotype orogenic model (Zwart, 1967) involves the partial melting of oceanic crust and/or upper mantle during the subduction of an oceanic plate under a continental margin (e.g., Hamilton and Myers, 1967 and Pitcher, 1978). The Hercynotype orogenic setting (Zwart, 1967) involves the partial melting of metasedimentary rock during a continent-marginal arc or continent-continent plate collision (e.g., Bateman and Eaton, 1967 and Beckinsale, 1979). The characteristics of these two very dissimilar magma-tectonic models as presented by Zwart (1967) and later modified by Pitcher (1978) are given in Table 7, columns 1 and 2.

During the Huntington Lake Granite Conference of 1978 (Peck and Wones, 1980), a third model for the

Table 7. Contrasting characteristics of the Hercynotype; Andinotype orogens and anorogenic environments; S-type; I-type; A-type granites; and their relationships to their Silver Plume Thermal Event and granites.

Andinotype	Hercynotype	Anorogenic-type	Characteristics of the Silver Plume-age plutons of the Front Range, Co.
1. Inland arc-volcanic and and associated with volcaniclastic sediment	1. Non-volcanic associated with continentally-derived sediment	1. Associated with peralkaline volcanic and volcaniclastic rocks	1. Plutons not associated with volcanic environment
2. Gabbro/tonalite/granite proportions 15:50:15	2. Gabbro/tonalite/granite proportions 2:10:80	2. Gabbro/syenite/tonalite/granite proportions 10/70/10/60	2. Gabbro/syenite/tonalite/granite proportions 0:0:5:95
3. Associated with burial metamorphism	3. Associated with regional metamorphism	3. Not associated with regional metamorphism; post-dates metamorphic event	3. Post dates regional metamorphic event
4. Disharmonious cauldron batholiths	4. Harmonious diapir batholith	4. Disharmonious cauldron batholiths and stocks and ring dikes	4. Harmonious and disharmonious intrusives. Major intrusives are diapirs.
5. Vertical movements with minimum crustal shortening	5. Tectonic shortening	5. Vertical movements and major faulting; generally rifting	5. Minimum crustal shortening associated with the Ilse Fault
6. Epizonal plutons	6. Mesozonal and catazonal plutons	6. Epizonal plutons	6. Mesozonal to catazonal plutons
7. Not associated with migmatites	7. Associated with migmatites	7. Not associated with the development of migmatites	7. Associated with some migmatites
8. I-type granites	8. S-type granites	8. A-type granites	8. S- and I-type granites
a. Calc-alkaline b. Quartz normative c. $^{87}Sr/^{86}Sr < 0.708$ d. Broad compositional range basic to acidic; rock primarily acidic e. Relatively high sodium content (>3.2% Na_2O) f. Peralkaline - no normative corundum g. Magnetite; a result of high oxygen fugacity h. Hornblende; sphene i. Rarely associated with regional metamorphism and migmatites	a. Calc-alkaline b. Quartz normative c. $^{87}Sr/^{86}Sr > 0.708$ d. Restricted compositional range; rocks mainly acidic e. Relatively low sodium content (<3.2% Na_2O) f. Peraluminous - normative corundum g. Ilmenite; a result of low oxygen fugacity h. Muscovite, garnet; cordierite, sillimanite, two mica granites i. May be associated with regional metamorphism and extensive migmatites	a. Alkalic b. Many analysis contain no normative quartz c. $^{87}Sr/^{86}Sr$ ranges widely but generally < 0.706 d. Broad compositional range from basic to acidic, mainly acidic, some silica-poor acidic e. Relatively high sodium content (>3.2% Na_2O) f. Peralkaline with some peraluminous rocks g. Both magnetite and ilmenite present h. Hornblende, sphene, riebeckite, fayalite, aegerine, arfvedsonite i. Not associated with regional metamorphism	a. Calc-Alkaline b. Quartz normative c. $^{87}Sr/^{86}Sr > 0.7014$ (Hedge, 1980) d. Restricted compositional range; rocks mainly acidic e. 45 analyses with Na_2O<3.2% 19 analyses with Na_2O>3.2% f. All rocks analyzed have normative corundum g. Metal iron oxides contain Ti h. Hornblende, biotite, sphene, muscovite i. Post-dates regional metamorphic event by 300 million years, but is associated with local development of migmatites

origin of granites (the Anorogenic-type) was suggested. The characteristics of this model were not discussed in any detail. In general, the magma produced by this type of event is characteristically peralkaline, and the tectonic environment in non-orogenic. The anorogenic continental peralkaline event is considered to be a result of either crustal swelling, rifting (Sorensen, 1974) or the effect of hot spot activity (Bowden, 1974). The descriptions and average values for some typical peralkaline granitic rocks and their plutons are given in column 3 of Table 7. These descriptions and values are taken from a variety of continental peralkaline terrains: the Younger Granite complex of Nigeria and Niger (Greenwood, 1951; Jacobson, *et. al.*, 1958; and Turner, 1963), the White Mountain Series of New England (Chapman and Williams, 1935; Turner and Verhoogen, 1960; and Ballard and Uchupi, 1975), the peralkaline granites of Newfoundland (Taylor, *et. al.*, 1980), the Tertiary granites of Skye, Scotland (Turner and Verhoogen, 1960; Thompson, 1969; and Dickin, 1981), the peralkaline granites of Georgia (Butler and Ragland, 1969; Waskom and Butler, 1971; and Fullagar and Butler, 1976), and the peralkaline rocks of the Sudan and Saudia Arabia (Neary, *et. al.*, 1976 and

Nasseef and Gass, 1977).

The granitic rocks that characterize the two orogenic and anorogenic models are markedly different in their various mineralogical, structural, and geochemical parameters (Chappell and White, 1974; Peck and Wones, 1980). This is due to the differences in the development and evolution of the three types of granitic magmas (Kleeman, 1965). The Hercynotype orogens are characterized as developing granitic magmas of an S-type while the Andenotype orogen develops granitic magmas of an I-type. The anorogenic-type environment develops an "A-type" granite. The general characteristics of the three types of granitic magmas are given in Table 7 and are easily compared to the structural, mineralogical, and geochemical data compiled from the Silver Plume-age plutons of the central and southern Wet Mountains (column 4, Table 7).

As seen in Table 7, the physical appearance of the Wet Mountains plutons seems to associate themselves with the characteristics of the Hercynotype orogenic event in seven of the eight plutonic characteristics favoring this type of orogen. The rock-type classification (I-type, S-type, or A-type) is not so clear. Six of the nine characteristics

favor the S-type granite, while four of the nine characteristics favor an I-type granite with some of these characteristics common to both magma types. As for the A-type granite and anorogenic environment, only three of the total seventeen characteristics listed in Table 7 are clearly related to the Silver Plume-age granites and plutons. The interpretation that can be made from these observations is that a Hercynotype orogenic event is a probable setting for the development and evolution of the Silver Plume-age granites of the Wet Mountains. However, it is not clear from Table 7 which type of granite (I- or S-type) developed as a result of this hypothetical Hercynotype event. Presumably, it should be the S-type granite.

Because the three contrasting types of granitic magmas are produced by very different tectonic processes, the development and differentiation of the magma should leave a profound imprint in the rock's geochemistry. Using the Or-Ab-An face of the $Or-Ab-An-SiO_2$ tetrahedron, it is possible to trace the differentiation of the two different orogenic (Kleeman, 1965) and the anorogenic granitic magma types. The normative values obtained from granitic rocks which developed via each of the three granitic magma types are given in Figure 20. Normative data for the various

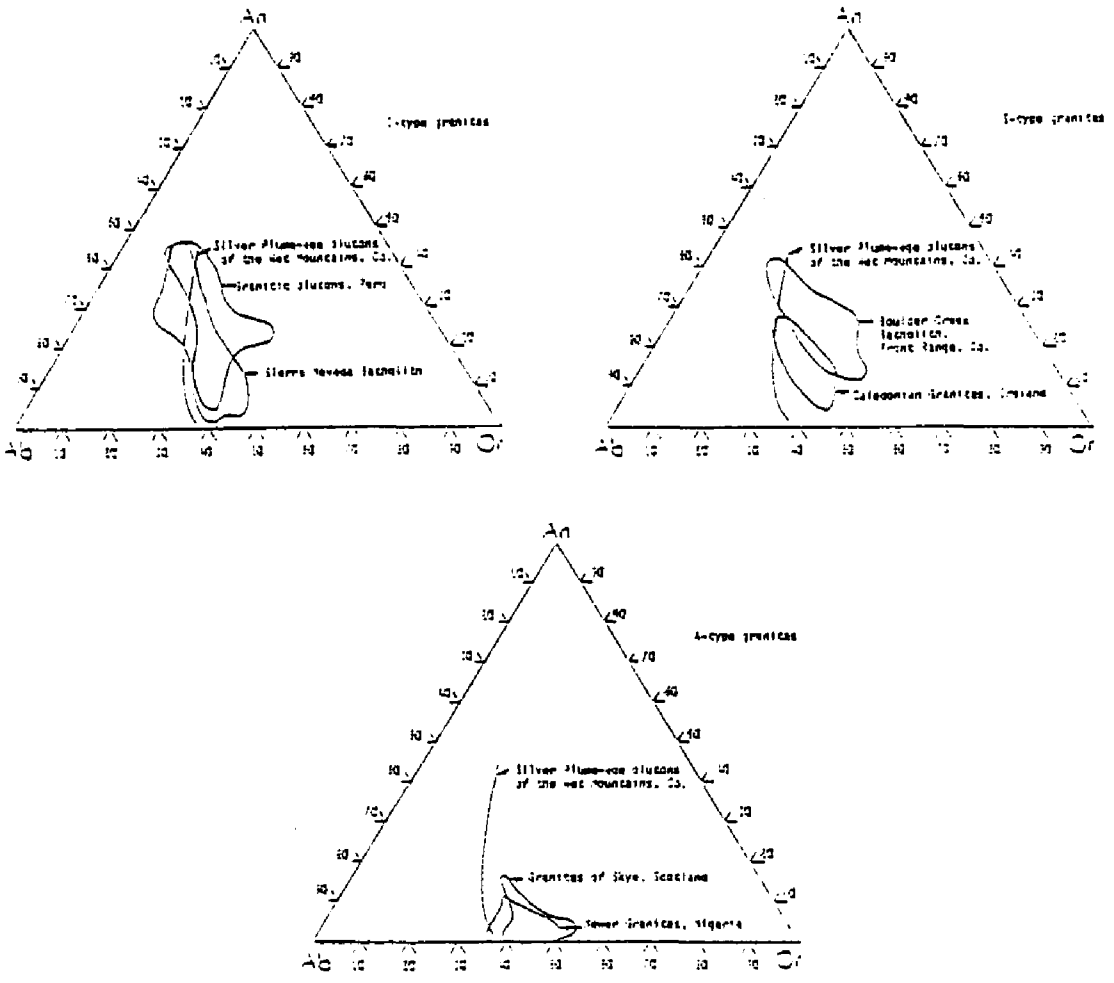

Figure 20. Generalized plots of various plutonic and volcanic rock suites plotted on the SiO_2-saturated surface of the Or-Ab-An-SiO_2 system at 5000 bars P_{H_2O} projected onto the Or-Ab-An face of the tetrahedron (Kleeman, 1965).

igneous provinces are depicted as inscribed circles, while the normative data from the Wet Mountains' Silver Plume-age granites is depicted as a single line. The I-type granitic norms are obtained from chemical analyses of the Sierra Nevada batholith (Ross, 1972) and Peruvian Coastal batholiths (Atherton and Tarney, 1979). S-type granitic norms are obtained from the Caledonian granites of Ireland (Pitcher and Berger, 1972) and the Precambrian Boulder Creek batholiths of Colorado (Gable, 1980). Figure 20 also includes norms calculated from the published chemistry obtained from the Younger granites of northern Nigeria (Jacobson, *et. al.*, 1958) and the granites of Skye, Scotland (Thompson, 1969).

A remarkable variation in the size, shape, and location of the various inscribed circles is easily noted in Figure 20, and was predicted by Kleeman (1965). The figure shows the relationship of the Silver Plume-age granites to the three varieties of granite evolution. The short and restrictive nature of the S- and A-type granites' normative distribution does not overlap or fit the distribution curve of the Wet Mountain granites. The figure does illustrate a relatively close fit of the normative differentiation trends of the Wet Mountains granites and the typical

I-type granites.

The Silver Plume-age plutons of the Wet Mountains, according to the characteristics listed in Table 7, appear to have developed in a Hercynotype setting. This implies converging continental plate boundaries and the production of S-type granites. Herein lies a major inconsistency. The plutons exhibit a cross-cutting structural relationship with the Idaho Springs gneiss. The gneiss must, therefore, pre-date the time of plutonic emplacement. Tectonically, the gneiss is a product of an orogenic event, and that event, because of structural evidence, cannot be the same event from which the Wet Mountain plutons were produced. The San Isabel granite has also been radioactively dated at 1.45 billion years (Boyer, 1962). This post-dates the 1.75 billion year Idaho Springs orogenic event by a minimum of 300 million years (Hutchinson, 1976). In fact, the orogenic event that produced the Idaho Springs gneiss has produced its own late-syntectonic plutonism -- the Boulder Creek granodiorite. The case for the Wet Mountain plutons being a product of some orogenic process is weak, since the plutons post-date the only orogenic event preserved in the Wet Mountains.

Because the Silver Plume-age plutons do not appear

to be a product of any tectonic event, they must have had their genesis in an anorogenic setting. Herein lies a second major inconsistency. The granites of these plutons are not typical A-type granites. On the contrary, they display a strong orogenic imprint. According to the characteristics listed in Table 7, the granites have a moderate S-type granitic character, while Figure 20 appears to show an I-type differentiation trend for these same granites.

The inability to classify these mid-Proterozoic granites may lie in their comparison to the modern tectonic models. The criteria established to characterize the development of granitic plutons has been taken from phanerozoic events (Zwart, 1967). By virtue of their names the Hercynotype and Andinotype orogens are products of phanerozoic events. The characteristics of these orogens have been applied successfully to a variety of different phanerozoic and a few Precambrian events (White and Chappell, 1977; Pitcher, 1978; and Hyndman, *et. al.*, 1980). Our present knowledge of modern plate tectonics, involving the global movements and interactions of very large lithic plates, has influenced our interpretation of Precambrian events. However, the modern tectonic models are inadequate to explain all Precambrian

events. The Silver Plume-age plutons are, based on their structural, mineralogical, and geochemical characteristics, particularly ill-suited for any modern tectonic explanation.

CONCLUSIONS: A FINAL MODEL

The Silver Plume-age plutons of the central and southern Wet Mountains are an example of an anorogenic plutonic complex that has been emplaced into a much older granitic and metasedimentary orogenic terrain. The anorogenic granites of the Wet Mountains are not part of a local or isolated event. They are part of a broad zone of correlatable intrusive calc-alkaline to alkaline granite, syenite, and anorthosite plutons (Silver, *et. al.*, 1977 and Hedge, 1980), which were emplaced into the North American craton. The zone extends from Labrador through Colorado into California and northern Mexico. The oldest plutons (1500 to 1485 million years ago) were emplaced along the present-day east coast of the North American continent, while the youngest plutons were emplaced along the west coast at about 1410 million years ago. The time interval for the magmatic event for any particular area is relatively short, about 25 $\pm$ 10 million years. According to Silver, *et. al.* (1977)

no existing modern plate tectonic or "hot spot" model is adequate to explain the development of this mid-Proterozoic anorogenic event. The failure of the Wet Mountains' Silver Plume-age granitic and plutonic characteristics to match those characteristics of the three modern plate tectonic models (Table 7) is consistent with Silver's observations.

Lawford Anderson (1982) suggests that the mid-Proterozoic transcontinental anorogenic belt, of which the Silver Plume plutons are a part, evolved from a succession of melting events originating in the mantle and passed upward into the crust. He suggests that the granitic magma is a product of the partial melting of the lower crust. This may explain the mineralogical, chemical, and isotopic inconsistencies seen on Table 7. If the granitic magma is a product of partial melting of the lower crust, then the geochemical evolution of the lower crust during the earlier Idaho Springs and Boulder Creek events should leave a strong imprint on the Silver Plume magmas. These earlier Proterozoic events are characterized by Hutchinson (1976), Gable (1980), and Hedge (1980) as being calc-alkaline and containing rock of metaigneous (I-type) composition with low initial $^{87}Sr/^{86}Sr$ ratios. These same characteristics seem to have been

inherited by the anorogenic granites of the Wet Mountains.

An anorogenic model explaining the development and evolution of the Silver Plume-age plutons of the Wet Mountains is given in Figure 21. The model involves the partial melting of lower crustal material. Partial melting could be accomplished by a moderate to high rise in the heat flow from the upper mantle (Kistler, *et. al.*, 1971). As the temperature rises in the lower crust, a zone of partial melting creates magma of a dominately granitic composition. The magma collects in discrete zones or diapirs, and because of the difference in density between the liquid and its surrounding host, the silica-rich granitic magma begins to rise. Individual plutons at first rise through the hot plastic country rock by "shouldering" aside their metasedimentary and metaigneous hosts. As cooler host rocks are encountered, stoping becomes the more common means of emplacement. The first pulse of magma to rise from the source area is a tongue-shaped diapir of the San Isabel batholith.

As the granitic liquids migrate from their zone of generation, and as the temperature in the zone of generation rises, the partial melting of the residue material continues. The mafic inclusions and high

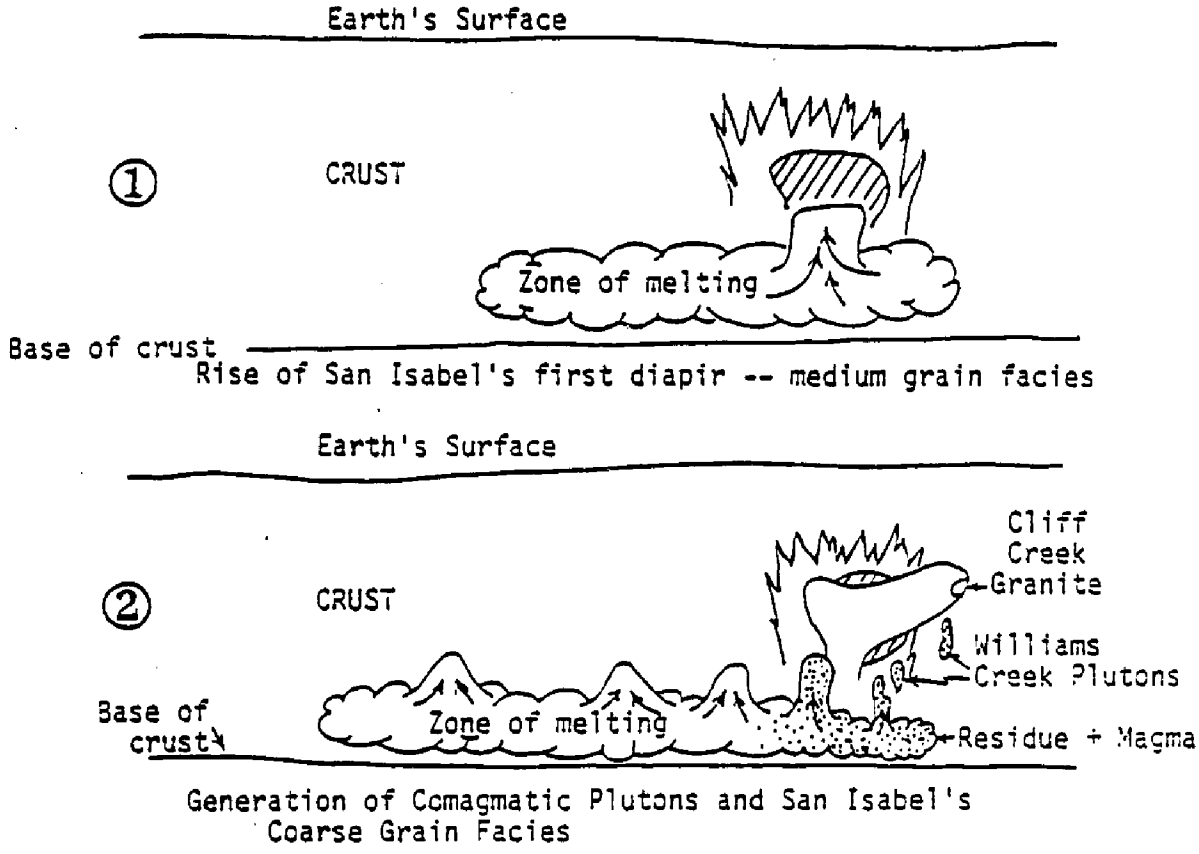

Figure 21. A conceptual model for the development of the Silver Plume-age plutons of the southern and central Wet Mountains, Colorado. Cross-section is from the northwest to the southeast.

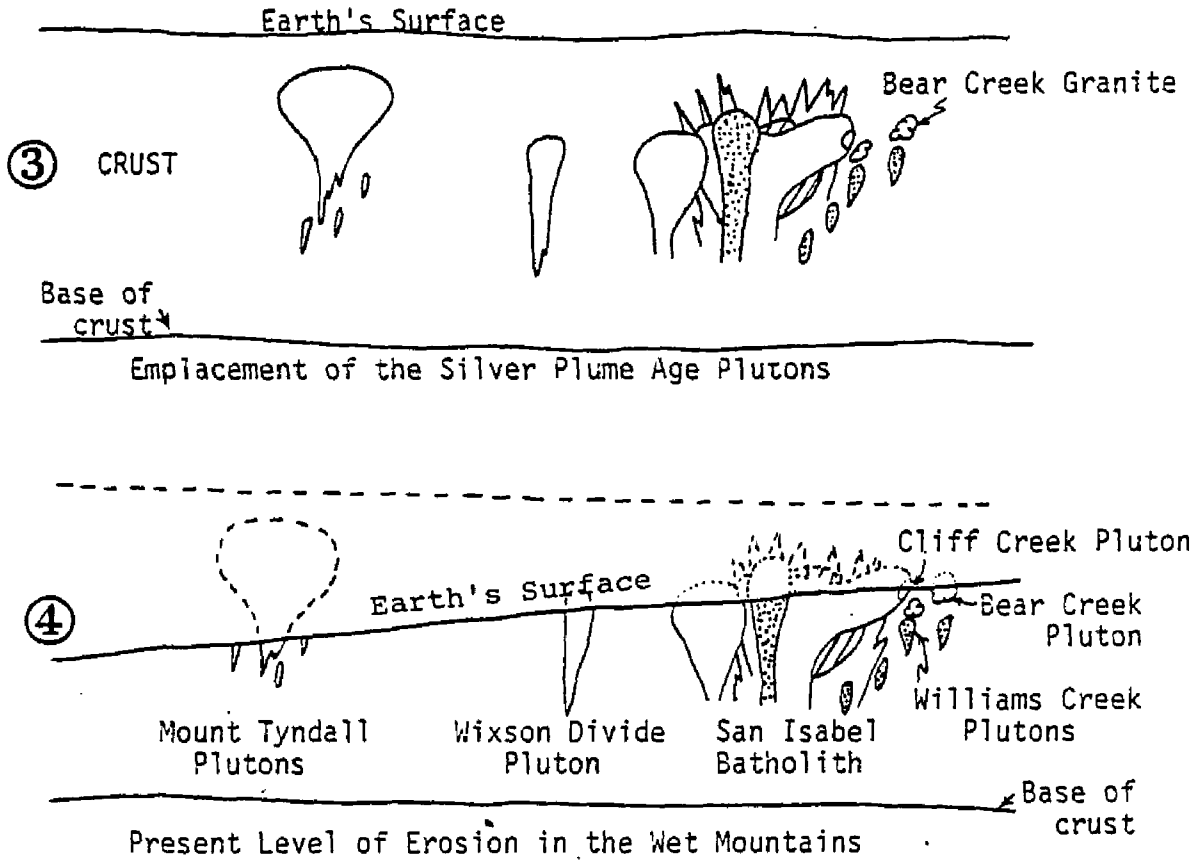

Figure 21. (cont'd). A conceptual model for the development of the Silver Plume-age plutons of the southern and central Wet Mountains, Colorado. Cross-section is from the northwest to the southeast.

concentration of refractory material in later granitic migrations are a result of the mobilization of the magmatic residue. The refractory material rose as part of a highly viscous mush, which became the youngest diapiric intrusions of the San Isabel batholith and the intrusives of Williams Creek. It is likely that during their ascent the various plutons underwent diversification by several processes. These processes included the loss of volatiles and ions to the host wall rock, contamination involving incorporation of solid materials by stoping, the inclusions of liquid materials by localized partial melting, and the incorporation of ions by diffusion. These processes, along with the mobilization of the mafic residue in the zone of generation, caused the modal and chemical variations that are common to these plutons.

The elevated temperatures produced at the time of the intrusion of the San Isabel batholith and the Williams Creek granites may have caused local partial melting or remelting of the adjacent host rock, the results of which may have been the formation of the two eutectic leucocratic granites -- the granites of Bear Creek and the granites of Cliff Creek. The Wixson Divide and Mount Tyndall plutons, which had

their origin in the northern portion of the zone of generation, appear to be the result of single emanations. They are expressed as single diapirs, with much of the Mount Tyndall diapir having been removed by erosion.

CITED REFERENCES

Anderson, J. L., 1982, Petrogenetic Evolution of Proterozoic Anorogenic Granites of North America: Geol. Soc. America Abstract with Programs, v. 14, p. 432.

Atherton, M. P. and J. Tarney (ed.), 1979, Origin of Granite Batholiths Geochemical Evidence: 1st ed., Shiva (London), 148 p.

Ballard, R. D. and E. Uchupi, 1975, Triassic Rift Structure in the Gulf of Maine: Am. Assoc. Petro. Geol. Bull., v. 59, p. 1041-1072.

Bateman, P. C. and F. C. W. Dodge, 1970, Variation of Major Chemical Constituents across the Central Sierra Nevada Batholith: Geol. Soc. Am. Bull., v. 81, p. 409-420.

Bateman, P. C. and J. P. Eaton, 1967, Sierra Nevada Batholith: Science, v. 158, p. 1409-1417.

Beckinsale, R. D., 1979, "Granite Magmatism in the Tin Belt of South-East Asia," Origin of Granite Batholiths Geochemical Evidence, ed. Atherton, M. P. and J. Tarney: 1st ed., Shiva (London), p. 34-44.

Bernas, B., 1968, A New Method for Decomposition and Comprehensive Analysis of Silicates by Atomic Absorption Spectrometry: Analytical Chemistry, v. 40, p. 1682-1686.

Biskopsky, U. S., 1965, Fast and Complete Decomposition of Rocks, Refractory Silicates, and Minerals: Analytica Chimica Acta, v. 33, p. 33-34.

Bowden, P., 1974, Oversaturated Alkaline Rocks: Granite Pantellerites and Comendites, in Sorensen, H., ed., The Alakaline Rocks: New York, John Wiley & Sons, Inc., p. 109-123.

Bowen, N. L., 1928, The Evolution of Igneous Rocks: Princeton University Press, Princeton, N. J., 334 p.

Boyer, Robert E., 1962, Petrology and Structure of the Southern Wet Mountains, Colorado: Geol. Soc. Am. Bull., v. 73, p. 1047-1070.

Boyer, R. E. and H. D. King, 1964, Petrogenetic Significance of Heavy Minerals in the San Isabel Batholith, Wet Mountains, Colorado (abstract): Geol. Soc. Am. Special Paper 68, p. 84-85.

Brock, M. R. and Q. D. Singewald, 1968, Geologic Map of the Mount Tyndall Quadrangle Custer County, Colorado: U. S. Geol. Survey, Geologic Quadrangle Map of the U. S., Map G. Q. 596.

Buddington, A. F., 1959, Granite Emplacement with Special Reference to North America: Geol. Soc. America Bull., v. 70, p. 671-747.

Butler, J. R., and P. C. Ragland, 1969, A Petrochemical Survey of Plutonic Intrusions in the Piedmont Southern Appalachians, U. S. A.: Cont. Mineralogy and Petrology, v. 24, p. 164-190.

Carmichael, I. S. E., 1963, The Crystallization of Feldspar in Volcanic Acid Liquids: Quart. J. Geol. Soc. London, v. 119, p. 95-131.

Chapman, R. W. and C. R. Williams, 1935, Evolution of the White Mountain Magma Series: Am. Mineralogist, v. 20, p. 502-530.

Chappell, B. W. and A. J. R. White, 1974, Two Contrasting Granite Types, Pacific Geology, v. 8, p. 173-174.

Chayes, F., 1952, Notes on the Staining of Potash Feldspar with Sodium Cobaltinitrite in Thin Section: Am. Min., v. 37, p. 337-348.

Dickin, A. P., 1981, Isotope Geochemistry of Tertiary Igneous Rocks from the Isle of Skye, N. W. Scotland: Jour. Petrology, v. 22, p. 155-189.

Dickinson, W. R., 1970, Relations of Andesites, Granites and Derivative Sandstones to Arc-Trench Tectonics: Rev. Geophys. Space Phys., v. 8, p. 813-860.

Eskola, P., 1932, On the Origin of Granite Magmas, Tschermaks Mineral. Petrog. Mitt, v. 42, p. 445-481.

Flanagan, F. J., 1969, U. S. Geological Survey Standards -- II. First Compilation of Data for the New U. S. G. S. Rocks: Geochim. Cosmochim. Acta, v. 33, p. 81-120.

Flanagan, F. J., 1973, 1972 Values for International Geochemical Reference Samples: Geochim. Cosmochim. Acta, v. 37, p. 1189-1200.

Fullagar, P. D. and J. R. Butler, 1976, Petrochemical and Geochronologic Studies of Plutonic Rocks in the Southern Appalachains: II, The Sparta Granite Complex, Georgia: Geol. Soc. Am. Bull., v. 87, p. 53-56.

Fyfe, W. S., 1970, Some Thoughts on Granite Magmas, "Mechanism of Igneous Intrusions," ed. Newall, G. and N. Rast: Geol. J. Spec. Issue 2, Liverpool, Gallery Press, p. 201-216.

Gable, D. J., 1980, the Boulder Creek Batholith, Front Range, Colorado: U. S. Geol. Surv. Prof. Paper 1101, p. 88.

Gilluly, J., 1969, Oceanic Sediment Volumes and Continental Drift: Science, v. 166, p. 992-994.

Greenwood, R., 1951, Younger Intrusive Rocks of Plateau Province, Nigeria, Compared with the Alkalic Rocks of New England: U. S. Geol. Surv. Bull., v. 62, p. 1151-1178.

Hamilton, W. B., 1969, Mesozoic California and the Underflow of Pacific Mantle: Geol. Soc. Am. Bull., v. 80, p. 2409-2430.

Hamilton, W. B. and W. B. Myers, 1967, The Nature of Batholiths, U. S. Geol. Surv. Prof. Paper 554-C, p. C 1-C 30.

Harper, W. F., 1975, Structure of Precambrian Metamorphic Rocks West of the Ilse Fault Zone, Hardscrabble Mountain Quadrangle, Wet Mountains, Colorado: unpublished Masters Thesis, 102 p.

Hedge, C. E., 1980, personal communications, U. S. Geol. Surv., Denver, Colorado.

Hutchinson, R. U., 1976, Precambrian Geochronology of Western and Central Colorado and Southern Wyoming: in Epis, R. C. and R. J. Weimer, (ed.), Professional Contributions of Colo. School of Mines: Colo. School of Mines Field Trip Guide 1976, p. 73-77.

Hydman, D. W., 1969, The Development of Granitic Plutons through Anatexix in the Northern Cordillera, British Columbia: Geol. Soc. Am. Spec. Paper, V. 121, 146 p.

Hyndman, D. W., C. J. Vitaliano, and L. J. Suttner, 1980, Granite II -- Near-Surface Batholiths, Related Volcanism, Tectonism, Sedimentation, and Mineral Deposition: Geology, v. 8, No. 2, p. 107-110.

Jacobson, R. R. E., W. N. MacLeod, and R. Black, 1958, Ring-Complexes in the Younger Granite Provinces of Northern Nigeria: Mem. Geol. Soc. Lond., v. 1, 71 p.

Johannsen, A., 1939, A Descriptive Petrography of the Igneous Rocks: University of Chicago Press (Chicago), 519 p.

Kerr, P. F., 1977, Optical Mineralogy: 4th ed., McGraw-Hill (New York), 492 p.

Kistler, R. W., J. F. Evernden, and H. R. Shaw, 1971, Sierra Nevada Plutonic Cycle; Part I: Origin of Composite Granitic Batholiths: Geol. Soc. Am. Bull., v. 82, p. 853-868.

Kleeman, A. W., 1965, The Origin of Granite Magmas: J. Geol. Soc. Aust., v. 12, p. 35-52.

Larsen, E. S., 1948, Batholith and Associated Rocks of Corona, Elsinore, and San Luis Rey Quadrangles, Southern California: Geol. Soc. America Mem. 29, 182 p.

Murray, M. M., 1970, Petrology, Structure, and Origin of the San Isabel Batholith, Wet Mountains, Colorado: Rice University, Houston, Texas, 51 p.

Nasseef, A. O. and I. G. Gass, 1977, Granite and Metamorphic Rocks of the Taif Area Western Saudia Arabia: Geol. Soc. Am. Bull., v. 88, p. 1721-1730.

Neary, C. R., I. G. Grass, and B. J. Cavanagh, 1976, Granite Association of Northern Sudan: Geol. Soc. Am. Bul., v. 87, p. 1501-1512.

Peacock, M. A., 1931, Classification of Igneous Rock Series: J. Geol., v. 39, p. 54-67.

Peck, D. L. and D. R. Wones, 1980, Penrose Conference Report -- Granite I: Origin and Evolution of Granite Magmas: Geology, v. 8, p. 452-253.

Pitcher, W. S., 1978, The Anatomy of a Batholith: J. Geol. Soc. London, v. 135, p. 157-182.

Pitcher, W. S. and A. R. Berger, 1972, The Geology of Donegal: A Study of Granite Emplacement and Unroofing: John Wiley and Sons, Inc. (New York), p. 435.

Pinwinskii, A. J. and P. J. Wyllie, 1968, Experimental Studies of Igneous Rock Series: A Zoned Pluton in the Wallows Batholith, Oregon: Jour. Geol., v. 76, p. 205-234.

Ross, D. C., 1972, Petrographic and Chemical Reconnaissance Study of Some Granite and Gneissic Rocks near the San Andreas Fault from Bodega Head of Kajon Pass, California: U. S. Geol. Survey Prof. Paper 698, 92 p.

Scott, G. R. R. C. Epis, R. B. Taylor, and C. E. Chapin, 1976a, Cenozoic Volcanic, Tectonic, and Geomorphic Features of Central Colorado: in Epis, R. C. and R. J. Weimer (ed.), Professional Contributions of Colo. Shcool of Mines: Colo. School of Mines Field Trip Guide, 1976, p. 323-338.

Scott, G. R. and R. B. Taylor, 1974, Reconnaissance Geologic Map of the Rockvale Quadrangle, Custer and Fremont Counties, Colorado: U. S. Geol. Survey Mineral Investigation Field Studies Map, MF-562, Rockvale Quadrangle, Colorado.

Scott, G. R., R. B. Taylor, R. C. Epis, and R. A. Wobus, 1976b, Geologic Map of the Pueblo 1^{o} x 2^{o} Quadrangle, South-Central Colorado: U. S. Geological Survey Misc. Field Studies Map, MF-775.

Shapiro, L., 1960, A Spectrophotometric Method for the Determination of FeO in Rocks: U. S. Geol. Survey Research Short Paper, No. 226, p. B496-B497.

Silver, L. T., M. E. Bickford, W. R. van Schmus, J. L. Anderson, T. H. Anderson, and L. G. Medaris, 1977, The 1.4-1.5 B. Y. Transcontinental Anaorogenic Plutonic Perforation of North America: Geol. Soc. America Abstracts with Programs, v. 9, p. 1176-1177.

Singewald, Q. D., 1966, Description and Relocation of Part of the Ilse Fault Zone, Wet Mountains, Colorado: U. S. Geol. Survey Prof. Paper 550C, p. 21-24.

Slemmons, D. B., 1962, Determination of Volcanic and Plutonic Plagioclases using a Three- or Four-Axis Universal Stage: Geol. Soc. America Spec. Paper, No. 69, 64 p.

Sorensen, H. (ed.), 1974, The Alkaline Rocks: John Wiley and Sons, Inc., (New York), 622 p.

Streckeisen, A. L., 1967, Classification and Nomenclature of Igneous Rocks: N. Jb. Miner. Abb., v. 107, No. 2, p. 144-214.

Taylor, R. B., G. R. Scott, R. A. Wobus, and R. C. Epis, 1975 , Reconnaissance Geologic Map of the Royal Gorge 15-minute Quadrangle, Fremont and Custer Counties, Colorado: U. S. Geol. Survey Misc. Inv. Series Map, I-869.

Taylor, R. P., D. F. Strong, and B. F. Kean, 1980, The Topailo Igneous Complex: Silurian-Devonian Peralkaline Magmatism in Western Newfoundland: Can. Jour. Earth Sci., v. 17, p. 425-439.

Thompson, R. N., 1969, Tertiary Granites and Associated Rocks of the Marsco Area, Isle of Skye: Q. J. Geol. Soc. Lond., v. 124, p. 349-385.

Turner, D. C., 1963, Ring Structures in the Sara-Fier Younger Granite Complex, Northern Nigeria: Q. J. Geol. Soc. Lond., V. 119, p. 345-366.

Turner, F. J. and J. Verhoogen, 1960, Igneous and Metamorphic Petrology: 2nd ed., McGraw-Hill (New York), 694 p.

Tuttle O. F. and N. L. Bowen, 1958, Origin of Granite in Light of Experimental Studies in the System $NaAlSi_3O_8$-$KAlSi_3O_8$-SiO_2-H_2O: Geol. Soc. America Mem. 74, 153 p.

Tweto, Ogden, 1979, Geologic Map of Colorado: U. S. Geological Survey.

Van Der Plas, L. and A. C. Tobi, 1965, A Chart for Judging the Reliability of Point Counting: Am. Jour. Sci., v. 263, p. 87-90.

von Platen, H., 1965, Experimental Anatexis and Genesis of Migmatites, in Controls of Metamorphism, ed. Pitcher, W. S. and G. W. Flinn: Oliver and Boyd (London), p. 203-218.

Waskon, J. D. and J. R. Butler, 1971, Geology and Gravity of the Lilesville Granite Batholith, North Carolina: Geol. Soc. Am. Bull., v. 82, p. 2827-2844.

White, A. J. R. and B. W. Chappell, 1977
Ultrametamorphism and Granitoid Genesis: Tectonophysics, v. 43, p. 7-22.

White, A. J. R., B. W. Chappell, and J. R. Cleary, 1974, Geologic Setting and Emplacement of Some Australian Paleozoic Batholiths and Implications for Intrusive Mechanism: Pacific Geol., v. 8, p. 159-171.

Whitten, E. H. T. and R. E. Boyer, 1964, Process-Response Models Based on Heavy-Mineral Content of the San Isabel Granite, Colorado: Geol. Soc. America Bull., v. 75, p. 841-862.

Winkler, H. G. F., 1976, Petrogenesis of Metamorphic Rocks: 4th ed., Springer-Verlag (New York), 334 p.

Winkler, H. G. F. and H. von Platen, 1958, Experimentelle Gesteinsmetamorphose -- II -- Bildung von Anatektischen Granitishchen Schmelzen bei der Metamorphose von NaCl -- Fuhrenden Kalkfreien Tonen: Geochem. Cosmochim. Acta, v. 15, p. 91-111.

Zwart, H. J., 1967, The Duality of Orogenic Belts: Geol. Mijnbouw, v. 46, p. 283-309.

APPENDIX A

Sampling Techniques

Field work was conducted during the summers of 1974 and 1975 for three purposes: 1) to obtain a detailed facies map of the Wixson Divide pluton, 2) to perform reconnaissance mapping of the northern third of the San Isabel batholith, and 3) to sample both plutons. In 1976 the other four major Silver Plume-age rock types were mapped and sampled. Two weeks of field work early in August, 1978 were needed to determine the potassium feldspar megacryst concentrations within and immediately adjacent to the San Isabel batholith.

Base maps used in both the detail and reconnaissance geologic mapping projects were 7.5 minute topographic maps. The reconnaissance mapping of the San Isabel batholith was completed on six adjacent topographic maps (Wetmore, Saint Charles Peak, San Isabel, Deer Peak, Bear Creek, and Rhy Quadrangles). The Wixson Divide pluton was mapped in detail on two adjacent topographic maps (Deer Peak and Hardscrabble Creek Quadrangles). Reconnaissance mapping within the Rosita and in the

northern half of the Hardscrabble topographic Quadrangles has revealed small lenses and pods of Mount Tyndall- and Williams Creek-type granites which until now have never been mapped. The other plutons crop out on the Mount Tyndall, Bear Creek, and San Isabel topographic Quadrangles.

Samples were collected from all the major plutonic outcroppings in a random manner. This is due largely to the randomness of fresh exposures. Samples were sparsely collected in some areas of the larger plutonic masses, and sampling within some of the smaller granitic lenses or pods was impossible because of the lack of fresh outcrops in these areas. Large selections of the San Isabel batholith and the Wixson Divide pluton were also sparsely sampled or either remained unsampled due to the existence of deep soil zones that developed along the myriad of faults associated with the Ilse Fault Zone.

Petrographic Technique

Thin sections for petrographic study were prepared from 306 samples. The microscope used for the analysis was a Ziess MF 40. A Ziess 10613000 mechanical stage which advances 0.60 mm after each point was used to determine the mineral volume percentages of each thin section. For those samples with grain sizes exceeding 20 mm, the rocks were slabbed and stained. Counts were made from the stained surface with the aid of a ruled glass plate.

The staining procedures follow the method established by Chayes (1952):

1) The rock is slabbed and washed to remove excess saw lubricant. The rock slab is then dried at 200^{o}C for four hours to volitalize lubricants trapped within the slab interstices.

2) The slab is cooled and treated with hydrofluoric acid for 15 seconds, then rinsed and dried.

3) The slab is then treated with sodium cobalt nitrite solution for 1 minute and dried. The stained minerals make feldspar identification easy. Potassium feldspars appear yellow, while sodium-rich plagioclase appear white. Quartz and accessory minerals are unaffected by staining.

The point counting procedure for these treated slabs is as follows (Chayes, 1952):

1) A plate glass with a ruled grid of etched lines approximately 1 mm apart and at right angles to one another was placed on the stained slab.

2) One thousand points were counted as quartz, alkali feldspar, plagioclase, and total accessory minerals.

3) The volume percentage for individual mafic and accessory minerals for each rock sample was determined by counting 1000 points off a prepared thin section. Statistical accuracy for the derived volume percentage of counts taken by this method is estimated to be between 1 and 2 percent (Van der Plas and Tobi, 1965).

For those rock specimens where few or no grains exceed 20 mm, volume percentages were taken exclusively from the thin sections. On these thin sections, staining was not necessary to distinguish potassium feldspar from plagioclase. Potassium feldspars were easily recognized due to perthite development and/or a very distinctive "grid iron" pattern. Plagioclase also was easy to detect due to the ubiquitous dusting of grains with alteration products, and to a lesser extent, its development of albite twins.

Anorthite content was determined by two methods: the Michel-Levy method as explained by Kerr (1977) and the Slemmons method (1962). The Slemmons method, because

of the amount of time needed to gather the necessary optical data and because of its accuracy, was used as a check on the Michel-Levy method.

In the Slemmons method, plagioclase grains displaying albite twinning in the thin section are oriented on the Universal Stage so that the three principal optical directions "x," "y," and "z" are located exactly with reference to the plane of the thin section. The optical directions are determined for each compositional twin plane, and the angle at which the composition plane crosses the plane of the thin section is also measured. All data is plotted on a stereographic net to determine "z" optical direction of the first and second compositional twin. The net is rotated so that "z_1," to "z_2," and the compositional plane all lie on a great circle. The total angular distance from "z_1" to "z_2" across the compositional plane is measured. The anorthite percentage is directly related to the mean angle between the two "z" optical directions and is readily determined from Plate I of Slemmons (1962).

Several methods were tried during the course of this study to optically determine the total amount of exsolved albite in microcline. The only method that achieved any precision was a method of point counting the macro- and microperthite. In this method, as microcline crystals

are crossed during a normal point counting traverse (obviously all points in the crystal would be counted as microcline) any exsolved albite encountered is tallied separately, thereby giving a count of not only the volume percent of microcline present in the rock, but also the volume percent of macro- and microperthite albite in the microcline.

Whole Rock Analysis: Analytical Technique

The knowledge that analytical work would eventually be performed on the rock samples collected in the field was taken into consideration at the time of sample collection. To eliminate any bias due to grain size, the sample sizes were made directly proportional to the maximum grain size. In other words, the coarser the grain size, the larger the sample needed to give a representative rock chemistry. The fine-grain facies' (grain size 1 mm to 5 mm) sample sizes were 7 cm by 10 cm. Medium-grain facies' (grain size 5 mm to 10 mm) sample sizes were 13 cm by 16 cm, and the coarse-grain as well as the porphyritic facies (grain size larger than 10 mm) sample sizes were 15 cm by 20 cm.

The degree to which a sample has been altered is a critical determination in any chemical analysis. The freshest samples used in the chemical analyses were collected in the recent road cuts along Colorado State Highway 165. These rocks were, in general, completely unaltered. Other samples used in the analyses needed to be petrographically analyzed before being chosen for analyses. Only those samples that had low concentrations of alteration products were considered for chemical study.

A total of 79 samples were analyzed for major element composition. Methods used in the studying of these samples were x-ray fluorescence, atomic absorption spectorscopy, and flame photometry. X-ray fluorescence studies were made to determine the chemical abundance of the major elements Si, Al, K, Ca, Ti, and total Fe. Atmoic absorption spectrochemical analyses were made for Mg, Mn, and Na. Flame photometry spectroscopy was used to determine FeO concentrations.

Before x-ray fluorescence pellets or atomic absorption solutions could be made, the samples were ground into a fine powder. The sample preparation and grinding procedures are as follows:

1) The relatively unaltered plutonic samples were first sawed into large slabs approximately 1 to 2 cm thick.

2) These slabs were washed to remove supperficial lubricating oil. The slabs were then dried in an oven at 200^{o}C for four hours to volitalize any of the remaining lubricant.

3) Slabs were then crushed in a steel jaw crusher to sand size. The amount of sample prepared varied according to the sample's grain size. The weight of the fine grained material was about 200 grams. Rocks with the largest megacrysts had several kilograms of sample crushed.

4) Obviously these large volumes of samples were not needed, therefore each sample was split by a standard sedimentary sample splitter to approximately 30 grams.

5) Samples were then ground by hand with a clean porcelain mortar and pestle to an approximate 15 to 20-mesh size.

6) The entire sample was then ground into a fine powder of about 600-mesh. The powder was produced after 1 to 3 minutes of grinding on a Baldor grinder with a revolving alumina disc. The grinding procedure undoubtedly oxidized some of the iron present in the sample but oxidation was kept to a minimum because of the short grinding time needed to produce the sample powder. Regardless of the amount of time used to grind the sample, small flakes of biotite were still visible in some samples.

7) Sample powders were then stored for future use.

X-ray fluorescence samples preparation procedures are as follows:

1) Six grams of rock powder were carefully weighed and placed in a clean plastic vial with exactly one gram of bakelite (phenal formaldehyde resin: British Bakelite Company Resin #R0214) and two well cleaned small plastic balls.

2) The vial was shaken vigorously for 10 minutes in a mechanical agitator.

3) The well-mixed rock powder and binder were then placed in a one-inch diameter die. The sample and binder were placed in a hydraulic press at 15 tons per square inch for 20 minutes. A heat jacket was placed around the press. The pellet produced by this procedure is one inch in diameter and approximately ¼ inche thick.

The x-ray fluorescence analyses were carried out on an NMINT Norelco x-ray fluorescence spectrometer. Analyses were made using both the tungsten and chromium targets. Table A.1 gives the operating conditions for the x-ray fluorescence spectrometer for each element. Peak positions for the elements are only approximate because of peak drift. The reasons for peak drift are many. Two common reasons are the minute movements of the analyzing crystal during analysis and the temperature changes produced during prolonged use. For these reasons maximum peak positions were determined each day.

Counts were read after ten ten-second intervals of time on each element's peak and on an adjacent background wavelength. Total elapsed time for each analysis was 100 seconds. This procedure was used to help evaluate the precision of the analysis and to eliminate those

Table A.1. Operating Conditions for the NMIMT Norelco X-Ray Fluorescence Spectrometer

Element	Tube	Analyzing Crystal	Atmosphere	Vacuum	2θ Peak	2θ Background	Counter	Voltage or Detector	Baseline	Window	Time(sec)	Voltage (Current to tube)
Si	Cr	EDDT	MA	Yes	78.20	81.22	FPG	1.827	1.5	2.6	100	40/30
Al	Cr	EDDT	MA	Yes	112.60	109.00	FPG	1.853	1.8	3.3	100	40/30
Ca	Cr	EDDT	MA	Yes	15.70	14.70	FPG	1.739	2.0	2.0	100	40/30
K	Cr	EDDT	MA	Yes	21.15	19.80	FPG	1.800	1.5	2.5	100	40/30
Ti	W	LiF	MA	Yes	85.47	89.30	FPG	1.792	2.1	2.0	100	40/30
Fe	W	LiF	Air	No	57.58	55.75	Scint.	0.727	1.0	4.0	100	40/30

readings that had abnormally high bursts of x-ray radiation during the ten ten-second intervals. This procedure also helps in the recognition of anonymous values produced by peak drift.

United States Geological Society rock standards AGV-1, GSP-1, T-1, BCR-1, and G-2 were used as standards for these analyses (Flanagan, 1969). A linear plot of standards for each element was made daily. Rock standard G-2 was run after each three samples as an internal standard. The composition for the unknown samples was determined graphically from the linear plot of the standards. Graphing was aided by the use of a Texas Instruments SR-52 linear regression program.

The atomic absorption spectrochemical analyses follows the procedure established by Bernas (1968). The procedure begins with the acid digestion of the 600-mesh sample. The acid digestion procedure employs the use of a Teflon-lined bomb. This method for dissolving silicate rock samples is both rapid and safe. Its main advantage over other methods is that the digestions occurred in a completely closed system. No volatile fluorides could be lost during the digestion process as is the problem with some other methods tried (Biskopsky, 1965). The method used to digest the samples is as follows:

1) Fifty mg of the rock powder are very accurately weighed into a Teflon (Dupont TFE fluorocarbon resin) crucible.

2) Aqua regia (0.5 ml) is added as a wetting agent. Special care is taken to insure that the entire sample is wet.

3) Fifty two per cent solution of hydrochloric acid (3.0 ml) is added to the vessel. The bomb is closed and quickly placed in the Teflon bomb holder. The holder is hand tightened.

4) The bomb and holder are placed in a drying oven (110^{o}C) for 40 minutes.

5) The bomb is allowed to cool to room temperature (2 hours).

6) The bomb is opened and the contents are washed from the Teflon crucible into a 50 ml polystyrene Spex vial containing 2.2 grams of boric acid. No more than 40 ml of water are used to wash out the Teflon crucible. The boric acid will help dissolve any fluorides that may have formed during digestion.

7) The solution is transferred to a 100 ml volumetric flask and the volume is adjusted to the mark.

8) The solution is then quickly transferred from the glass volumetric flask and stored in a polyethylene container. All water used in this procedure is 2 mega-ohm water distilled in glass for its high purity.

All samples were run on a Perkin-Elmer Atomic Absorption Spectrometer Model 306 with automatic concentration readout. The tube and setting used for each element analyzed follows the suggestions set forth by the manufacturer. The operating conditions for the Perkin-Elmer 306 are given in Appendix Table A.2. Each sample was run 4 to 8 times to check the precision of the analysis.

Elemental concentrations of Mg, Mn, and Na for the standard samples were graphed and the samples' unknown concentrations were determined from those graphs.

FeO Determination Techniques

A spectrophotometric procedure for the determination of ferrous iron content is used in this study (Shapiro, 1960). This procedure is used because of its application to rapid analysis of a large number of samples without sacrificing precision or accuracy.

The excess 600 mesh sample material left over from the preparation of x-ray fluorescence pellets is used in this analysis. The sample powder is carefully weighed (10 mg) into a clean plastic bottle, which already contains 20 mg of the ferrous iron indicator, orthophenanthroline. The sample is then digested with sulfuric acid and carefully titrated with 52% hydrofluoric acid solution. To accelerate the digestion

Table A.2. Operating Conditions for the Perkin-Elmer 306

Element	λ	Phase	Slit	Range	Function	Fuel	Fuel Flow	Oxidant Flow
Mg	2852Å	Normal	4	UV	ABS	Acetylene-NO_2	6.5	5.5
Na	2890Å	Normal	4	Vis	Ems	Acetylene-air	8.0	9.0
Mn	2794Å	Normal	3	UV	Abs	Acetylene-air	9.5	9.0

process, the bottles are placed in a steam bath for exactly thirty minutes. After digestion 20 ml of 10% sodium citrate is immediately added. The contents of the bottle is added to a 100 ml volumetric flask already containing a boric acid solution and brought to the mark and then mixed well (Shapiro, 1960). The sample solution is poured into 25 ml rectangular silicon cells and analyzed in a Perkin-Elmer Hetachi 139, Vis-UV Spectrophotometer. Absorption readings are made at wavelengths of 550 mu (peak) and 640 mu (background) (Shapiro, 1960).

Calculations are made by substracting the absorbance at 640 mu from the absorbance at 550 mu, to obtain absorbance due to color intensity. The FeO content for the standard sample, BCR-1 (Flanagan, 1973) is divided by the known's absorbance due to color. This ratio is multiplied by the unknown's sample weight, by its absorbance due to color, and by 100 to obtain the unknown's FeO's volume percent (Shapiro, 1960).

The results obtained by the spectrophotometric procedure are in close agreement with the absolute value given by Flanagan (1973) for the four known samples, G-2, GSP-1, SY-1, and AGV-2. The measure of accuracy for the FeO value obtained by this method was within $\pm$ 0.82 for four runs of SY-1. These results are similar to those obtained by Shapiro (1960).

Accuracy and Precision of Results

One sample of known chemical composition was analyzed along with the rest of the samples in this study as an internal check on the accurracy of the methods used. The sample known used was the U. S. G. S. rock standard SY-1 (Flanagan, 1973). The comparison of the recommended values of Flanagan (1973) with the theoretical values of this study are presented in Table A.3.

Table A.3a. Accuracy: Results Obtained in the Analysis of the International Rock Standard SY-1

	Theoretical Values (This work)	Recommended Values (Flanagan, 1973)
SiO_2	60.64	59.50
TiO_2	0.36	0.49
Al_2O_3	10.12	9.60
Fe_2O_3	1.29	2.15
FeO	5.09	5.45
MnO	0.44	0.40
MgO	4.82	4.20
CaO	10.50	10.20
Na_2O	3.36	3.30
K_2O	2.14	2.67
	98.76	96.96

b - Precision: Results of Ten Replicate Analysis of the International Rock Standard SY-1

	Mean	S. D.
SiO_2	60.64	0.54
TiO_2	0.36	0.29
Al_2O_3	10.12	2.51
Fe_2O_3	1.29	1.36
FeO	5.09	0.81
MnO	0.44	0.49
MgO	4.82	1.31
CaO	10.50	1.60
Na_2O	3.36	0.10
K_2O	2.14	1.08

APPENDIX B

SUMMARY OF MODAL AND CHEMICAL DATA OF THE SAN ISABEL BATHOLITH

A total of 150 sample modes has been made in the San Isabel batholith and its satellite plutons. These modes include 133 samples collected and petrographically analyzed by Murray (1970). The locations of the samples within the granitic batholith are shown on the index map (Figure B.1). It is easily recognizable from the index map that sampling was rather unsystematic. This is largely due to the limited exposures of fresh rock. Several large areas in the southern portion of the batholith seem to be unsampled. However, the lack of modal representation is primarily due to the areal expression of another pluton, the granites of Cliff Creek, which will be discussed later.

Modes of the San Isabel granites are given in Table B.2. For ease of comparison of such an abundance of data, the table of modal analyses is summarized in a series of triangular diagrams (Figure B.3). The trigonal diagrams represent standard quartz-potassium feldspar-plagioclase diagrams, following the general method

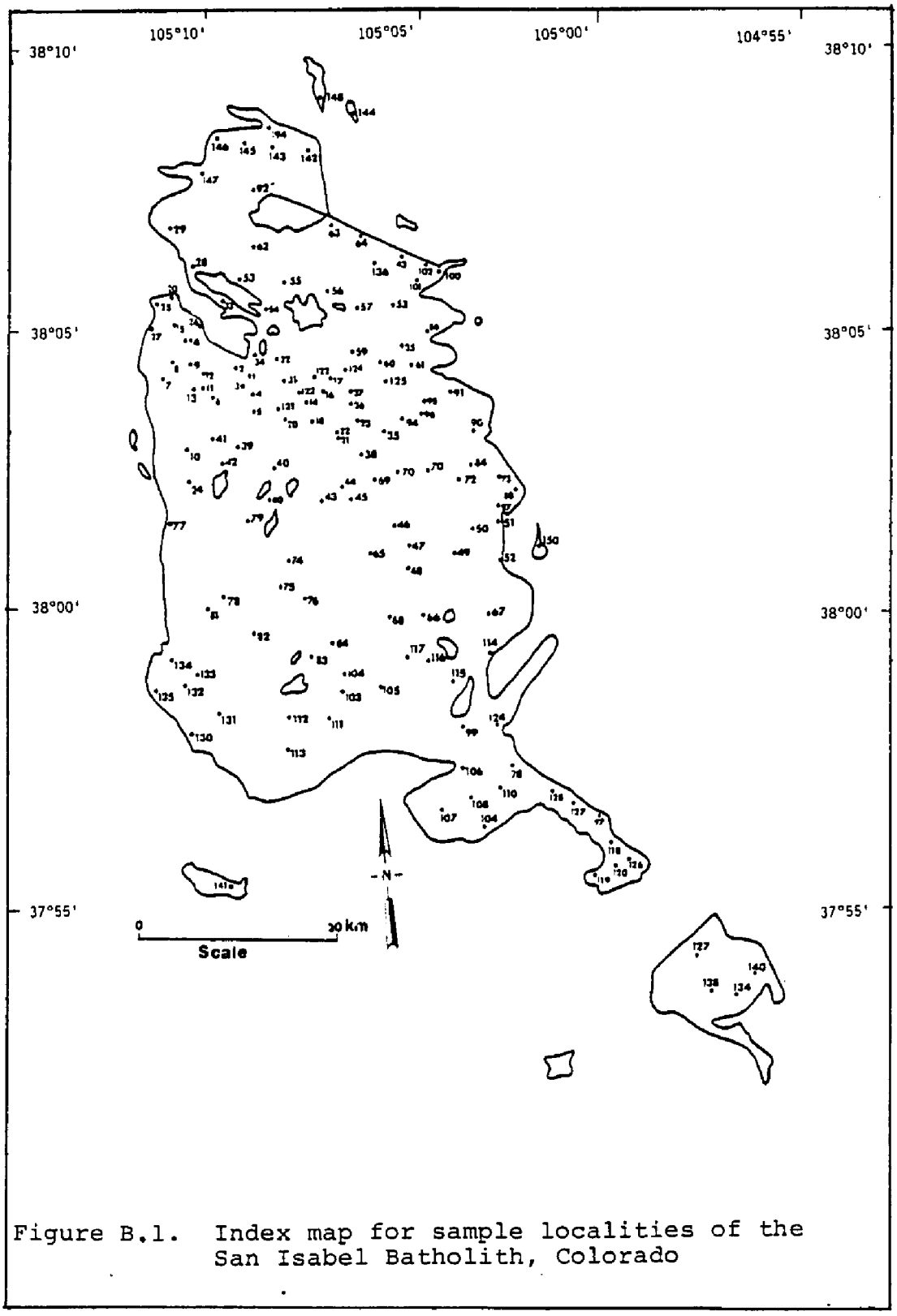

Figure B.1. Index map for sample localities of the San Isabel Batholith, Colorado

Table B.2. Modal analysis of rock samples collected from the San Isabel Batholith. The facies from which each samples was collected is given in the "Facies" column. Abbreviations used are as follows: SIC, coarse-grain facies: SIM, medium-grain facies; and SIP, porphyritic facies. Specimens numbered 1-120, 126-136, and 150 are taken from Murray (1970).

Sample Number	Kspar	Plag	Qtz	Biot	Mag	Sph	Hbl	Zir	Ap	Ep	Sericite	Chl	Hem	Others	Total	Facies
1	29.0	33.7	21.5	5.7	4.7	0.5	---	---	0.8	---	0.8	---	2.7	Calcite 0.3	99.8	SIC
2	36.0	24.5	29.4	1.0	0.5	---	---	---	---	---	0.1	---	0.9	Calcite 7.2	99.6	SIC
3	18.4	35.4	19.4	10.9	3.9	2.7	1.1	0.1	1.1	1.6	---	4.2	---	---	99.9	SIC
4	32.7	25.5	20.9	7.0	3.4	4.9	---	---	0.2	1.2	0.6	3.7	---	---	100.0	SIC
5	28.1	37.0	15.4	9.7	1.8	3.1	0.3	tr	0.8	2.2	---	1.5	---	---	99.9	SIC
6	32.1	27.8	18.1	7.7	5.8	2.2	1.7	0.2	2.2	1.7	0.4	0.2	---	---	100.0	SIC
7	12.5	48.1	20.8	11.3	2.5	2.5	---	0.1	0.7	1.6	---	---	---	---	100.1	SIC
8	36.7	25.4	18.4	8.0	2.3	2.5	1.3	0.1	1.8	3.4	0.1	---	---	---	100.0	SIC
9	28.7	34.1	13.7	7.4	1.5	4.4	1.7	0.3	0.5	3.1	---	4.4	---	---	99.9	SIC
10	40.6	22.7	35.0	1.2	0.1	0.1	---	---	---	---	0.1	0.1	---	---	99.9	SIM
11	20.9	36.5	16.3	9.9	4.4	4.0	3.4	---	2.0	1.3	---	0.6	0.6	---	100.0	SIC
12	23.5	35.5	19.2	12.7	2.4	2.5	1.6	---	0.8	1.8	---	---	0.1	---	99.9	SIC
13	32.9	21.9	21.7	14.4	3.3	3.2	0.2	---	0.5	1.8	---	---	---	---	99.9	SIC
14	24.7	37.2	16.6	7.5	2.9	2.7	2.1	0.1	0.9	5.3	---	---	---	---	100.0	SIC
15	25.0	26.9	19.0	10.1	1.9	5.5	2.7	0.3	1.3	3.9	---	2.7	0.6	---	99.9	SIC
16	33.5	31.5	19.2	8.5	2.3	2.5	0.4	0.3	1.3	0.5	---	---	---	---	100.0	SIM
17	33.8	30.9	17.0	7.5	2.2	1.6	3.4	0.1	0.8	2.2	0.1	0.1	0.1	---	99.9	SIC
18	39.0	22.1	23.3	6.0	1.3	2.5	0.8	---	1.5	0.9	---	0.4	---	---	99.9	SIC
19	37.9	22.3	22.3	8.3	1.9	2.3	0.5	---	0.8	0.8	---	2.7	0.3	---	100.0	SIC
20	16.2	32.2	25.6	15.0	2.4	2.9	---	---	0.8	2.2	0.7	1.9	---	---	99.9	SIC

Table B.2 (cont'd)

Sample Number	Kspar	Plag	Qtz	Biot	Mag	Sph	Hbl	Zir	Ap	Ep	Sericite	Chl	Hem	Others	Total	Facies
21	37.6	23.8	24.7	7.4	2.0	1.4	---	0.1	1.2	0.6	1.2	---	---	---	100.0	SIC
22	29.9	29.1	17.5	12.0	3.1	4.8	---	0.3	1.2	1.7	0.4	---	---	---	100.0	SIM
23	37.2	31.0	22.9	3.9	1.6	1.6	---	---	0.5	1.5	---	---	---	---	100.1	SIM
24	27.6	34.3	16.0	9.9	3.4	2.9	3.4	0.1	1.1	1.2	---	1.1	0.1	---	100.0	SIC
25	20.7	38.6	19.8	6.8	4.1	2.2	5.4	---	1.1	0.7	---	0.4	0.1	---	99.9	SIC
26	19.8	39.4	21.6	---	2.3	0.8	---	---	1.4	3.9	4.4	6.4	---	---	100.0	SIM
27	25.1	32.7	20.6	8.4	3.8	3.2	3.5	---	1.0	1.2	0.1	---	0.1	---	99.8	SIC
28	32.9	29.9	19.9	8.1	1.6	1.3	---	0.1	0.3	0.3	---	5.4	---	---	100.0	SIM
29	35.5	27.2	15.3	10.9	2.6	3.3	1.0	0.1	1.8	1.1	---	0.8	0.4	---	100.0	SIM
30	31.2	30.9	24.3	6.5	2.3	2.3	0.1	0.1	1.3	1.0	---	---	---	---	100.0	SIC
31	36.3	25.2	21.7	9.4	1.5	1.5	1.0	---	0.5	2.8	---	---	---	---	99.9	SIC
32	29.9	29.0	19.7	8.6	3.5	3.5	0.6	---	2.1	2.7	---	---	0.3	---	100.0	SIM
33	38.2	26.0	21.8	7.2	3.5	0.7	---	---	0.9	0.9	---	---	0.7	---	99.9	SIM
34	40.9	30.6	17.7	6.2	2.1	1.1	---	---	0.6	0.2	---	0.5	---	---	99.9	SIC
35	43.7	22.1	20.0	8.2	2.0	2.5	---	0.4	0.6	0.2	0.2	---	---	---	99.9	SIM
36	33.0	30.8	19.4	1.7	2.3	2.3	2.8	---	---	0.5	---	6.6	0.2	---	100.0	SIP
37	26.3	28.9	23.3	7.6	3.6	2.5	1.2	---	1.8	1.0	0.5	2.9	0.3	---	100.0	SIP
38	38.7	22.2	20.6	9.3	3.9	---	---	---	0.8	3.1	0.6	---	---	Leuc. 0.8	100.0	SIM
39	19.4	35.8	14.7	9.1	5.5	4.0	3.2	---	1.2	4.5	---	2.0	0.5	---	100.0	SIC
40	20.0	28.8	25.0	11.4	2.6	3.4	1.3	---	0.9	5.1	---	---	0.4	---	100.0	SIC
41	45.2	21.0	24.8	7.6	0.5	0.2	---	---	---	0.4	---	0.2	---	---	99.9	SIC
42	29.1	30.7	15.7	7.9	3.6	3.7	1.3	0.4	0.3	5.6	---	1.8	---	---	100.1	SIC

Table B.2 (cont'd)

Sample Number	Kspar	Plag	Qtz	Biot	Mag	Sph	Hbl	Zir	Ap	Ep	Sericite	Chl	Hem	Others	Total	Facies
43	41.1	25.1	19.0	4.5	2.3	3.1	2.0	0.1	0.9	1.6	---	0.1	0.1	---	100.0	SIC
44	38.9	27.3	20.4	7.1	2.6	2.6	0.4	0.2	0.1	0.2	---	---	0.2	---	100.0	SIC
45	36.6	26.4	19.3	9.2	3.1	2.7	1.1	0.2	0.7	0.5	---	---	---	---	100.0	SIC
46	34.3	28.2	20.5	8.6	3.5	3.1	0.6	---	0.8	0.4	---	---	---	---	100.0	SIM
47	33.5	29.7	18.1	11.9	2.9	0.9	0.9	---	0.4	1.9	---	---	---	---	100.1	SIM
48	30.0	33.0	17.0	10.4	2.5	2.4	2.0	0.1	0.4	1.9	---	---	0.1	---	99.9	SIM
49	27.9	31.7	12.5	10.1	5.7	3.2	3.5	---	0.9	4.4	---	---	---	---	99.9	SIM
50	31.2	28.1	20.9	10.1	2.8	3.0	0.2	---	1.7	1.9	---	---	0.1	---	100.0	SIM
51	34.0	28.8	21.8	8.2	2.1	2.0	0.1	0.3	1.3	1.4	---	---	---	---	99.9	SIM
52	39.7	28.3	20.8	6.0	2.0	2.0	tr	---	0.6	0.1	---	---	0.5	---	100.0	SIM
53	44.7	21.8	22.2	1.2	1.2	0.6	---	---	0.4	1.6	---	6.3	---	---	99.9	SIM
54	38.5	29.5	19.2	0.7	3.2	0.3	0.1	---	0.7	2.8	---	4.7	0.1	---	99.9	SIM
55	42.3	25.1	26.0	---	0.1	0.6	---	---	0.1	2.5	---	3.2	---	---	100.1	SIM
56	40.6	29.5	23.1	4.6	1.0	0.1	---	---	0.4	0.1	0.4	---	0.1	---	99.9	SIP
57	31.2	35.8	21.6	6.2	2.2	1.2	0.1	---	0.6	0.8	---	---	0.1	Alan. 0.4	100.1	SIP
58	35.6	22.8	28.4	4.9	1.3	2.0	---	0.1	1.1	3.0	0.1	0.6	0.1	---	100.0	SIP
59	29.7	29.3	20.9	8.1	3.3	0.6	---	---	0.4	2.3	0.6	3.5	1.2	---	100.0	SIP
60	35.3	31.5	19.1	5.3	1.5	2.2	1.7	0.1	0.8	1.9	--	0.3	0.1	---	99.9	SIP
61	39.5	25.3	22.5	5.3	2.6	1.5	---	0.3	1.0	1.5	---	---	0.4	---	99.9	SIP
62	36.1	30.1	17.8	8.7	1.6	3.1	---	---	0.3	0.3	0.1	1.1	0.1	Alan. 0.7	100.0	SIM
63	27.9	32.2	31.1	2.8	2.8	---	---	---	1.0	0.4	0.8	---	1.0	---	100.0	SIM

Table B.2 (cont'd)

Sample Number	Kspar	Plag	Qtz	Biot	Mag	Sph	Hbl	Zir	Ap	Ep	Sericite	Chl	Hem	Others	Total	Facies
64	44.1	24.2	27.0	4.4	0.1	---	---	---	---	0.1	---	---	---	---	100.0	SIM
65	30.4	30.2	18.4	7.7	4.0	1.4	---	0.2	0.7	3.5	---	0.4	3.0	---	100.0	SIP
66	32.7	27.1	19.4	10.0	1.8	1.2	0.5	---	0.5	3.7	---	1.7	0.2	Alan. 1.2	99.9	SIM
67	29.9	28.4	22.3	10.0	2.2	2.1	2.6	0.1	0.4	1.9	--	---	0.1	---	100.0	SIM
68	37.4	25.0	24.0	9.4	0.6	2.5	---	---	0.4	0.1	---	0.1	0.3	---	100.0	SIC
69	32.1	24.5	24.5	8.1	3.3	3.4	0.9	0.1	1.9	0.9	---	0.2	---	---	100.0	SIC
70	32.0	27.2	25.7	6.8	1.6	2.1	2.8	---	1.1	0.3	0.1	---	0.3	---	100.0	SIM
71	29.1	30.8	16.0	4.3	2.3	3.4	0.6	---	2.6	6.6	3.7	---	0.6	---	100.0	SIM
72	23.3	31.9	23.8	4.4	4.4	3.8	0.3	0.1	1.6	5.7	0.1	---	---	---	99.9	SIM
73	36.5	31.8	18.0	7.0	1.6	2.2	---	0.3	0.8	0.9	0.8	---	---	---	100.0	SIM
74	19.1	32.9	17.3	7.9	6.2	7.7	5.8	0.1	1.7	1.2	---	0.1	---	---	99.9	SIC
75	31.2	34.8	16.1	5.2	1.9	2.7	0.3	---	0.3	4.8	---	2.2	0.3	---	99.9	SIC
76	17.0	33.3	19.3	9.0	6.4	5.9	2.1	0.5	0.5	5.9	---	---	---	---	100.0	SIC
77	16.7	39.3	18.9	9.0	3.1	3.6	3.5	---	1.5	2.8	---	1.5	---	---	99.9	SIC
78	22.7	30.3	25.3	10.0	2.5	2.2	1.9	0.1	1.3	1.8	---	1.8	0.1	---	100.0	SIC
79	29.0	35.7	17.6	3.5	1.4	2.2	4.9	0.2	0.4	4.3	0.1	0.6	---	---	99.9	SIC
80	20.5	39.1	17.3	10.0	2.8	1.4	1.1	0.2	1.8	3.2	---	1.8	0.6	---	99.9	SIC
81	26.1	35.7	18.5	5.3	2.3	3.6	0.2	---	0.5	7.0	0.1	---	0.6	---	100.0	SIC
82	25.3	33.7	21.7	9.5	2.5	1.9	0.3	---	0.6	4.5	---	---	---	---	100.0	SIC
83	34.7	22.4	19.2	10.0	4.8	3.7	1.0	0.1	1.2	2.7	---	---	---	Alan. 0.3	100.1	SIC
84	21.3	31.4	15.6	10.2	7.0	4.3	2.5	---	0.8	6.2	---	---	0.4	---	99.9	SIC
85	24.8	33.4	15.9	9.2	2.3	3.0	3.3	0.1	2.3	5.1	0.5	---	---	---	99.9	SIP

Table B.2 (cont'd)

Sample Number	Kspar	Plag	Qtz	Biot	Mag	Sph	Hbl	Zir	Ap	Ep	Sericite	Chl	Hem	Others	Total	Facies
86	22.9	35.8	18.2	13.3	2.2	1.8	0.9	---	1.1	0.8	---	1.8	1.1	---	100.0	SIP
87	20.4	30.8	22.7	15.9	2.2	2.5	2.0	0.1	0.4	2.2	0.7	---	---	---	99.9	SIM
88	28.6	31.4	16.7	11.3	1.8	2.1	2.4	---	0.8	3.8	---	1.1	---	---	100.0	SIM
89	49.0	19.1	20.2	7.7	0.8	1.0	---	---	0.4	0.4	1.2	---	---	---	99.8	SIM
90	29.6	28.0	16.1	13.0	4.0	1.5	0.3	0.2	1.5	4.3	---	---	0.9	White Mica 0.1	100.0	SIM
91	28.6	30.4	20.0	8.9	2.9	3.4	0.4	0.1	1.6	2.9	---	0.5	---	---	99.9	SIP
92	34.4	26.3	21.6	10.0	2.3	1.7	---	---	1.6	0.2	1.8	---	---	---	100.0	SIM
93	46.7	22.7	26.7	0.9	0.8	---	---	---	0.1	0.2	0.7	---	1.3	---	100.1	SIM
94	17.1	22.2	20.4	15.9	6.5	6.2	6.8	---	2.1	2.7	---	---	---	Calcite 0.1	99.9	SIM
95	31.1	31.4	17.2	9.1	1.0	1.7	0.2	0.2	0.7	3.6	1.0	2.7	---	---	100.0	SIM
96	41.1	24.7	28.8	1.0	0.5	1.5	---	---	0.5	0.9	0.2	0.8	---	---	100.0	SIM
97	35.7	24.7	22.7	10.6	1.0	0.3	---	0.3	0.8	0.3	2.2	1.5	---	---	100.0	SIM
98	33.9	25.8	19.1	12.8	4.4	2.5	---	0.1	0.6	0.5	---	0.2	---	---	100.0	SIM
99	44.3	23.5	25.5	4.9	1.1	0.2	---	0.3	0.2	---	---	---	0.3	---	100.1	SIM
100	28.8	34.0	27.7	2.8	1.1	---	---	---	0.6	0.4	---	---	4.4	---	99.9	SIP
101	32.5	24.8	32.5	6.5	1.8	0.5	---	---	0.4	0.4	0.5	---	0.1	Alan. 0.1	100.1	SIP
102	39.0	21.9	27.2	5.4	3.8	---	---	0.1	0.8	0.1	0.1	0.4	0.1	---	100.0	SIP
103	24.4	27.7	22.3	11.5	5.3	1.0	---	---	2.6	5.3	---	---	---	---	100.0	SIC
104	24.7	33.0	14.9	11.4	3.1	2.3	6.1	0.2	1.6	1.5	---	1.0	---	Alan 0.2	100.1	SIC
105	16.6	40.6	19.0	9.1	4.0	3.9	2.4	0.2	1.2	1.9	---	0.8	0.3	---	100.0	SIC

Table B.2 (cont'd)

Sample Number	Kspar	Plag	Qtz	Biot	Mag	Sph	Hbl	Zir	Ap	Ep	Sericite	Chl	Hem	Others	Total	Facies
106	38.5	14.1	41.3	4.2	0.8	0.3	0.1	---	0.1	---	0.4	--	0.1	---	100.0	SIM
107	26.6	27.3	20.9	18.1	1.9	1.9	---	---	0.6	3.2	0.2	---	---	---	99.9	SIM
108	35.4	22.8	23.4	9.5	0.9	1.8	---	0.1	0.9	1.3	1.0	---	---	Alan. 2.8	100.0	SIM
109	33.4	22.5	17.5	15.9	3.3	2.5	---	0.5	0.8	2.5	0.6	0.1	0.3	---	99.9	SIM
110	26.0	25.9	22.2	14.7	3.7	3.9	---	0.2	1.5	1.3	0.3	---	---	---	99.9	SIM
111	17.3	37.7	20.6	10.4	4.1	3.5	4.6	---	0.8	0.6	---	0.3	---	---	100.0	SIC
112	16.5	35.8	16.2	18.8	1.9	2.2	5.2	---	0.9	2.1	---	---	0.4	---	100.0	SIC
113	17.1	34.9	23.4	0.8	2.5	1.6	19.7	---	---	---	---	---	---	---	100.0	FGR
114	22.7	31.0	19.4	8.4	4.8	4.1	3.9	0.1	2.0	2.8	0.1	0.5	0.1	---	100.0	SIM
115	28.1	35.9	19.0	6.9	2.0	3.4	0.6	---	0.9	1.6	3.4	1.7	---	---	100.1	SIM
116	25.7	34.0	17.5	9.8	3.0	2.8	1.6	---	0.9	2.1	---	0.5	---	Allan 0.2	100.0	SIM
117	24.1	35.5	15.9	12.7	2.9	2.1	2.8	---	0.6	2.9	0.1	---	0.3	Allan 0.1	100.0	SIM
118	25.1	29.3	24.6	10.8	3.1	2.4	---	---	0.7	2.7	0.9	---	0.3	---	99.9	SIM
119	31.9	25.8	24.0	7.9	4.0	1.3	0.3	---	1.3	---	1.2	2.1	---	---	99.9	SIM
120	26.2	28.4	28.2	12.6	1.6	0.3	---	---	0.4	2.1	0.1	---	---	---	99.9	SIM
121	24.9	28.6	26.3	10.1	1.5	2.9	4.9	0.3	---	---	---	0.4	---	White Mica 0.1	100.0	SIC
122	30.2	34.2	19.8	7.7	2.3	2.9	1.9	0.2	0.1	0.2	---	0.3	---	White Mica 0.2	100.0	SIC
123	30.5	34.4	24.0	8.2	1.8	0.5	0.2	0.3	0.1	---	---	---	---	---	100.0	SIC
124	29.9	30.4	25.1	5.1	2.4	1.7	4.1	---	0.1	0.4	---	0.4	---	White Mica 0.4	100.0	SIC
125	29.6	30.5	28.6	8.7	1.8	0.6	---	0.1	---	---	---	0.1	---	---	100.0	SIP
126	29.2	24.7	26.7	6.6	1.8	3.3	---	0.1	---	6.3	0.5	0.7	---	---	99.9	SIC
127	39.3	33.5	24.8	1.7	0.4	---	---	0.1	---	---	0.1	---	0.2	---	100.1	SIM

Table B.2 (cont'd)

Sample Number	Kspar	Plag	Qtz	Biot	Mag	Sph	Hbl	Zir	Ap	Ep	Sericite	Chl	Hem	Others	Total	Facies
128	35.8	36.2	25.7	1.7	0.3	---	---	---	---	---	---	---	0.3	---	100.0	SIM
129	35.3	30.7	24.4	7.2	0.3	---	---	---	---	---	1.8	---	---	---	100.0	SIM
130	26.2	32.5	15.1	7.0	3.6	3.4	4.7	---	0.8	4.2	---	2.4	---	---	99.9	SIC
131	35.8	26.8	17.4	11.5	2.7	1.7	0.3	---	0.6	0.6	---	2.6	0.4	---	100.0	SIC
132	16.2	38.6	25.1	13.1	2.3	2.9	0.3	---	0.7	0.6	---	---	0.2	---	100.1	SIC
133	37.7	25.0	19.3	6.5	1.0	1.8	0.8	0.1	1.1	3.5	---	3.1	0.1	---	100 0	SIM
134	27.2	30.8	21.4	5.2	5.0	2.6	---	---	1.9	3.5	---	2.0	---	Alan. 0.4	100 0	SIM
135	36.2	27.1	23.0	3.0	3.5	0.7	---	---	0.5	3.6	---	2.3	0.2	---	100.0	SIC
136	29.3	36.2	23.4	5.3	2.1	1.7	---	---	0.3	0.3	---	1.1	0.3	---	100.0	SIM
137	31.7	25.1	23.3	11.5	2.9	3.1	1.4	0.4	---	---	---	---	---	White Mica 0.1 Garnet 0.3	99.8	SIP
138	32.2	34.4	17.4	7.0	3.8	3.6	0.4	0.3	---	0.5	---	---	---	Garnet 0.4	100.0	SIC
139	37.9	34.6	24.3	3.2	---	---	---	---	---	---	---	---	---	---	100.0	SIC
140	31.6	30.5	31.9	3.5	0.9	0.7	---	0.1	---	0.7	---	---	---	Garnet 0.1	100.0	SIP
141	32.2	41.8	19.4	6.2	---	---	---	---	---	---	---	0.4	---	---	100.0	SIC
142	29.8	28.5	29.6	7.7	1.0	1.0	---	---	0.1	1.7	---	---	---	White Mica 0.6	100.0	SIM
143	18.6	38.0	27.4	9.7	2.9	0.2	---	0.1	---	0.9	---	---	---	White Mica 2.2	100.0	SIM
144	24.2	31.1	25.3	12.3	3.7	0.9	---	0.1	0.1	---	---	---	---	White Mica 2.3	100.0	SIM
145	30.9	27.2	27.2	9.5	1.8	1.0	---	0.1	---	1.6	---	---	---	White Mica 0.5	99.8	SIM
146	33.2	32.8	25.9	4.2	1.8	1.4	---	0.2	---	---	---	---	---	White Mica 0.4	99.9	SIM
147	29.6	27.7	25.7	10.0	3.6	1.7	---	0.4	0.4	0.5	---	---	---	White Mica 0.4	100 0	SIM
148	24.3	30.6	24.1	13.3	2.4	2.6	---	0.2	0.3	0.3	---	---	---	White Mica 0.8 Rutile 0.1	99 0	SIM

Table B.2 (cont'd)

Sample Number	Kspar	Plag	Qtz	Biot	Mag	Sph	Hbl	Zir	Ap	Ep	Sericite	Chl	Hem	Others	Total	Facies
149	26.6	30.5	26.8	10.4	2.6	1.5	---	0.1	0.1	0.9	---	---	---	White Mica 0.4 Rutile 0.1	100.0	SIM
150	40.1	29.0	11.1	11.4	2.2	3.3	---	---	1.4	1.2	---	---	0.4	---	100.0	SIM

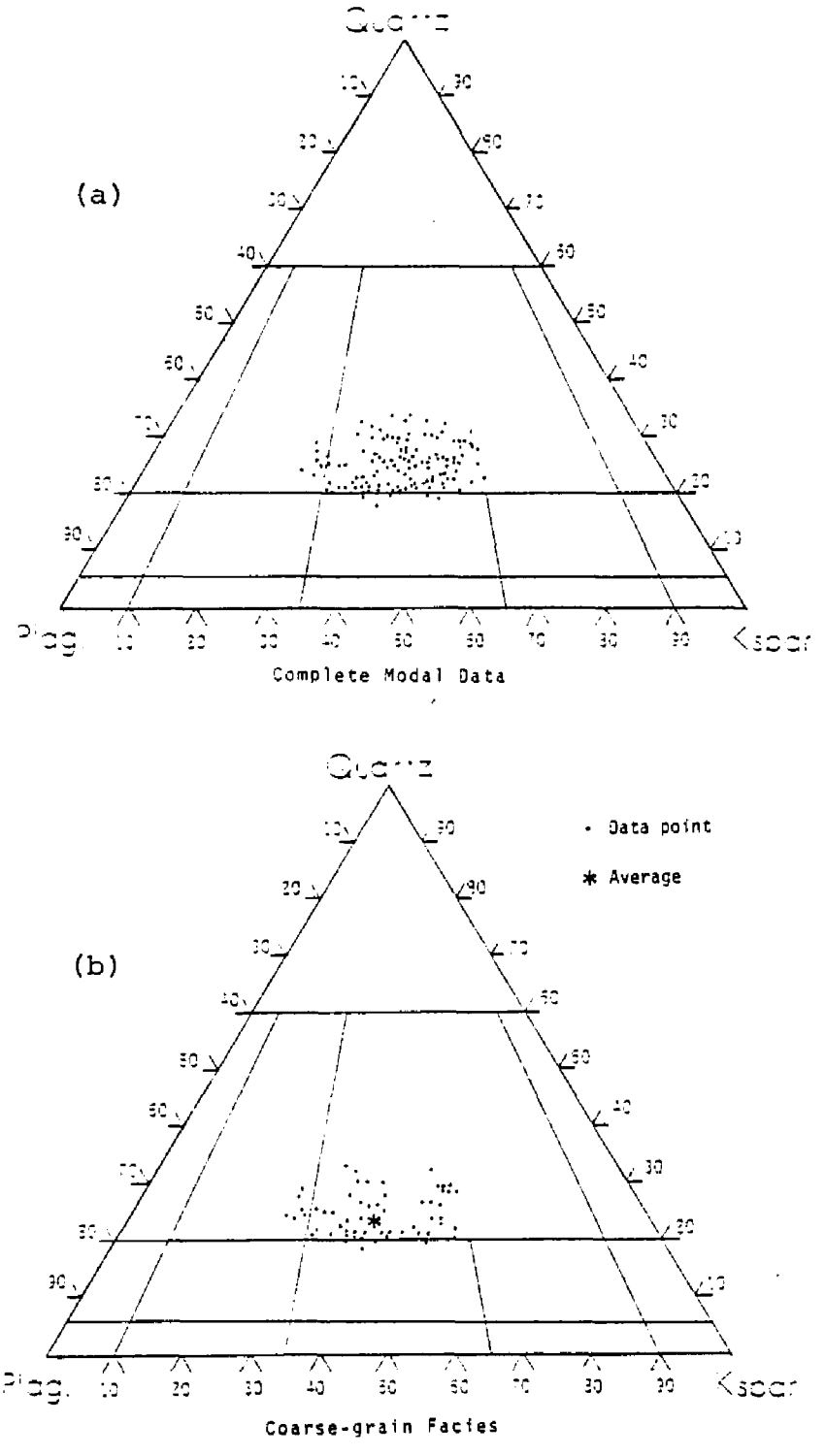

Figure B.3. Modal distribution of quartz, Kspar, and plagioclase in 150 samples of the San Isabel granite

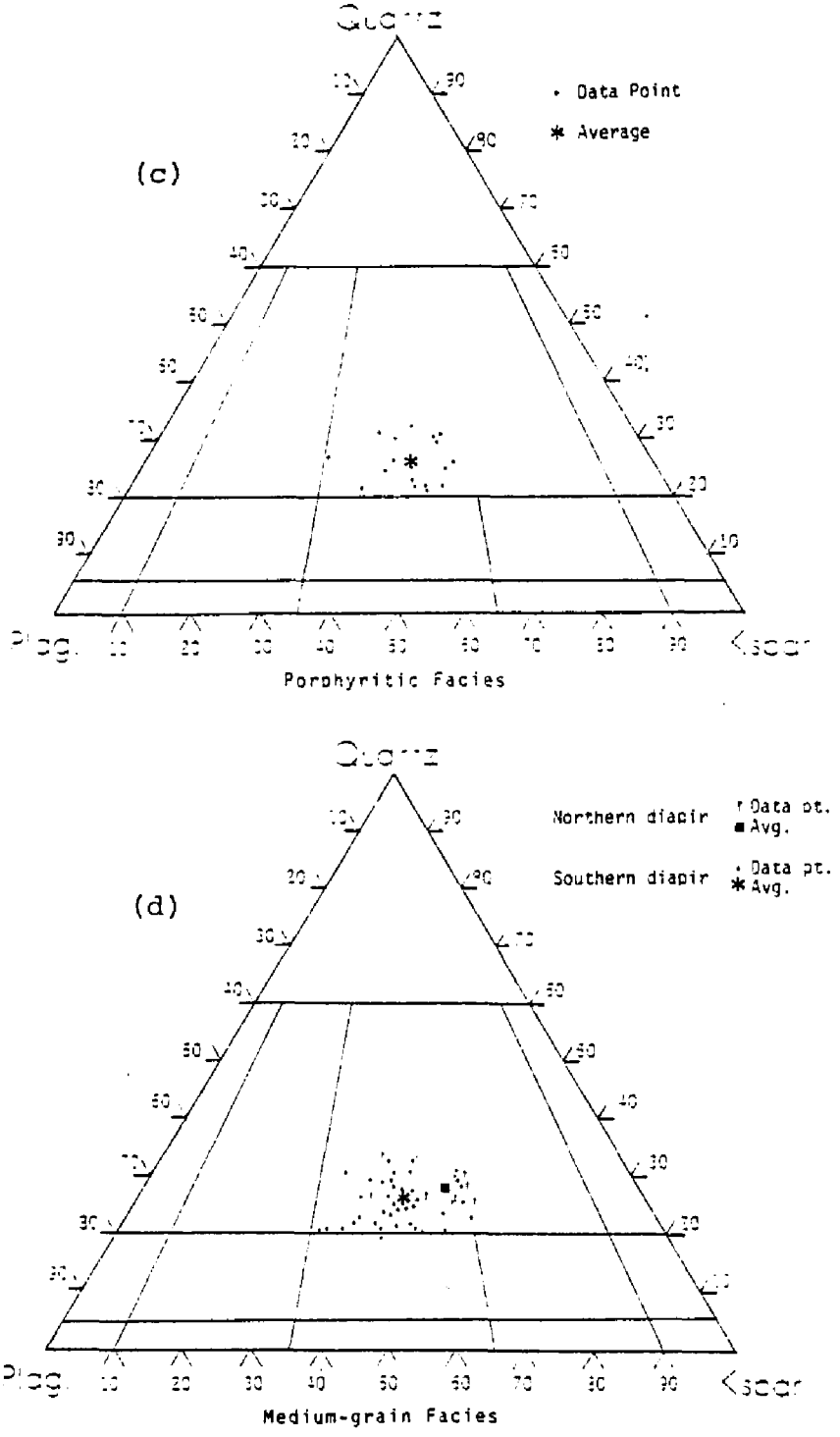

Figure B.3 (cont'd)

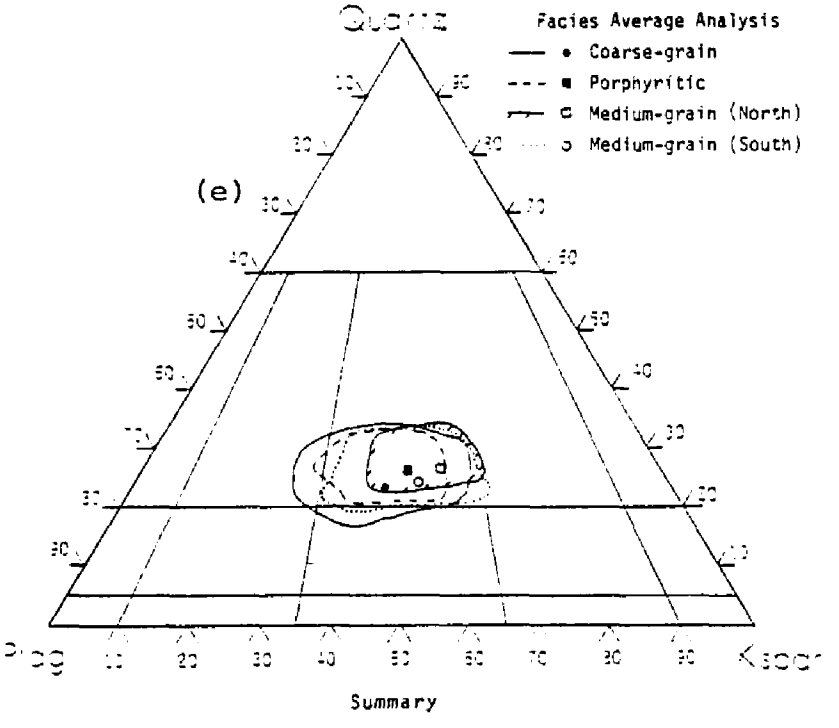

Figure B.3 (cont'd)

established by Johannsen (1939). The petrologic rock names that appear on the trigonal diagrams are taken from Streckeisen (1967).

Thirty-six rock samples from the San Isabel batholith were analyzed for major elements. The CIPW norms were also calculated (Table B.4). Figure B.5 displays cation oxide percentages plotted against SiO_2 percentages.

Table B.4. Chemical analysis and CIPW norms of the San Isabel batholith (percent weight)

Sample #	3	9	11	17	21	22
Chemical#	1	2	3	4	5	6
SiO_2	65.49	66.51	58.41	66.23	69.63	65.41
Al_2O_3	16.35	15.89	18.08	15.51	15.92	15.58
Fe_2O_3	2.56	2.15	1.99	3.39	2.25	2.02
FeO	2.66	2.26	3.57	1.99	0.39	3.05
MnO	0.13	0.12	0.09	0.10	0.03	0.13
MgO	1.53	1.00	1.92	1.45	0.24	1.83
CaO	3.45	3.43	5.41	1.98	2.14	2.95
Na_2O	3.45	3.13	3.64	3.40	3.34	2.98
K_2O	3.10	4.22	3.22	4.90	5.02	4.06
TiO_2	1.19	0.75	1.13	0.85	0.52	1.38
	99.91	99.46	97.46	99.99	99.48	99.39
Qtz	23.19	22.41	9.67	22.29	26.14	22.53
Or	18.37	25.05	18.92	23.94	29.50	23.94
Ab	29.37	26.75	30.54	28.84	28.32	25.18
An	17.25	16.69	23.37	14.75	10.57	14.75
C	0.92	---	---	---	1.12	0.92
En	4.02	2.61	4.22	3.75	0.60	4.72
Fs	0.79	1.32	2.51	---	---	1.58
Mt	3.70	3.01	2.78	3.94	0.75	3.01
Il	2.28	1.37	2.12	1.67	0.16	2.58
Mg Di	---	0.21	1.52	---	---	---
Fe Di	---	---	1.24	---	---	---
Cr	---	---	---	0.10	---	---
He	---	---	---	0.64	2.24	---
Wo	---	---	---	---	---	---
Hm	---	---	---	---	---	---
Rt	---	---	---	---	---	---

Table B.4 (cont'd). Chemical analysis and CIPW norms of the San Isabel batholith (percent weight)

Sample #	34	35	36	43	48	49
Chem #	7	8	9	10	11	12
SiO_2	72.21	68.20	69.93	69.40	66.43	62.05
Al_2O_3	13.90	16.07	16.20	15.26	15.90	17.48
Fe_2O_3	1.16	1.23	0.81	1.39	2.21	2.64
FeO	0.45	2.02	0.95	1.15	2.65	3.29
MnO	0.03	0.09	0.02	0.01	0.13	0.09
MgO	0.45	1.14	0.44	0.29	1.50	1.45
CaO	2.00	2.34	2.77	2.07	2.36	3.78
Na_2O	3.67	2.93	2.99	4.00	2.87	3.02
K_2O	5.17	4.59	4.25	5.08	4.59	4.13
TiO_2	0.20	0.71	0.28	1.29	1.22	0.98
	99.24	99.32	98.54	99.94	99.86	98.91
Qtz	26.49	26.14	29.62	21.99	24.33	17.24
Or	30.62	27.28	25.05	30.06	27.28	24.49
Ab	30.94	24.65	25.17	34.09	24.12	25.69
An	6.12	11.68	13.63	8.62	11.68	18.64
C	---	---	---	---	1.94	---
En	---	2.91	1.10	0.10	3.91	3.71
Fs	---	1.45	0.52	---	1.06	2.24
Mt	0.69	1.85	1.16	---	3.24	3.94
Il	0.46	1.36	0.61	2.43	2.28	1.82
Mg Di	2.38	---	---	1.31	---	---
Fe Di	---	---	---	---	---	---
Cr	---	2.04	1.73	---	---	1.12
He	---	---	---	---	---	---
Wo	1.27	---	---	---	---	---
Hm	0.64	---	---	1.44	---	---
Rt	---	---	---	---	---	---

Table B.4 (cont'd). Chemical analysis and CIPW norms of the San Isabel batholith (percent weight)

Sample #	52	54	59	60	64	70
Chem. #	13	14	15	16	17	18
SiO_2	73.27	70.68	66.83	70.91	70.59	67.78
Al_2O_3	14.57	14.66	16.07	14.53	14.53	16.25
Fe_2O_3	1.75	1.13	3.81	2.33	0.67	1.61
FeO	1.07	1.35	1.83	1.09	1.09	2.13
MnO	0.04	0.04	0.07	0.09	0.12	0.11
MgO	0.05	0.44	1.01	1.18	0.41	1.02
CaO	1.14	2.00	2.11	2.00	2.14	2.35
Na_2O	3.02	3.18	3.52	3.34	3.36	3.48
K_2O	4.69	4.66	4.01	4.16	5.04	3.53
TiO_2	0.21	0.81	0.65	0.83	0.33	1.01
	99.81	98.95	99.91	100.46	98.28	99.27
Qtz	34.97	29.44	24.63	29.44	26.20	27.16
Or	27.83	27.28	23.94	24.49	30.06	20.60
Ab	25.70	26.75	29.89	28.32	28.32	29.37
An	5.56	10.02	10.57	10.02	9.46	11.68
C	2.45	0.82	2.04	0.92	---	2.45
En	0.20	1.20	2.61	3.01	---	2.71
Fs	0.13	0.26	---	---	0.66	0.92
Mt	2.55	1.62	3.94	1.15	0.92	2.32
Il	0.45	1.52	1.21	1.52	0.61	1.97
Mg Di	---	---	---	---	0.43	---
Fe Di	---	---	---	---	0.50	---
Cr	---	---	---	---	---	---
He	---	---	---	---	---	---
Wo	---	---	---	---	---	---
Hm	---	---	1.12	1.60	---	---
Rt	---	---	---	---	---	---

Table B.4 (cont'd). Chemical analysis and CIPW norms of the San Isabel batholith (percent weight)

Sample #	74	77	84	85	89	98
Chem. #	19	20	21	22	23	24
SiO_2	56.16	73.61	61.75	63.04	71.42	61.57
Al_2O_3	17.89	13.67	17.03	15.91	14.14	16.21
Fe_2O_3	2.97	1.27	3.03	3.88	1.83	2.68
FeO	5.29	0.43	3.75	3.79	1.52	4.09
MnO	0.16	0.09	0.12	0.13	0.09	0.15
MgO	2.49	0.54	1.64	1.54	0.76	2.43
CaO	7.28	1.33	4.25	3.71	0.64	2.05
Na_2O	3.09	3.35	3.21	2.56	3.96	3.57
K_2O	2.53	4.58	3.21	3.83	4.71	5.36
TiO_2	1.51	0.42	0.96	1.33	0.51	0.86
	99.37	99.29	98.95	99.72	99.59	98.87
Qtz	8.77	32.75	17.79	22.41	27.93	10.70
Or	15.03	27.28	18.93	22.82	27.83	31.71
Ab	26.22	28.32	27.27	21.50	33.04	30.41
An	27.26	6.67	21.14	18.36	3.06	10.29
C	---	0.71	0.51	0.82	1.53	0.71
En	---	1.40	4.32	4.01	2.01	6.22
Fs	3.30	---	2.77	1.58	0.53	2.51
Mt	4.40	0.23	4.40	5.55	2.55	3.94
Il	2.88	0.76	1.82	2.58	0.91	3.19
Mg Di	4.76	---	---	---	---	---
Fe Di	2.48	---	---	---	---	---
Cr	---	---	---	---	---	---
He	---	---	---	---	---	---
Wo	---	---	---	---	---	---
Hm	---	1.12	---	---	---	---
Rt	---	---	---	---	---	---

Table B.4 (cont'd). Chemical analysis and CIPW norms of the San Isabel batholith (percent weight)

Sample #	101	104	106	107	112	121
Chem. #	25	26	27	28	29	30
SiO_2	75.24	64.91	75.55	60.92	64.72	70.29
Al_2O_3	13.21	16.15	12.47	16.95	16.85	14.61
Fe_2O_3	1.10	1.64	1.25	1.24	1.66	2.20
FeO	0.67	3.20	0.30	4.16	3.02	1.08
MnO	0.05	0.10	0.02	0.19	0.10	0.12
MgO	0.56	1.46	0.11	2.49	1.80	1.80
CaO	0.81	4.19	0.82	4.63	4.25	0.71
Na_2O	3.00	3.37	2.79	3.23	3.37	3.28
K_2O	4.82	3.19	5.20	3.99	3.26	4.71
TiO_2	0.36	0.83	0.25	1.50	0.76	0.98
	99.82	99.04	98.76	99.30	99.79	99.78
Qtz	36.95	20.67	37.49	11.96	19.94	28.78
Or	28.39	18.93	30.62	23.38	19.48	27.83
Ab	25.17	28.32	23.60	27.27	28.32	27.80
An	3.89	19.47	4.17	20.04	21.14	3.12
C	---	---	0.71	---	---	2.75
En	1.51	3.51	0.30	5.82	4.62	4.72
Fs	---	3.03	---	3.56	1.72	---
Mt	---	2.32	---	1.85	2.32	---
Il	1.36	1.52	0.61	2.88	2.88	2.28
Mg Di	---	0.65	---	1.52	---	---
Fe Di	---	0.50	---	0.99	---	---
Cr	1.73	---	---	---	---	---
He	---	---	---	---	---	---
Wo	---	---	---	---	---	---
Hm	1.12	---	1.28	---	---	2.24
Rt	---	---	0.16	---	---	---

Table B.4 (cont'd). Chemical analysis and CIPW norms of the San Isabel batholith (percent weight)

Sample #	129	131	141	142	145	147
Chem. #	31	32	33	34	35	36
SiO_2	74.61	72.60	70.03	69.23	71.49	68.41
Al_2O_3	14.45	14.92	14.60	16.23	15.50	14.99
Fe_2O_3	0.32	0.86	0.68	0.64	0.67	0.81
FeO	0.27	1.47	2.13	1.87	1.23	2.98
MnO	0.01	0.13	0.02	0.01	0.02	0.06
MgO	0.13	0.57	1.05	0.58	0.98	1.29
CaO	1.38	2.13	2.22	2.16	1.84	2.56
Na_2O	3.43	2.86	3.50	3.12	3.43	2.99
K_2O	4.65	4.76	4.51	4.19	4.25	4.13
TiO_2	0.14	0.38	0.59	0.74	0.42	0.69
	99.39	100.68	99.33	98.77	99.83	98.91
Qtz	34.07	31.48	25.12	29.02	29.56	26.14
Or	27.28	28.39	26.72	24.29	25.05	24.49
Ab	28.84	24.12	29.36	26.22	28.84	25.17
An	6.68	10.57	10.85	10.85	9.18	12.80
C	1.43	1.13	---	2.65	1.94	0.92
En	0.30	1.61	2.51	1.41	2.41	3.31
Fs	---	1.32	2.51	1.72	1.06	3.56
Mt	0.23	1.16	0.93	0.93	0.93	1.16
Il	0.46	0.76	1.06	1.37	0.76	1.37
Mg Di	---	---	0.22	---	---	---
Fe Di	---	---	---	---	---	---
Cr	---	---	---	---	---	---
He	---	---	---	---	---	---
Wo	---	---	---	---	---	---
Hm	0.16	---	---	---	---	---
Rt	---	---	---	---	---	---

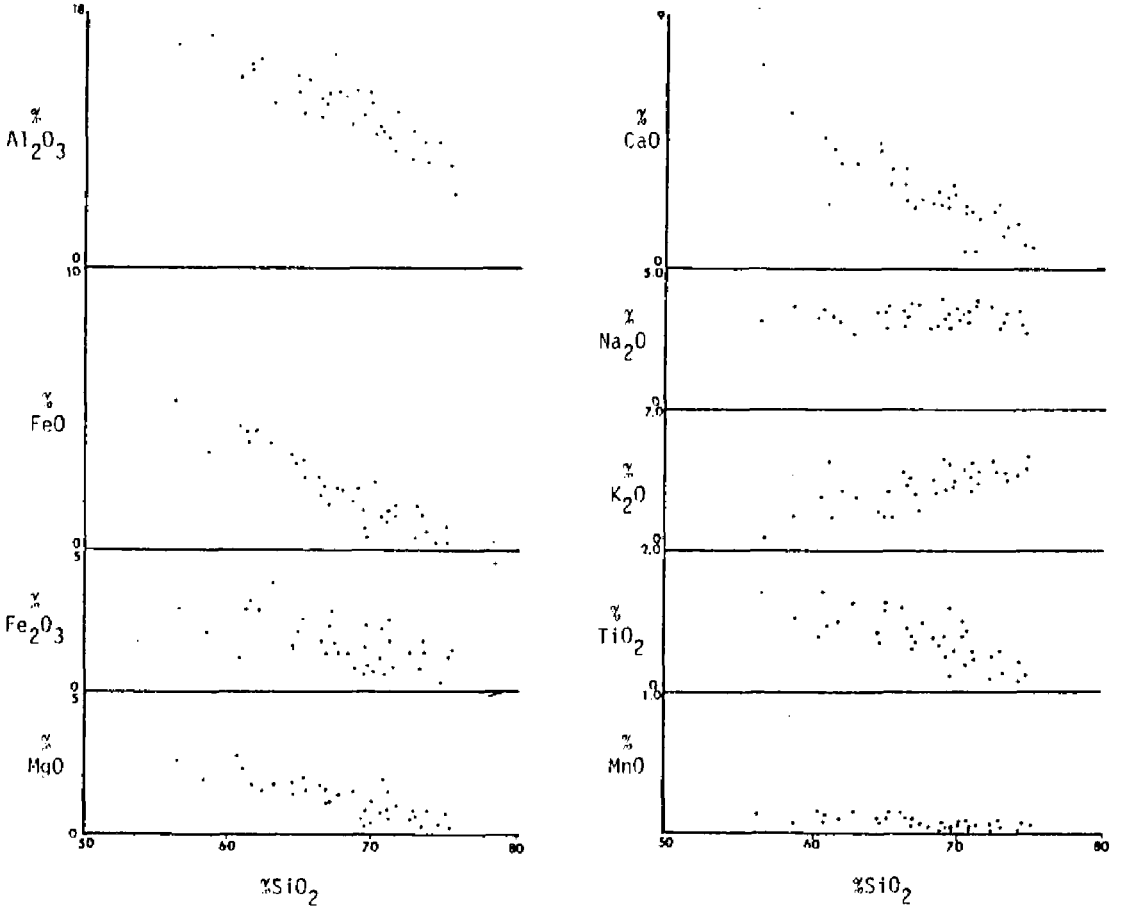

Figure B.5. Variation diagrams for the various cation oxides of the San Isabel batholith

APPENDIX C

SUMMARY OF MODAL AND CHEMICAL DATA OF THE WIXSON DIVIDE PLUTON

Sample locations within the Wixson pluton are shown on the index map (Figure C.1). The index map shows several areas with relatively high density in the sample population. These areas represent limited exposures of fresh rock that could be easily sampled. Approximately 40% of the pluton is nearly devoid of collected samples and hence represent areas where granites are covered by alluvium, colluvium, or dense forest vegetation.

Modal analysis of 94 samples collected from the Wixson Divide pluton and some of its smaller adjacent satellites are listed in Table C.2. Included in the table are 14 samples collected along two traverses. The five samples collected along traverse "A" in Figure C.1 include three amphibolites from the wall rock and two granitic rocks from the pluton, while traverse "B" includes four granite gneisses and two granite samples. All traverse specimens were collected within 900 meters of the granite-gneiss contact. Two other samples included on Figure C.1 were collected as external

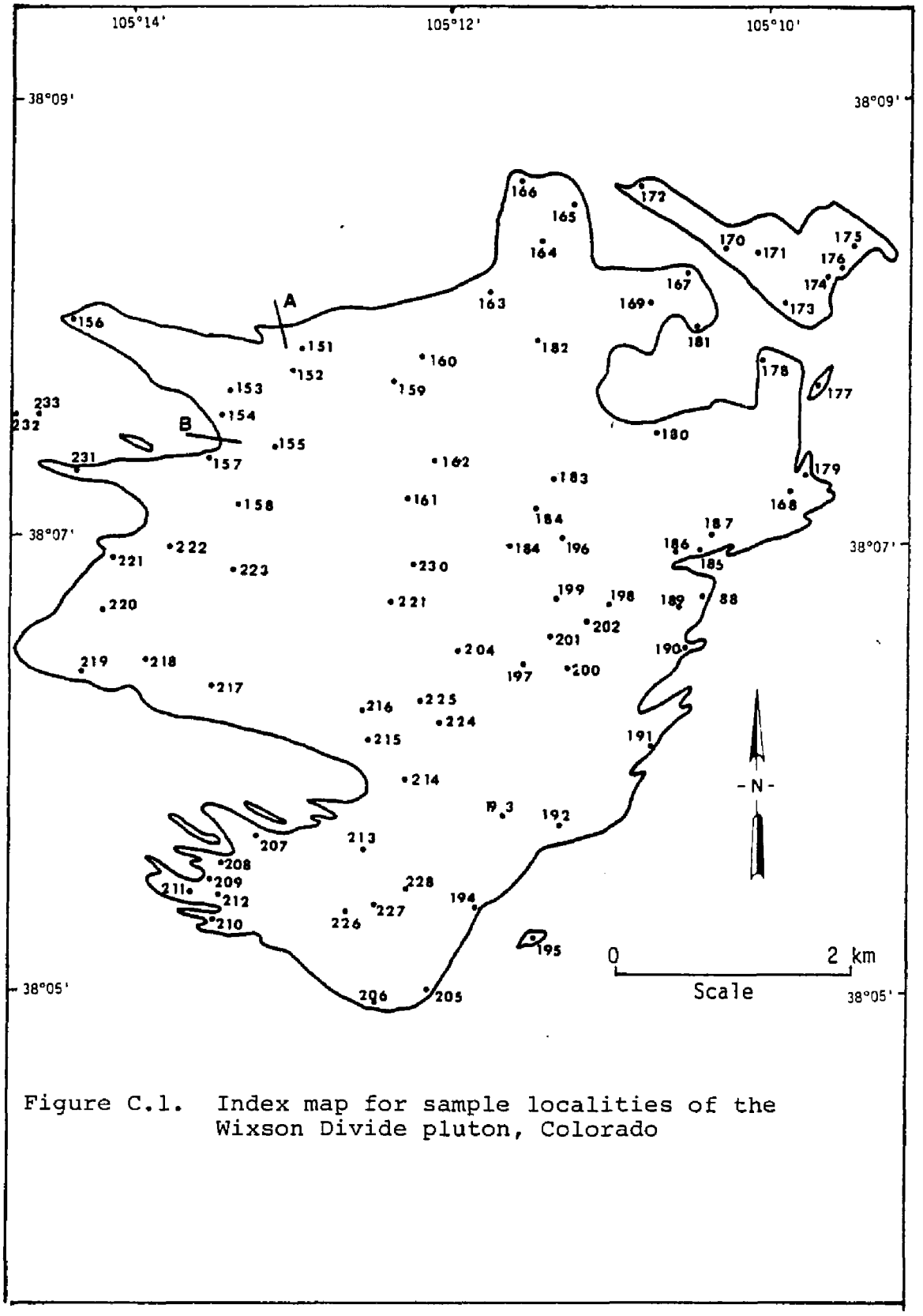

Figure C.1. Index map for sample localities of the Wixson Divide pluton, Colorado

standards for the wall rock. The two specimens were collected at a distance of 1000 meters from the plutonic border, so as to be unaffected by any chemical gradients that might be associated with the intrusion of the Wixson Divide granite.

Triangular diagrams (Figure C.3) graphically summarize the modes given in Table C.2. Chemical analysis and CIPW norms of 24 of the modal samples of the Wixson Divide pluton are shown in Table C.4. Figure C.5 displays cation oxide percentages plotted against SiO_2 percentages.

Table C.2. Modal Analysis of granitic rocks from the Wixson Divide pluton

Sample Number	Kspar	Plag	Qtz	Biot	Mag	Sph	Zir	Ap	Ep	Chl	Mus	All	Gr	Others	Facies	Total
151	31.9	25.9	36.9	2.9	1.3	0.9	0.2	---	---	---	---	---	0.1	---	Wdf	100.1
152	37.6	23.4	27.0	8.6	2.3	---	0.2	0.2	---	---	0.7	---	---	---	Wdf	100.0
153	39.5	16.5	26.1	8.0	1.8	3.9	0.4	---	---	---	3.7	---	0.1	---	Wdc	100.0
154	29.3	28.0	27.2	6.5	2.2	1.3	0.1	0.1	---	0.2	4.6	0.3	0.1	---	Wdm	99.9
155	37.6	21.7	25.3	7.5	3.4	1.9	0.1	---	---	---	2.5	---	---	---	Wdm	100.0
156	43.9	31.5	12.5	8.6	2.0	0.4	0.4	---	---	---	0.7	---	---	---	Wdm	100.0
157	39.1	22.3	26.1	10.2	1.0	0.4	0.2	0.2	0.2	0.1	0.1	---	0.1	---	Wdm	100.0
158	34.3	34.8	24.2	6.2	0.4	---	0.1	---	---	---	---	---	---	---	Wdc	100.0
159	33.6	32.8	20.3	8.8	1.2	0.9	0.1	0.1	0.3	0.1	1.8	---	---	---	Wdc	100.0
160	35.4	32.7	22.1	6.4	1.6	1.5	---	0.1	---	---	0.2	---	---	---	Wdc	100.0
161	26.7	35.7	22.5	8.5	1.8	0.0	0.1	0.1	0.7	0.1	3.8	---	---	---	Wdc	100.0
162	26.0	26.4	25.8	12.8	2.4	2.9	0.3	0.1	1.0	0.7	1.4	0.2	---	---	Wdc	100.0
163	25.2	31.5	27.4	8.2	2.8	0.2	---	---	0.5	---	4.1	---	0.1	---	Wdc	100.0
164	19.4	34.1	29.8	13.2	1.6	1.0	0.2	---	0.2	---	0.2	0.2	0.1	---	Wdc	99.6
165	32.0	23.9	29.3	9.5	1.9	1.9	0.1	---	---	---	1.4	---	---	---	Wdm	100.0
166	38.0	20.0	29.0	8.1	1.3	1.4	0.1	---	---	---	2.1	---	---	---	Wdc	100.0
167	63.7	10.7	21.6	2.9	0.1	0.1	---	---	---	---	0.9	---	---	---	Wdm	100.0
168	39.3	22.8	22.9	5.6	2.1	2.7	0.1	0.6	1.1	0.2	2.5	0.1	---	---	Wdm	100.0
169	40.4	27.3	22.6	5.3	0.9	0.1	0.1	0.1	---	---	3.2	---	---	---	Wdm	100.0

Table C.2 (cont'd).

Sample Number	Kspar	Plag	Qtz	Biot	Mag	Sph	Zir	Ap	Ep	Chl	Mus	All	Gr	Others	Facies	Total
170	38.7	25.7	22.1	10.5	0.7	---	---	---	---	---	1.8	---	---	Clay Min. 0.5	Wdm	100.0
171	45.4	20.4	30.8	1.9	0.3	---	---	---	---	0.3	0.9	---	---	---	Wdm	100.0
172	44.3	20.0	23.5	6.0	1.9	2.6	---	---	---	0.1	1.5	---	---	---	Wdm	99.9
173	40.2	22.9	31.3	3.3	---	---	---	---	---	---	2.3	---	---	---	Wdm	100.0
174	30.8	30.4	24.4	8.7	1.8	---	0.3	---	---	---	3.6	---	---	---	Wdf	100.0
175	35.9	22.4	25.5	5.3	1.8	2.5	0.1	0.2	0.2	0.1	4.2	---	0.1	Clay Min. 1.6	Wdm	99.9
176	37.0	19.0	29.7	8.7	1.4	1.4	0.1	0.3	---	0.4	2.0	---	---	---	Wdm	100.0
177	40.9	25.6	24.6	5.9	2.5	---	---	0.2	---	---	---	---	0.1	Fluorite 0.1	Wdf	99.9
178	39.5	19.8	25.6	8.9	2.6	1.1	---	0.1	---	---	2.3	---	---	Clay Min. 1.8	Wdm	100.1
179	49.4	28.4	18.6	1.8	0.5	---	---	---	0.6	---	0.7	---	---	---	Wdm	100.0
180	30.5	32.5	26.3	7.5	1.3	1.3	0.1	---	---	---	0.3	---	---	---	Wdc	99.8
181	36.4	29.3	23.7	6.5	1.9	0.8	0.1	---	0.3	0.1	0.8	0.1	---	---	Wdm	100.0
182	33.2	33.4	23.1	4.5	2.4	---	0.1	0.2	0.6	0.4	0.3	0.2	---	Clay Min. 1.2 Hematite 0.4	Wdm	100.0
183	31.5	33.9	24.2	6.6	1.2	1.8	0.2	0.1	---	---	0.5	---	---	---	Wdc	100.0
184	26.5	33.2	17.9	10.6	2.5	0.7	---	---	---	---	8.5	0.1	---	---	Wdc	100.0
185	32.1	21.9	34.1	2.8	2.9	0.3	0.1	0.3	1.8	0.4	2.2	---	---	Clay Min. 1.1	Wdf	100.0
186	42.1	20.3	23.6	7.1	1.5	1.4	---	0.2	0.6	---	3.2	---	---	---	Wdm	100.0
187	37.3	22.5	23.0	9.6	2.2	3.0	0.6	0.4	---	---	1.4	---	---	---	Wdf	100.0
188	46.8	18.0	22.1	6.5	2.6	1.0	0.1	0.1	---	0.1	2.6	0.1	---	---	Wdf	100.0
189	47.2	24.0	27.2	0.4	0.8	0.4	---	---	---	---	---	---	---	---	Wdf	100.0
190	35.7	29.7	28.2	4.2	1.2	0.5	---	---	---	---	0.3	---	0.1	---	Wdf	99.9

Table C.2 (cont'd).

Sample Number	Kspar	Plag	Qtz	Biot	Mag	Sph	Zir	Ap	Ep	Chl	Mus	All	Gr	Others	Facies	Total
191	27.7	29.1	29.1	6.9	2.4	1.7	---	---	---	0.1	2.9	---	0.1	---	Wdf	100.0
192	44.0	25.2	22.4	5.2	0.9	1.0	0.1	---	---	---	1.2	---	---	---	Wdf	100.0
193	36.2	23.3	27.1	6.9	2.3	0.5	0.3	0.1	0.8	---	2.4	---	---	Rutile 0.2	Wdf	100.1
194	39.8	22.4	30.4	3.7	1.4	---	0.2	0.2	---	1.6	0.2	---	0.1	---	Wdf	98.2
195	43.3	22.4	28.6	3.9	1.7	---	0.1	---	---	---	---	---	---	---	Wdf	100.0
196	26.9	30.7	27.5	9.7	3.0	1.1	---	---	0.3	---	0.8	---	---	---	Wdc	100.0
197	30.2	37.2	24.1	4.6	1.7	0.7	0.1	---	---	---	1.4	---	---	---	Wdc	100.0
198	33.6	26.3	24.7	7.4	1.6	1.4	0.4	---	---	0.1	4.5	---	---	Fluorite 0.1	Wdc	100.1
199	26.1	31.5	22.2	10.4	2.4	3.7	0.1	0.1	2.9	---	0.5	0.1	---	---	Wdc	100.0
200	40.9	26.6	20.9	6.9	1.8	1.7	0.1	---	0.2	---	0.8	---	0.1	---	Wdc	100.0
201	26.9	32.2	24.3	9.8	2.7	0.6	0.1	---	0.8	0.1	2.5	---	---	---	Wdc	100.0
202	29.8	27.6	27.3	10.1	1.5	1.6	0.3	---	0.3	0.4	0.9	---	---	---	Wdc	100.0
203	25.4	37.9	23.2	9.0	2.0	1.7	---	0.1	0.4	---	0.2	---	---	---	Wdc	99.9
204	38.2	21.6	29.8	5.5	2.1	0.3	0.3	0.2	---	---	1.7	---	---	Hornblende 0.2	Wdc	99.9
205	44.0	15.4	28.0	8.3	3.2	0.6	---	0.4	---	---	---	0.1	---	---	Wdm	100.0
206	34.9	27.0	27.4	7.2	1.0	---	0.2	---	---	---	2.3	---	---	---	Wdm	100.0
207	49.5	15.2	24.2	7.7	0.5	0.5	---	0.1	0.2	---	2.0	---	---	Hornblende 0.1	Wdm	100.0
208	38.9	18.4	32.3	6.1	1.2	0.7	---	---	---	---	2.4	---	---	---	Wdm	100.0
209	44.1	26.0	25.3	3.8	0.8	---	---	---	---	---	0.2	---	---	---	Wdm	100.0
210	37.4	27.8	29.7	3.6	1.3	0.2	---	---	---	---	---	---	---	---	Wdf	100.0
211	52.2	15.0	32.6	---	---	---	---	---	---	---	0.2	---	---	---	Wdf	100.0

Table C.2 (cont'd).

Sample Number	Kspar	Plag	Qtz	Biot	Mag	Sph	Zir	Ap	Ep	Chl	Mus	All	Gr	Others	Facies	Total
212	39.7	21.9	33.4	1.6	0.9	0.5	---	---	---	---	2.0	---	---	---	Wdm	100.0
213	34.7	28.7	28.8	4.2	0.9	0.5	---	---	---	---	2.3	---	---	---	Wdm	100.1
214	38.7	27.1	31.7	0.4	0.6	---	---	---	---	---	1.5	---	---	---	Wdc	100.0
215	47.4	17.2	26.7	3.4	0.9	1.1	0.1	0.2	0.5	0.6	1.8	---	0.1	---	Wdc	100.0
216	35.8	26.6	32.6	1.3	0.5	---	---	---	---	---	2.0	---	---	Clay Min. 1.0 Pyrolucite 0.1	Wdc	100.0
217	36.4	28.9	25.0	7.3	1.3	---	0.2	---	---	---	0.9	---	---	---	Wdc	100.0
218	41.8	25.1	23.1	7.5	0.4	---	0.1	0.1	---	---	0.6	---	---	Hornblende 0.7 Clay Min. 0.6	Wdm	100.0
219	34.2	21.2	22.8	14.1	1.7	2.8	0.4	0.3	---	---	2.5	---	---	---	Wdf	100.0
220	31.8	25.9	23.9	---	1.1	0.2	---	---	3.7	---	---	---	---	Clay Min. 3.3	Wdm	99.9
221	36.5	23.7	30.6	7.5	1.0	0.1	---	---	---	0.1	0.4	---	---	---	Wdf	99.9
222	35.3	12.7	30.7	9.2	2.5	1.8	0.3	0.1	---	0.1	2.2	---	---	Caly Min. 5.1	Wdc	100.0
223	45.9	28.2	18.6	3.9	0.7	0.3	---	0.1	0.3	0.2	2.7	---	---	Fluorite 0.1	Wdc	99.3
224	37.6	22.3	31.9	2.8	0.9	0.5	---	---	0.2	---	3.8	---	---	---	Wdc	99.8
225	44.1	30.4	15.7	5.8	0.5	1.4	0.2	---	---	---	1.9	---	---	---	Wdc	100.0
226	30.1	31.9	28.0	5.3	1.1	1.6	---	---	---	---	1.9	---	---	Rutile 0.1	Wdm	100.0
227	30.7	25.1	32.2	7.4	1.4	1.2	---	---	---	---	2.0	---	---	---	Wdm	100.0
228	35.9	20.6	39.4	1.8	0.8	---	0.1	0.1	---	---	1.2	---	---	---	Wdm	99.9
229	36.0	32.0	18.9	7.7	1.9	2.4	0.1	---	---	---	1.0	---	---	---	Wdc	100.0
230	22.2	33.1	27.1	9.9	2.3	---	0.1	0.1	0.6	---	4.5	---	---	---	Wdc	99.9

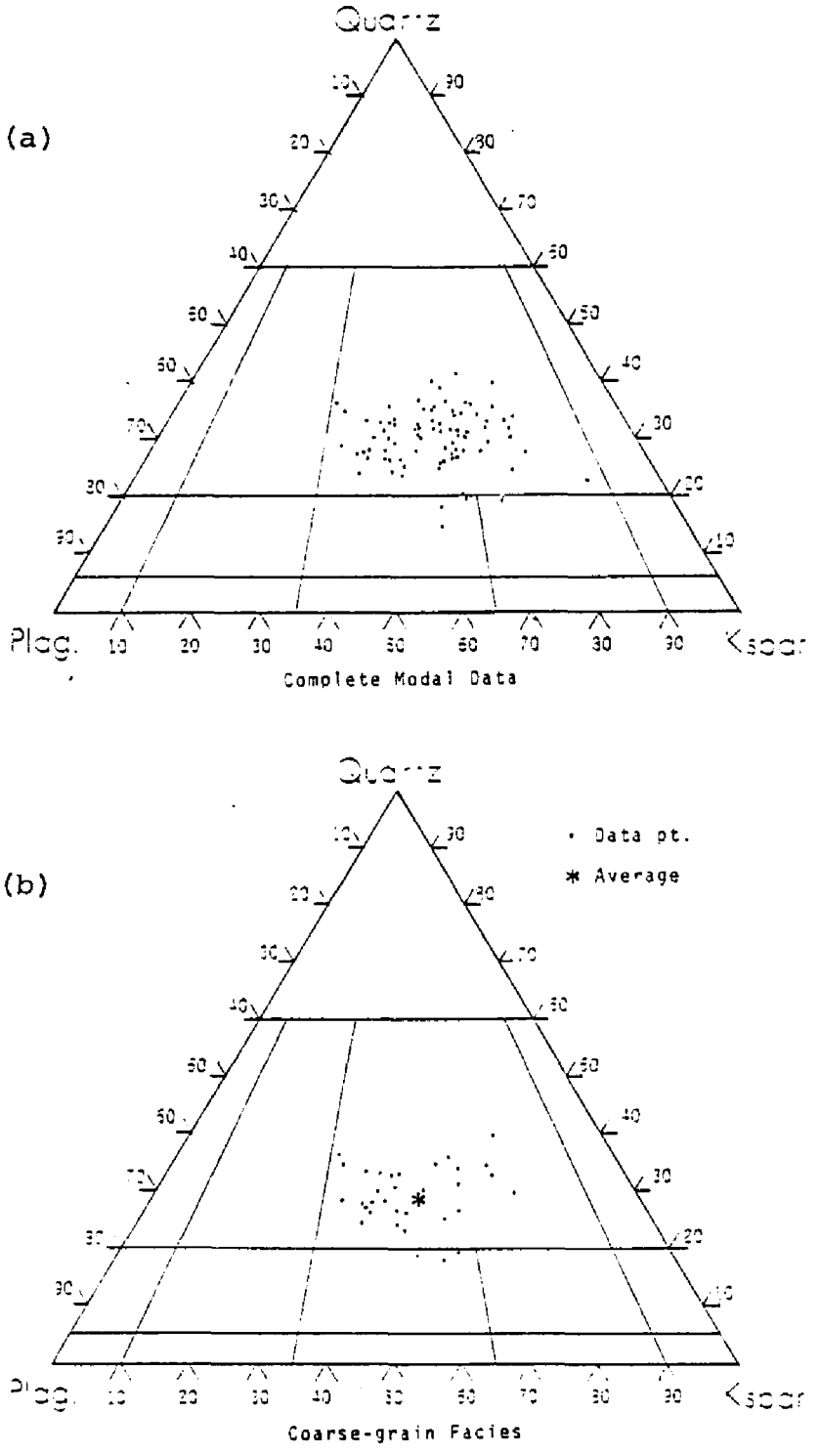

Figure C.3. Modal distribution of quartz, Kspar, and plagioclase in 94 samples of the Wixson Divide granite

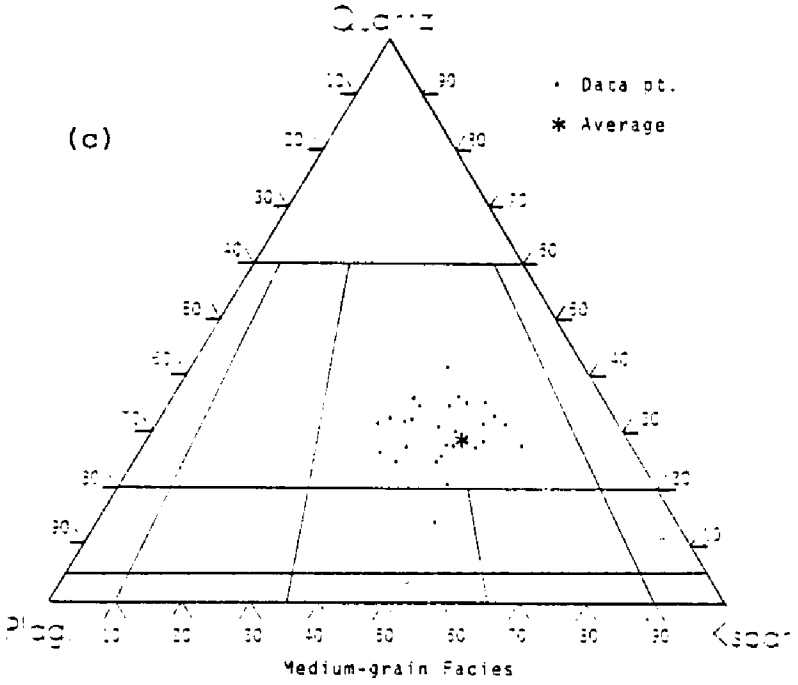

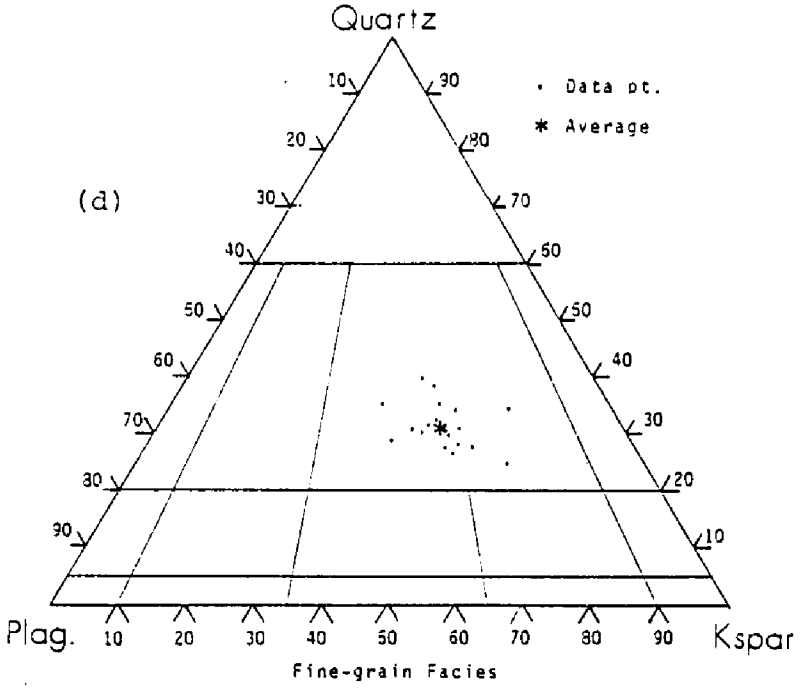

Figure C.3 (cont'd). Modal distribution of quartz, Kspar, and plagioclase in 94 samples of the Wixson Divide granite

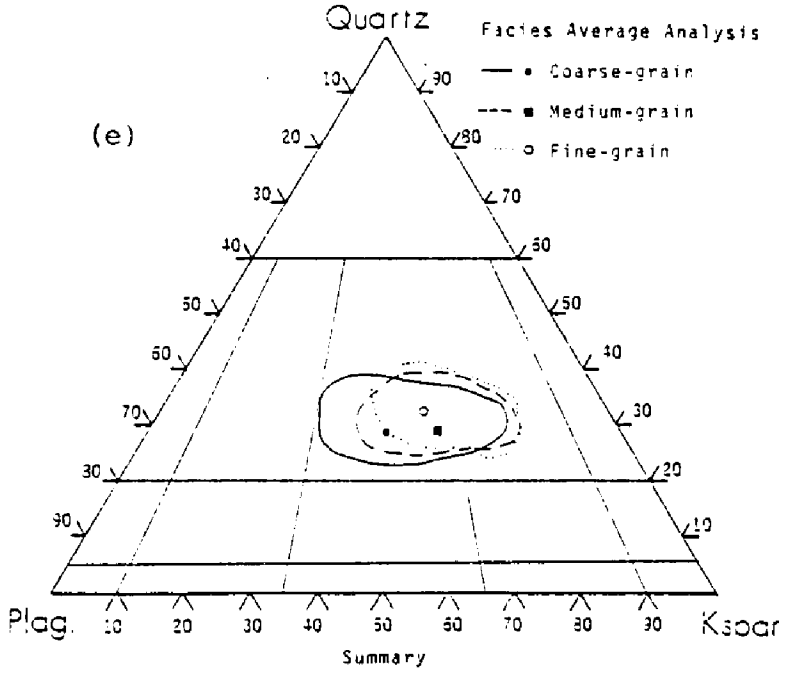

Figure C.3 (cont'd). Modal distribution of quartz, Kspar, and plagioclase in 94 samples of the Wixson Divide granite

Table C.4. Chemical Analysis and CIPW norms of the Wixson Divide pluton (percent weight)

Sample #	186	170	171	167	W35a	W35b
Chem. #	37	38	39	40	41	42
SiO_2	73.21	73.46	75.67	72.44	72.87	68.03
Al_2O_3	13.30	14.42	12.89	14.65	13.98	16.32
Fe_2O_3	0.93	0.88	0.53	0.82	0.80	0.57
FeO	2.38	0.94	0.20	0.52	2.40	1.97
MnO	0.05	0.09	0.01	0.01	0.05	0.16
MgO	0.56	0.50	0.54	0.37	0.61	0.97
CaO	0.66	0.80	0.10	0.50	1.36	1.99
Na_2O	3.12	3.09	2.97	3.18	2.82	3.27
K_2O	5.06	5.07	5.32	6.69	4.81	3.81
TiO_2	0.69	0.41	0.07	0.04	0.14	0.21
	99.96	99.66	98.29	99.22	99.84	97.30
Qtz	37.33	33.41	37.13	26.80	32.51	27.40
Or	30.06	30.06	31.17	39.52	28.39	22.27
Ab	26.22	26.22	25.17	26.75	24.13	27.80
An	3.34	3.90	0.56	2.50	6.68	10.01
C	1.52	2.35	2.04	1.33	1.63	3.16
En	1.51	1.31	1.30	0.90	1.61	2.61
Fs	2.38	0.26	---	0.13	3.43	2.64
Mt	0.50	0.50	0.46	1.16	1.16	0.92
Il	1.51	1.31	0.16	0.15	0.30	0.46
He	---	---	0.16	---	---	---
Mg Di	---	---	---	---	---	---
FeDi	---	---	---	---	---	---

Table C.4 (cont'd). Chemical analysis and CIPW norms of the Wixson Divide pluton (percent weight)

Sample #	190	184	202	163	164	226
Chem. #	43	44	45	46	47	48
SiO_2	75.22	66.04	70.03	69.52	66.82	71.13
Al_2O_3	13.11	16.65	15.08	15.69	16.74	15.25
Fe_2O_3	0.90	2.22	0.46	1.90	2.29	1.45
FeO	1.02	3.60	2.75	1.99	2.01	0.86
MnO	0.00	0.12	0.07	0.07	0.06	0.06
MgO	0.32	1.10	1.20	1.04	1.24	0.40
CaO	0.90	2.31	2.16	2.64	3.07	1.82
Na_2O	3.18	3.58	3.18	3.37	3.08	3.45
K_2O	4.97	3.88	4.47	4.09	3.89	4.25
TiO_2	0.24	1.25	0.49	0.49	0.50	0.29
	99.86	100.75	99.89	100.80	99.70	98.96
Qtz	35.03	22.47	26.44	27.64	25.00	30.58
Or	29.50	22.82	26.16	23.94	22.82	25.05
Ab	26.74	30.42	26.75	28.32	26.22	29.37
An	4.45	11.41	10.85	10.85	15.30	8.90
C	0.92	2.35	1.12	1.84	1.84	1.73
En	0.80	2.91	3.11	2.71	3.21	1.10
Fs	0.66	2.64	3.83	1.32	1.06	---
Mt	1.39	3.24	0.70	2.78	3.24	1.85
Il	0.46	2.43	0.91	0.91	0.91	0.61
He	---	---	---	---	---	0.16
Mg Di	---	---	---	---	---	---
Fe Di	---	---	---	---	---	---

Table C.4 (cont'd). Chemical analysis and CIPW norms of the Wixson Divide pluton (percent weight)

Sample #	227	205	208	221	215	197
Chem. #	49	50	51	52	53	54
SiO_2	69.89	71.24	74.31	74.47	71.12	69.53
Al_2O_3	15.91	14.87	13.13	13.81	14.21	16.59
Fe_2O_3	1.62	1.17	1.16	1.13	1.52	1.04
FeO	1.48	1.97	1.37	1.22	1.48	0.68
MnO	0.03	0.05	0.06	0.04	0.05	0.03
MgO	0.62	0.93	0.70	0.50	0.86	0.83
CaO	2.38	0.85	0.86	0.91	0.81	2.21
Na_2O	3.75	3.28	2.64	3.23	2.80	3.02
K_2O	4.00	5.13	5.04	4.72	5.22	4.02
TiO_2	0.76	0.64	0.54	0.25	0.47	0.25
	100.44	100.13	99.81	100.28	98.54	98.20
Qtz	26.74	27.88	36.17	34.55	31.76	30.40
Or	23.38	30.06	30.06	27.83	30.62	23.94
Ab	31.99	27.88	22.55	27.27	23.60	25.70
An	11.69	4.17	4.17	4.45	3.90	10.85
C	1.12	2.45	1.73	1.73	2.55	3.26
En	1.51	2.41	1.81	1.31	2.21	2.21
Fs	0.13	1.19	0.66	1.31	0.66	---
Mt	2.32	2.32	1.62	1.62	2.32	1.39
Il	1.52	1.21	1.06	0.46	0.91	0.46
He	---	---	---	---	---	0.16
Mg Di	---	---	---	---	---	---
Fe Di	---	---	---	---	---	---

Table C.4 (cont'd). Chemical analysis and CIPW norms of the Wixson Divide pluton (percent weight)

Sample #	203	155	223	162	166	151
Chem. #	55	56	57	58	59	60
SiO_2	64.81	71.67	69.80	68.68	70.56	75.39
Al_2O_3	16.04	14.62	15.28	15.56	15.62	13.40
Fe_2O_3	1.74	2.01	1.81	2.69	0.87	1.01
FeO	3.11	2.00	1.44	2.10	1.79	1.20
MnO	0.09	0.03	0.05	0.10	0.05	0.04
MgO	1.59	0.74	0.55	1.28	1.02	0.39
CaO	3.57	0.60	1.53	1.51	0.58	0.73
Na_2O	3.71	3.55	3.32	3.85	2.94	3.02
K_2O	4.24	4.55	5.16	4.30	4.96	4.19
TiO_2	0.74	0.56	0.54	1.43	0.76	0.78
	99.64	100.33	99.48	101.50	99.15	100.15
Qtz	16.94	30.94	28.18	27.40	31.06	39.59
Or	25.05	26.72	30.62	25.61	29.50	24.49
Ab	31.47	29.89	28.32	28.32	24.65	25.70
An	14.47	3.06	3.06	7.51	2.78	3.62
C	---	2.75	3.06	2.65	4.38	2.55
En	3.21	1.81	1.51	3.31	2.61	1.10
Fs	2.51	1.06	0.26	---	1.32	0.13
Mt	2.55	3.01	2.55	2.55	1.16	1.39
Il	1.37	1.06	1.06	2.73	1.52	1.52
He	---	---	---	0.96	---	---
Mg Di	1.73	---	---	---	---	---
FeDi	0.99	---	---	---	---	---

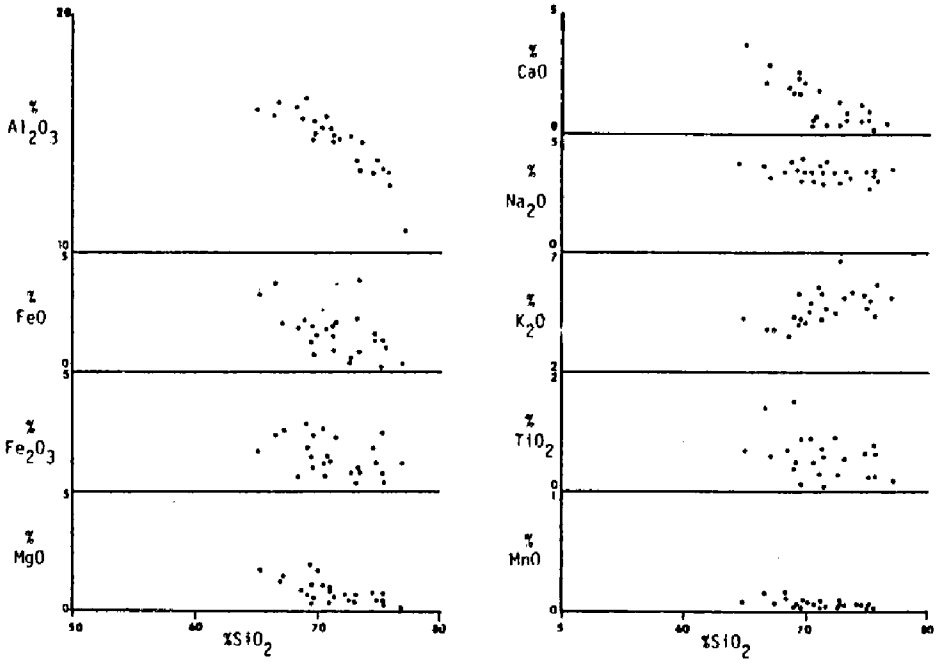

Figure C.5. Variation diagrams for the various cation oxides of the Wixson Divide pluton

APPENDIX D

SUMMARY OF MODAL AND CHEMICAL DATA OF THE GRANITES OF THE MOUNT TYNDALL QUADRANGLE

Locations of sample localities for the 16 specimens of the Mount Tyndall granite are shown on the index map (Figure D.1). Modal analyses of the twelve specimens collected from the "r" granites and 4 specimens from the "d" granite facies are given in Table D.2. Just as in the San Isabel and Wixson Divide plutons, there are some extensive areas within the outcrop area of the Mount Tyndall granites that are modally moderately to poorly represented. As before, this is due primarily to the lack of fresh exposures, or their inaccessibility. Fresh exposures in this area are quite scarce. This is due to their location on a high deeply weathered plateau which dominates the topography in the central portion of the Wet Mountains.

Modal Analyses of Table D.2 are summarized graphically on the standard trigonal diagram of major minerals (Figure D.3). Chemical analysis and CIPW norms for five of the modal specimens are listed in Table D.4. Figure D.5 displays cation oxide percentages plotted against SiO_2 percentages.

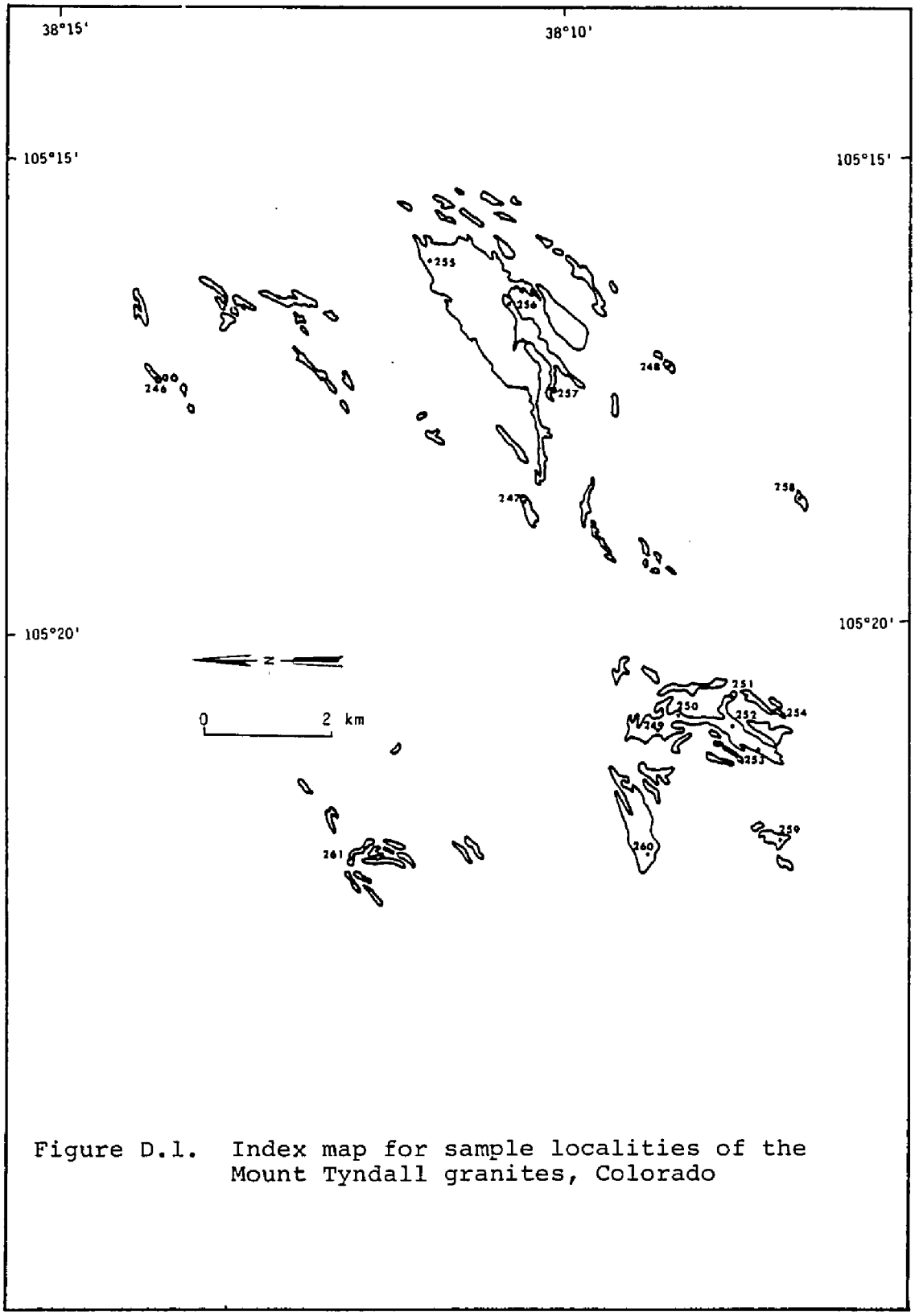

Figure D.1. Index map for sample localities of the Mount Tyndall granites, Colorado

Table D.2. Modal Analysis of the Granites Collected in the Mount Tyndall Quadrangle

Sample Number	Kspar	Plag	Qtz	Biot	Mag	Sph	Hbl	Zir	Ap	Ep	Sericite	Chl	Hem	Others	Total
246	32.9	30.4	28.8	5.5	2.1	---	---	---	0.1	---	---	0.2	---	---	100.0
247	31.8	23.0	33.0	4.2	1.6	2.3	0.4	0.1	0.4	0.1	---	---	---	White Mica 1.1	100.0
248	30.0	33.7	23.0	6.2	1.8	2.7	0.5	0.1	0.1	---	---	0.2	---	White Mica 1.7	100.0
249	20.1	40.9	24.0	13.3	1.2	---	0.1	---	0.4	---	---	---	---	---	100.0
250	37.6	33.2	21.6	6.3	1.0	---	---	---	---	0.3	---	---	---	---	100.0
251	28.1	39.7	26.5	5.2	0.5	---	---	---	---	---	---	---	---	---	100.0
252	35.3	30.6	25.9	7.1	0.7	---	---	---	---	---	---	---	---	White Mica 0.5	100.1
253	31.4	32.6	24.8	5.8	1.2	---	---	0.1	---	---	---	---	---	White Mica 2.1	100.0
254	34.1	32.4	25.3	6.7	1.3	---	---	---	---	---	---	---	---	White Mica 0.2	100.0
255	32.1	29.1	23.2	5.9	1.3	4.9	---	0.3	0.1	0.3	---	---	---	White Mica 2.8	100.0
256	27.7	33.8	20.4	11.0	3.2	1.3	0.2	0.1	---	1.5	---	---	---	White Mica 0.8	100.0
257	22.6	26.5	25.1	18.7	3.5	0.2	---	0.1	0.2	1.2	---	0.3	---	White Mica 1.6	100.0
258	24.0	27.9	31.7	9.5	3.0	1.8	0.3	0.1	0.1	1.2	---	---	---	White Mica 0.4	100.0
259	35.1	29.7	31.6	2.5	2.3	---	---	0.1	---	0.3	---	---	---	White Mica 0.4	100.0
260	34.6	30.1	23.9	9.2	1.5	---	---	0.1	---	---	---	---	---	White Mica 0.6	100.0
261	31.4	30.3	28.6	6.2	1.9	0.9	---	---	---	0.2	---	---	---	White Mica 0.5	100.0

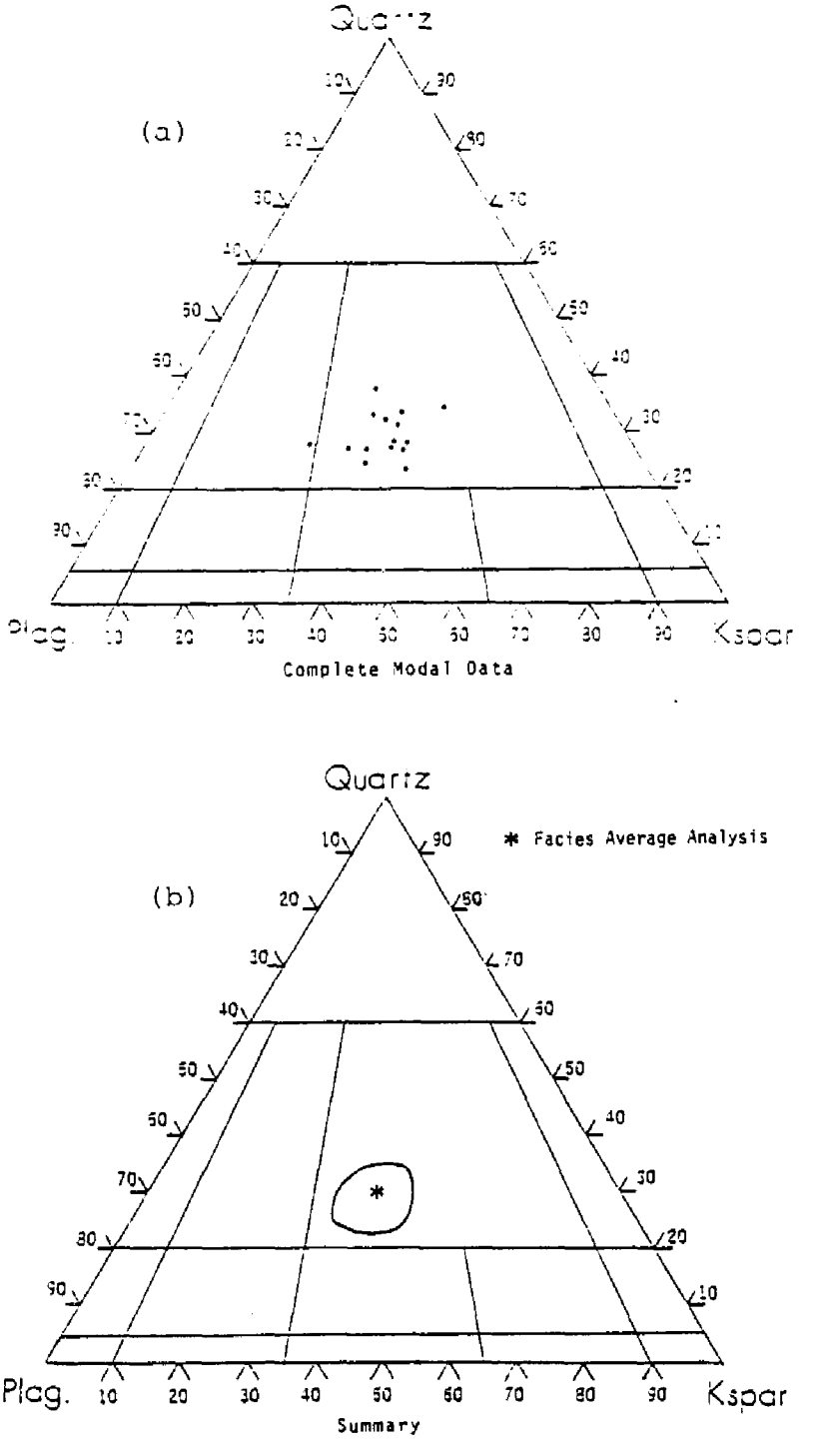

Figure D.3. Modal distribution of quartz, Kspar, and plagioclase in 16 samples of the Mount Tyndall granite

Table D.4. Chemical analysis and CIPW norms of the Granite of the Mount Tyndall Quadrangle (percent weight)

Sample #	246	248	252	255	257
Chemical #	75	76	77	78	79
SiO_2	72.22	69.29	70.85	69.67	69.00
Al_2O_3	14.92	16.31	14.63	15.67	15.80
Fe_2O_3	0.92	0.97	1.22	2.03	1.49
FeO	0.87	0.99	1.87	1.51	1.89
MnO	0.00	0.05	0.01	0.00	0.11
MgO	0.05	0.73	0.14	0.05	1.12
CaO	1.19	1.90	1.94	2.01	2.56
Na_2O	2.89	2.85	3.13	2.34	3.01
K_2O	4.79	4.96	5.39	4.98	4.38
TiO_2	0.37	0.55	0.62	0.66	0.77
	98.22	98.60	99.80	98.92	100.13
Qtz	34.25	28.30	26.74	32.51	26.98
Or	28.39	29.50	31.73	29.50	25.61
Ab	24.65	24.12	26.75	19.93	25.70
An	5.84	9.46	9.78	10.02	12.80
C	2.75	2.75		2.75	1.43
En	0.10	1.91	0.20	0.10	3.01
Fs	0.13	0.13	1.32		0.92
Mt	1.39	1.39	1.85	3.01	2.08
Il	0.76	1.06	1.21	1.21	1.52
Mg Di			0.22		

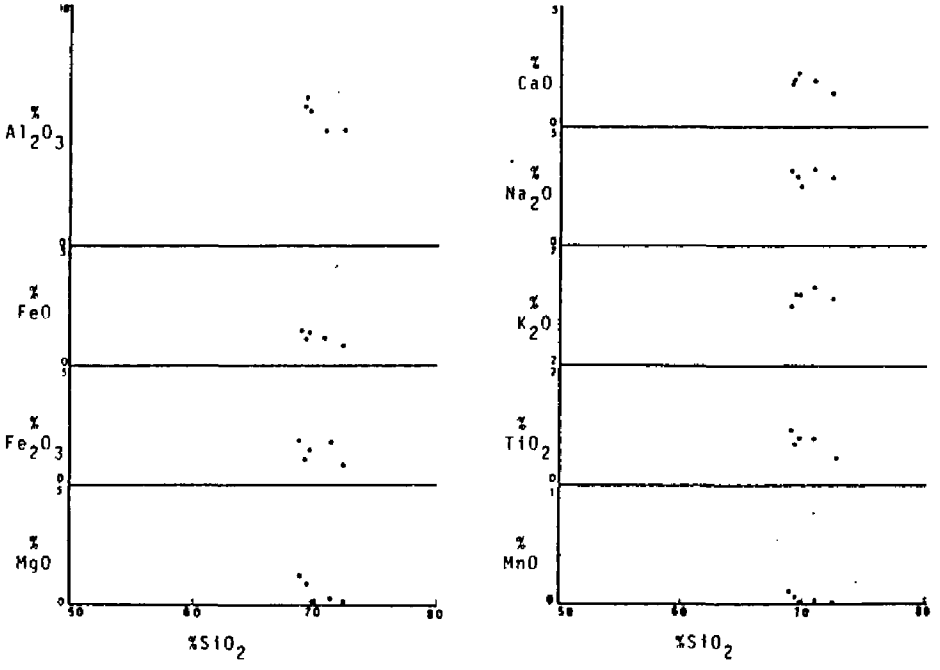

Figure D.5. Variation diagrams for the various cation oxides of the Mount Tyndall Quadrangle

APPENDIX E

SUMMARY OF MODAL AND CHEMICAL DATA FOR THE GRANITES OF THE WILLIAMS CREEK PLUTON

Sample localities within the various Williams Creek plutons are shown on the index map (Figure E.1). Sampling of these plutons could be best described as being erratic. West of Williams Creek in the largest granite exposure, sample specimens occurred typically in hummocky outcrops and boulder piles normally located at the top of widely spread hills. East of Williams Creek, specimens are taken from the rare cliff exposures found along tributaries of Williams Creek. Northern exposures in the Deer Peak quadrangle are so deeply altered that no fresh samples could be collected. Thus, sample localities for these plutons are sparse and appear to have a shotgun pattern. The twenty-two (22) modes made from Williams Creek granites are given in Table E.2.

Quartz, plagioclase, and Kspar modes, recalculated to 100 percent, are plotted on Figure E.3. Two thin section modes are given in Table E.2, but are not plotted on the trigonal diagram because heavy alteration has

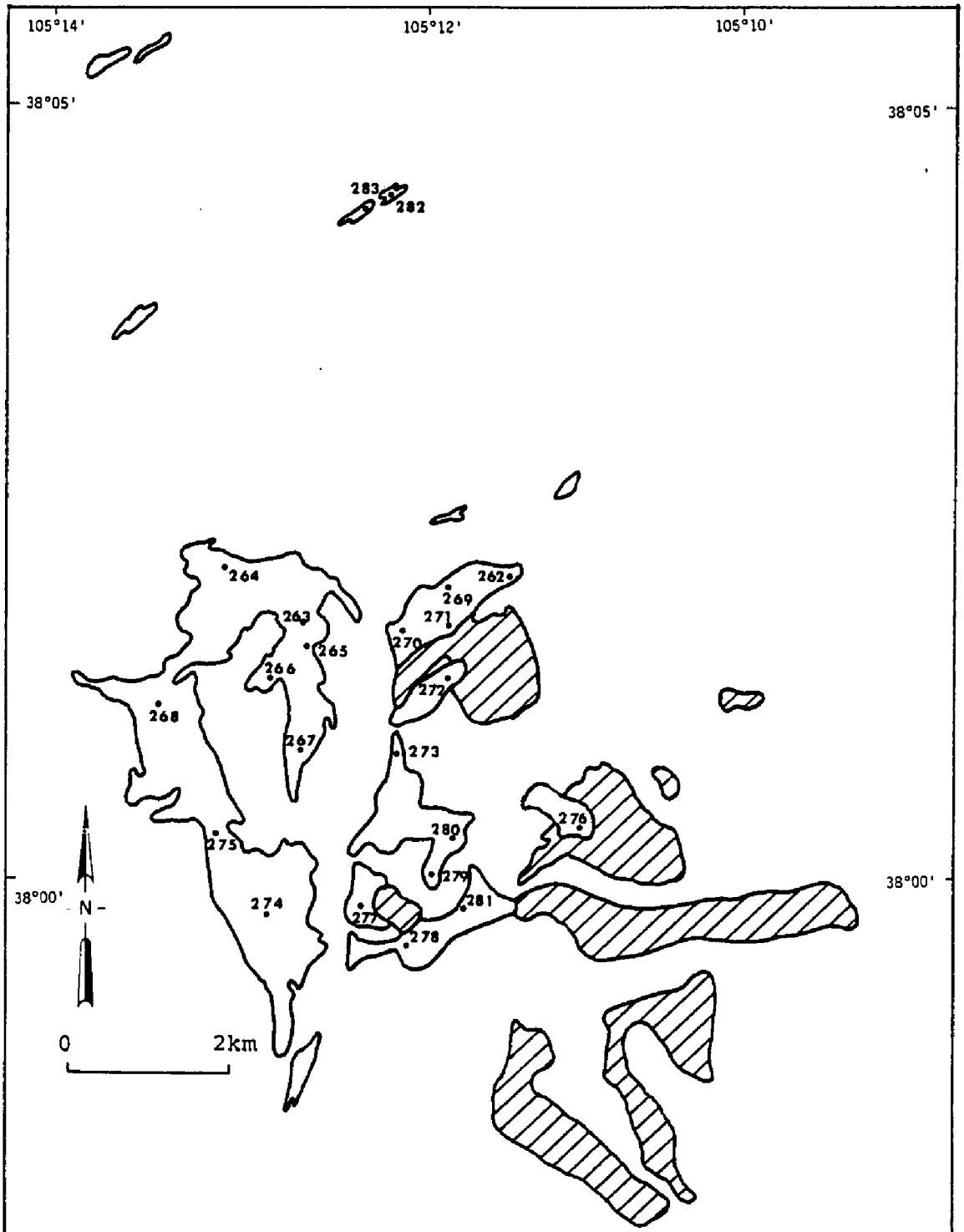

Figure E.1. Index map for sample localities of the Williams Creek plutons, Colorado. Bear Creek granites are depicted by diagonal lines.

Table E.2. Modal Analysis of the Granites of Williams Creek

Sample Number	Kspar	Plag	Qtz	Biot	Mag	Sph	Hbl	Zir	Ap	Ep	Sericite	Chl	Hem	Others	Total
262	26.2	35.3	22.9	11.1	0.9	---	2.7	---	---	---	---	0.9	---	---	100.0
263	34.2	30.2	19.7	9.4	3.1	0.8	0.2	---	0.1	0.6	---	0.2	---	White Mica 1.5	100.0
264	30.6	35.2	24.1	5.0	1.9	1.1	0.1	---	---	---	---	---	---	White Mica 2.0	100.0
265	35.8	28.6	31.3	2.7	0.8	0.3	---	---	---	---	---	---	---	White Mica 0.5	100.0
266	29.2	37.5	29.4	2.6	0.1	---	0.2	---	---	0.1	---	---	---	White Mica 0.9	100.0
267	29.1	28.4	38.1	3.4	0.6	0.1	0.2	---	---	---	---	---	---	White Mica 0.1	100.0
268	20.0	39.1	20.4	14.0	3.7	1.6	0.5	0.1	---	0.6	---	---	---	---	100.0
269	28.0	34.3	17.8	10.8	1.2	0.1	7.5	---	---	---	---	---	---	Garnet 0.3	100.0
270	21.8	32.5	24.9	15.8	2.3	1.3	0.4	0.1	0.1	0.2	---	---	---	White Mica 0.6	100.0
271	27.4	31.6	21.9	14.8	1.5	1.4	0.3	---	---	0.3	---	---	---	White Mica 0.8	100.0
272	41.2	32.6	12.8	9.0	1.1	1.4	1.6	---	0.1	0.2	---	---	---	---	100.0
273	25.6	41.2	24.0	8.7	0.5	---	---	---	---	---	---	---	---	---	100.0
274	35.4	38.7	10.3	12.0	2.7	0.4	---	0.1	---	0.2	---	---	---	Garnet 0.3	100.1
275	20.6	33.6	28.3	10.4	1.7	---	0.4	0.2	---	0.2	---	---	---	White Mica 4.6	100.0
276	32.2	25.4	35.1	4.5	0.6	---	---	---	0.1	0.3	---	---	---	White Mica 1.8	100.0
277	38.0	33.2	11.7	13.3	2.5	---	0.7	0.1	---	0.3	---	---	---	White Mica 0.2	100.0
278	28.7	37.8	24.9	5.9	1.6	0.8	---	---	---	---	---	0.3	---	---	99.9
279	33.9	26.3	26.7	10.8	1.8	0.4	---	---	---	---	---	---	---	White Mica 0.1	100.0
280	20.2	47.5	4.0	18.5	2.6	2.8	3.5	---	---	---	---	0.1	---	Garnet 0.8	100.0
281	27.0	28.6	21.3	19.1	2.3	0.4	1.2	---	---	---	---	---	---	Garent 0.1	100.0

Table E.2 (cont'd).

Sample Number	Kspar	Plag	Qtz	Biot	Mag	Sph	Hbl	Zir	Ap	Ep	Sericite	Chl	Hem	Others	Total
282	19.4	35.4	10.1	---	1.2	---	0.9	---	---	---	16.7	5.1	---	Clay min. 11.2	100.0
283	14.6	37.9	15	---	3.3	---	2.9	---	1.2	---	10.4	6.1	---	White Mica 2.0 Clay min. 6.6	100.0

masked many minerals and has made them non-representative of the Williams Creek granites.

Seven chemical analyses were run on the granitic rocks collected from the various plutons. The results and norms calculated from the analysis are shown in Table E.4. Figure E.5 displays cation oxide percentage plotted against SiO_2 percentage.

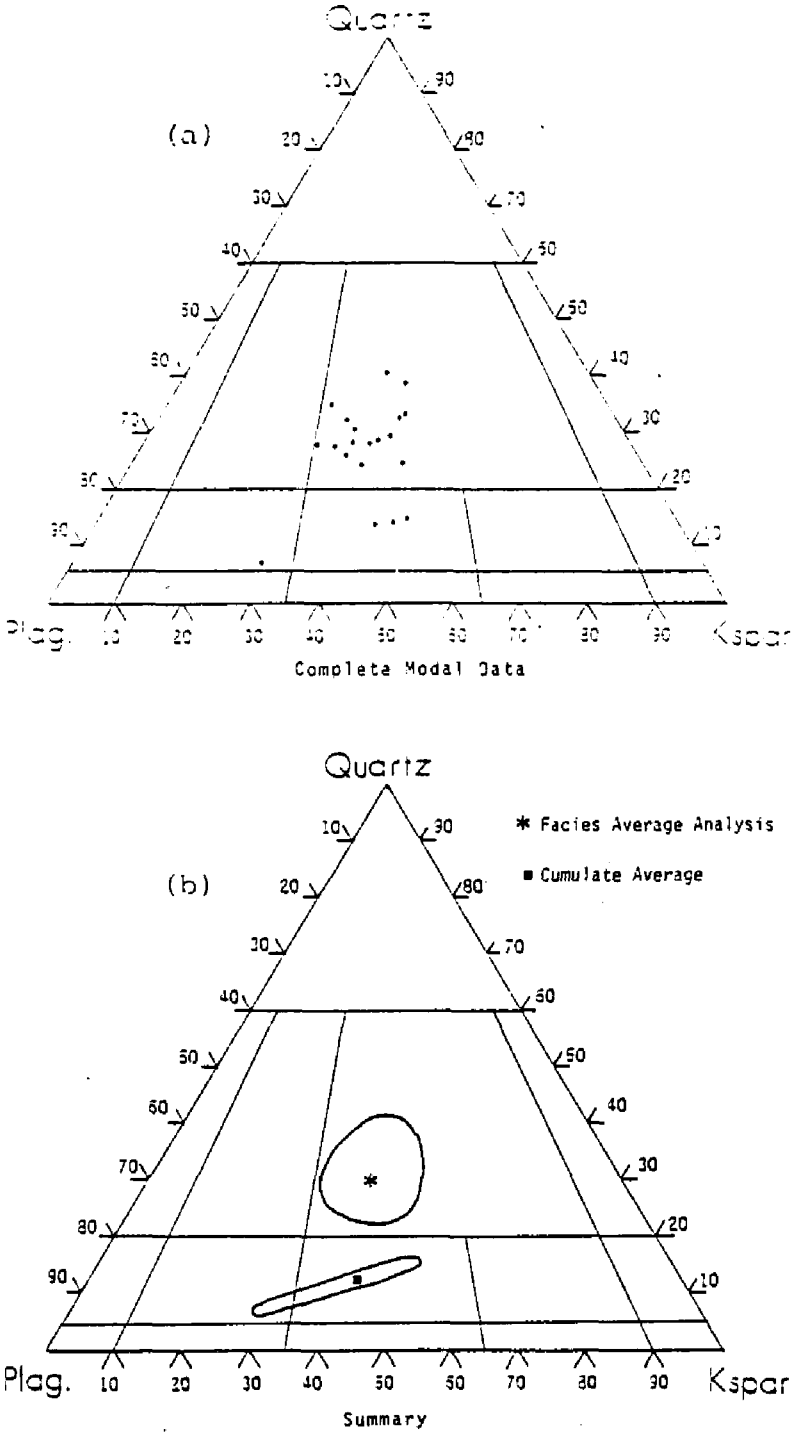

Figure E.3. Modal distribution of quartz, Kspar, and plagioclase in 22 samples of the Williams Creek pluton

Table E.4. Chemical analysis and CIPW norms of the Granite of Williams Creek (percent weight)

Sample #	266	268	272	274	276	278	280
Chemical #	80	81	82	83	84	85	86
SiO_2	68.50	63.69	62.55	64.33	73.94	67.16	55.15
Al_2O_3	16.11	16.89	17.09	16.70	13.85	14.85	19.67
Fe_2O_3	0.48	0.50	0.85	0.72	0.40	0.99	2.03
FeO	0.29	3.42	3.07	3.14	1.00	2.18	4.60
MnO	0.00	0.15	0.19	0.00	0.10	0.08	0.17
MgO	0.05	1.48	2.00	0.00	0.42	1.08	2.91
CaO	1.87	2.53	2.83	2.75	1.86	2.03	4.48
Na_2O	3.10	3.27	3.71	3.54	2.36	3.36	3.67
K_2O	4.92	3.63	5.28	4.89	5.25	4.53	3.57
TiO_2	0.51	1.01	0.86	1.12	0.35	0.78	1.28
	95.83	96.57	98.43	97.19	99.53	97.04	97.46
Qtz	27.70	20.85	9.91	17.66	35.02	26.44	4.03
Or	28.95	21.71	31.17	28.95	31.18	22.27	21.15
Ab	26.22	27.80	31.47	29.89	19.93	28.32	30.94
An	9.18	12.52	13.91	13.63	9.18	10.02	22.26
C	2.35	2.96	0.20	0.61	0.92	1.63	1.63
En	0.10	3.92	5.32		1.10	2.81	7.43
Fs		4.22	3.56	3.30	0.92	1.85	4.62
Mt		0.69	1.16	1.16	0.69	1.39	3.01
Il	0.61	1.97	1.67	2.12	0.61	1.52	2.43
Rt	0.16						
Hm	0.48						

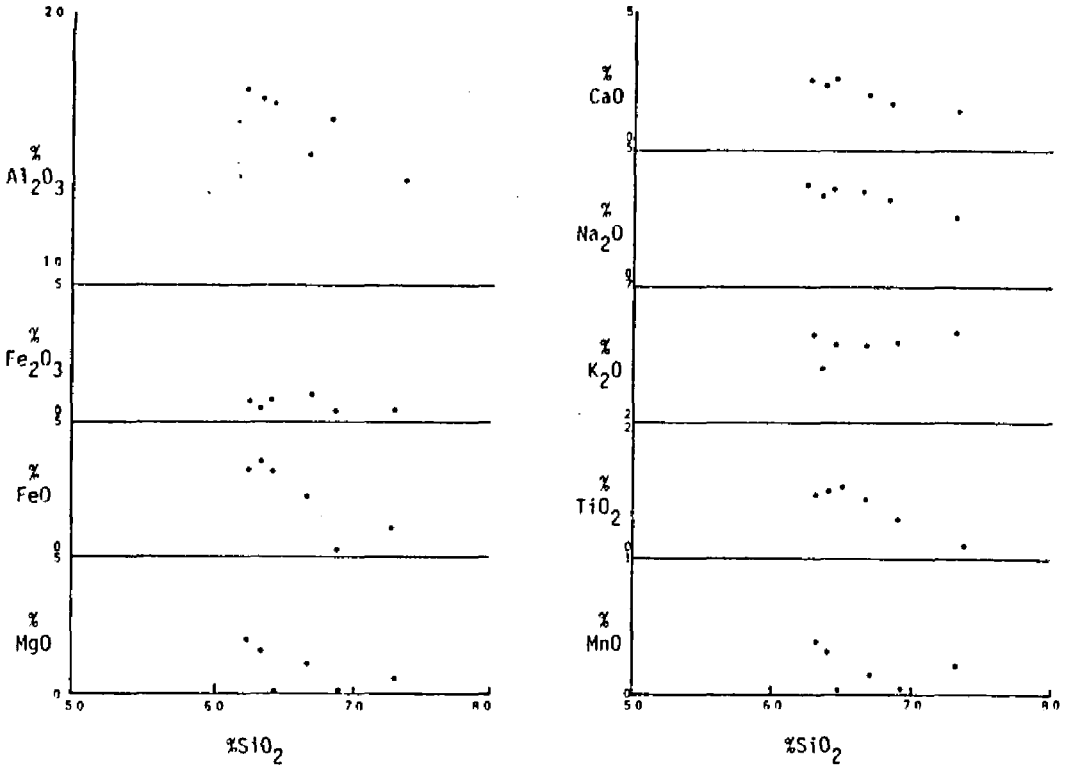

Figure E.5. Variation diagrams for the various cation oxides of the Williams Creek pluton

APPENDIX F

SUMMARY OF MODAL AND CHEMICAL DATA FOR THE GRANITES OF THE BEAR CREEK PLUTONS

Specimen collection sites of the various Bear Creek granitic plutons are shown on the index map (Figure F.2). Modal data taken from these specimens is given in Table F.2. Unlike other Silver Plume-age intrusives, each pluton of Bear Creek composition is modally represented. This is primarily due to the area of exposure being located on the highly dissected and tilted plateau just east of Williams and Bear Creeks. Here, deep canyons have cut into parts of most of the plutons. Therefore, each pluton could be effectively collected, and fresh samples are the rule rather than the exception. However, because of the dense cover of vegetation between canyons, as well as the inaccessibility of steep canyon walls, many plutons were not extensively sampled. Thus, sampling again appears to be random, and for some plutons, may give the appearance of being minimal.

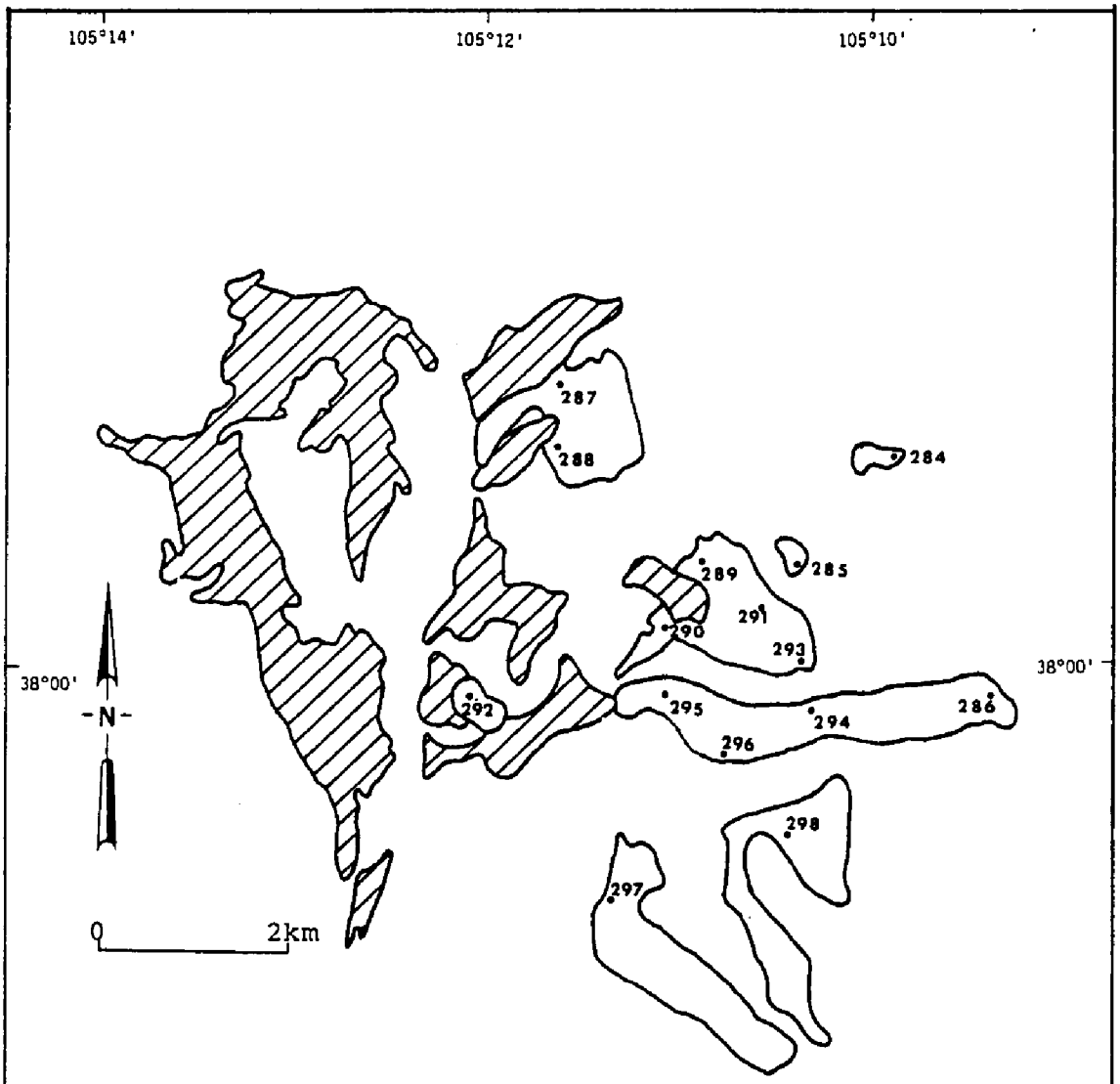

Figure F.1. Index map for sample localities of the Bear Creek plutons. Williams Creek plutons are depicted by diagonal lines.

The modal data for the major minerals of these granitic rocks are plotted on the standard trigonal diagram (Figure F.3). Chemical analyses of 5 specimens from the various plutons are listed in Table F.4 and are displayed on variation diagrams (Figure F.5).

Table F.2. Modal Analysis for the Granites of Bear Creek

Sample Number	Kspar	Plag	Qtz	Biot	Mag	Sph	Hbl	Zir	Ap	Ep	Sericite	Chl	Hem	Others	Total
284	33.9	29.0	33.1	2.6	1.4	---	---	---	---	---	---	---	---	---	100.0
285	28.9	34.4	22.8	8.5	1.5	---	0.1	0.1	---	0.4	---	---	---	White Mica 3.3	100.0
286	44.0	9.5	41.3	1.1	0.4	---	---	0.1	---	---	---	---	---	White Mica 3.6	100.0
287	38.7	29.8	27.2	2.8	0.8	0.7	---	---	---	---	---	---	---	---	100.0
288	40.4	21.7	29.5	5.3	0.8	---	---	0.2	---	0.4	---	---	---	White Mica 1.7	100.0
289	40.4	19.8	36.3	3.0	0.5	---	---	---	0.1	---	---	---	---	---	100.1
290	30.2	33.4	19.9	12.0	1.5	1.3	0.4	0.1	0.1	---	---	---	---	White Mica 1.0 Garnet 0.1	100.0
291	32.3	31.8	20.8	11.2	1.1	1.6	0.2	0.1	---	0.1	---	---	---	White Mica 0.8	100.0
292	39.9	25.4	25.3	6.7	1.2	---	0.1	0.1	0.1	0.1	---	---	---	White Mica 1.1	100.0
293	29.1	39.7	30.7	0.2	0.2	---	---	---	---	---	---	---	---	---	99.9
294	35.3	23.1	37.6	3.9	---	---	---	---	---	---	---	---	---	---	99.9
295	41.4	28.4	28.4	1.2	---	---	---	---	---	---	---	---	---	White Mica 0.5	99.9
296	41.3	24.1	33.1	1.0	0.4	---	---	---	---	---	---	---	---	White Mica 0.1	100.0
297	43.8	24.4	30.6	0.4	0.3	---	0.1	0.1	---	---	---	---	---	White Mica 0.3	100.0
298	38.8	25.4	28.6	5.2	0.2	---	---	---	---	---	---	---	---	White Mica 1.8	100.0

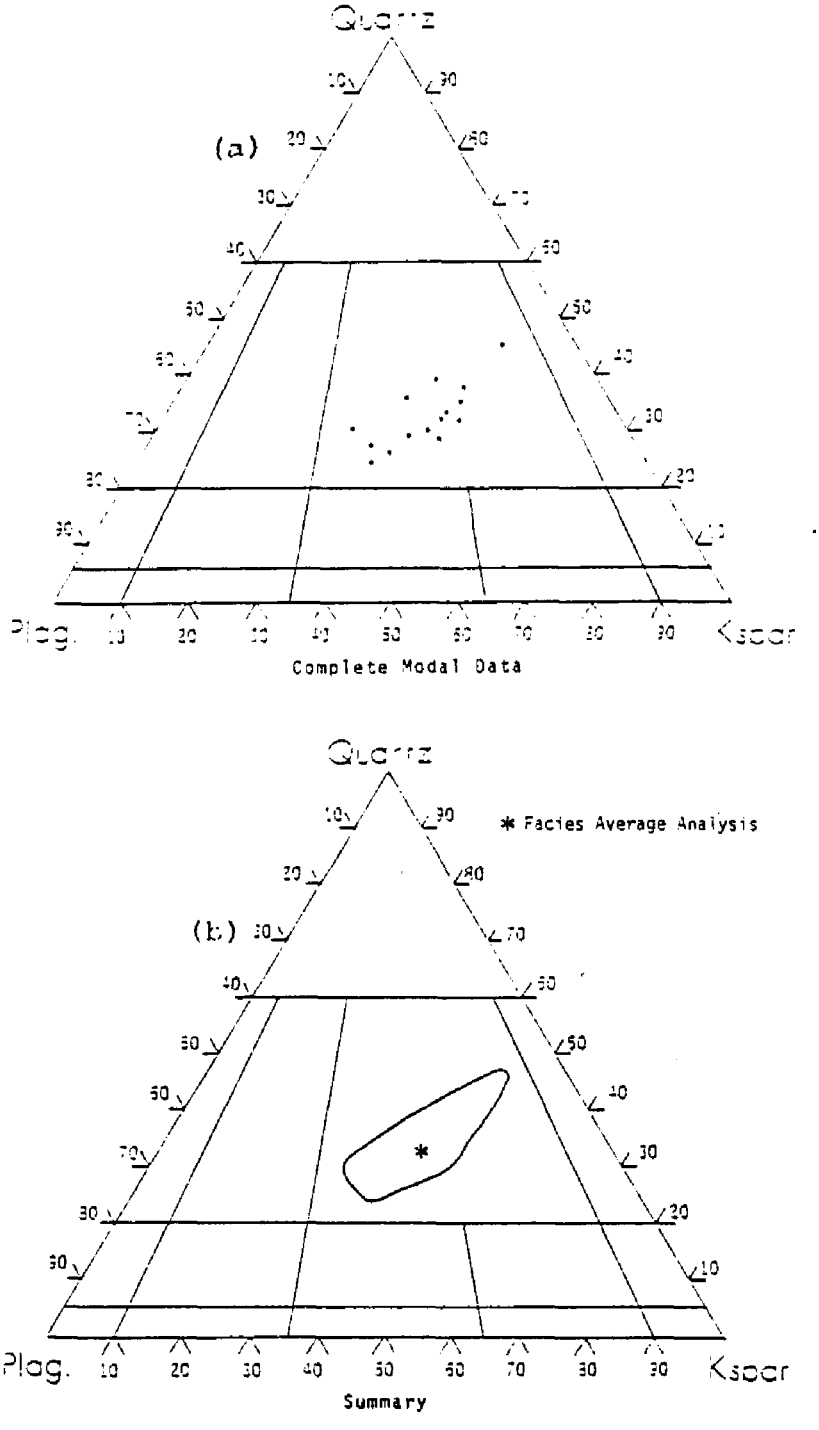

Figure F.3. Modal distribution of quartz, Kspar, and plagioclase in 15 samples of the Bear Creek granite

Table F.4. Chemical analysis and CIPW norms of the granites of Bear Creek (percent weight)

Sample #	286	288	289	297	298
Chemical #	87	88	89	90	91
SiO_2	74.31	74.51	76.49	75.98	73.22
Al_2O_3	13.52	14.29	12.88	12.86	14.74
Fe_2O_3	0.53	1.21	0.77	0.64	0.72
FeO	0.36	0.56	0.63	0.42	1.20
MnO	0.00	0.00	0.00	0.00	0.01
MgO	0.05	0.00	0.05	0.00	0.38
CaO	0.33	0.94	0.74	0.75	1.24
Na_2O	2.63	2.65	2.63	2.55	2.30
K_2O	5.67	5.35	5.07	5.18	5.42
TiO_2	0.21	0.42	0.21	0.25	0.49
	97.61	99.93	99.47	98.63	99.72
Qtz	36.77	36.42	40.98	39.84	35.69
Or	33.40	31.73	30.06	30.62	32.29
Ab	22.03	22.55	22.03	21.50	19.40
An	1.67	4.73	3.62	3.62	6.12
C	2.55	2.34	1.73	1.73	1.84
En	0.10		0.10		0.50
Fs			0.13		0.79
Mt	0.46	0.69	1.16	0.69	1.16
Il	0.46	0.76	0.46	0.46	0.91
Hm	0.16	0.80		0.16	

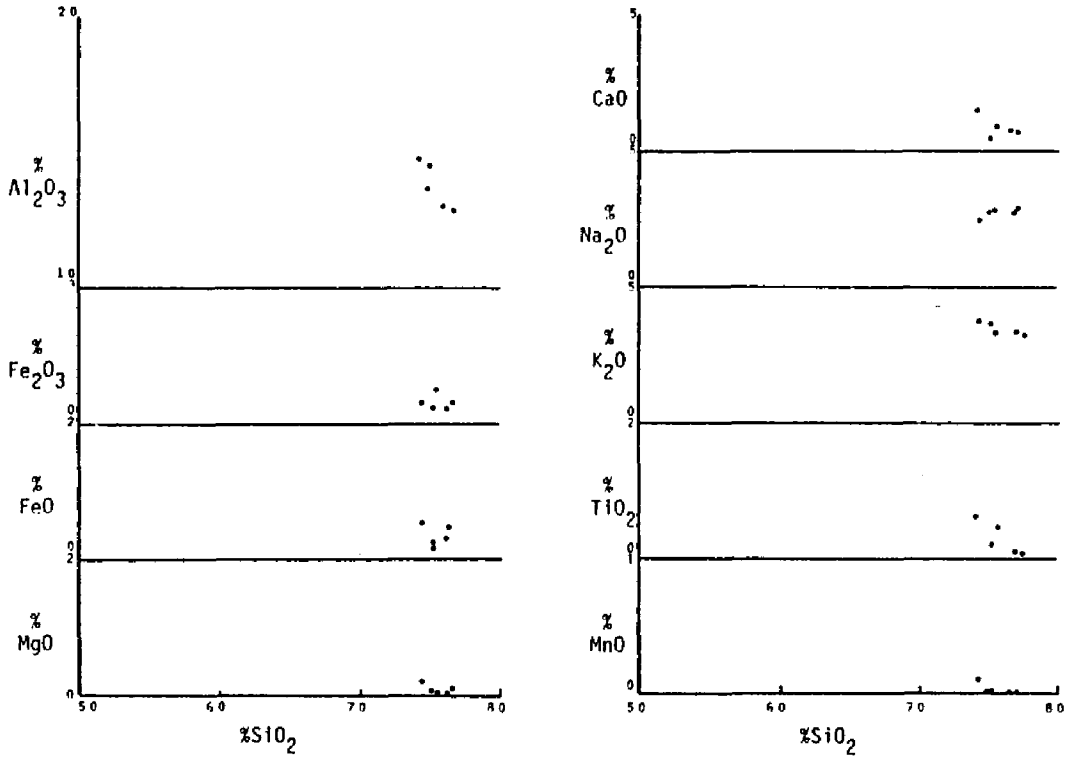

Figure F.5. Variation diagrams for the various cation oxides of the Bear Creek plutons

APPENDIX G

SUMMARY OF MODAL AND CHEMICAL DATA FOR THE GRANITES OF CLIFF CREEK PLUTONS

Sample localities for the Cliff Creek granites are shown on the index map (Figure G.1.). Table G.2 gives the modes of 8 thin sections taken from the granites of Cliff Creek. Two of the specimens, numbered 305 and 306, are taken from modal analyses compiled by Murray (1970). Samples are unusually clear of alterations. This is due in part to the abundance of fresh sample sites located along the deeply entrenched youthful streams of the area. Therefore, samples were collected from steep cliffs and canyon walls. This, in turn, produces fewer collected modes.

Stream channels are a rarity, and only in those channels could granite penetrate the widespread colluvial and alluvial cover. East of the Ilse fault few plutons were collectable, and only two specimens were collected from this area. Topographic relief is moderate to low, and many of the pluton's surface expressions are primarily

those of a bright red to light orange soil horizon. Therefore, samples from this area are generally uncollectable because of their high degree of friability and their high degree of alteration. Two samples of the Cliff Creek granite have been analyzed chemically (Table G.4). The table also gives the calculated CIPW norms.

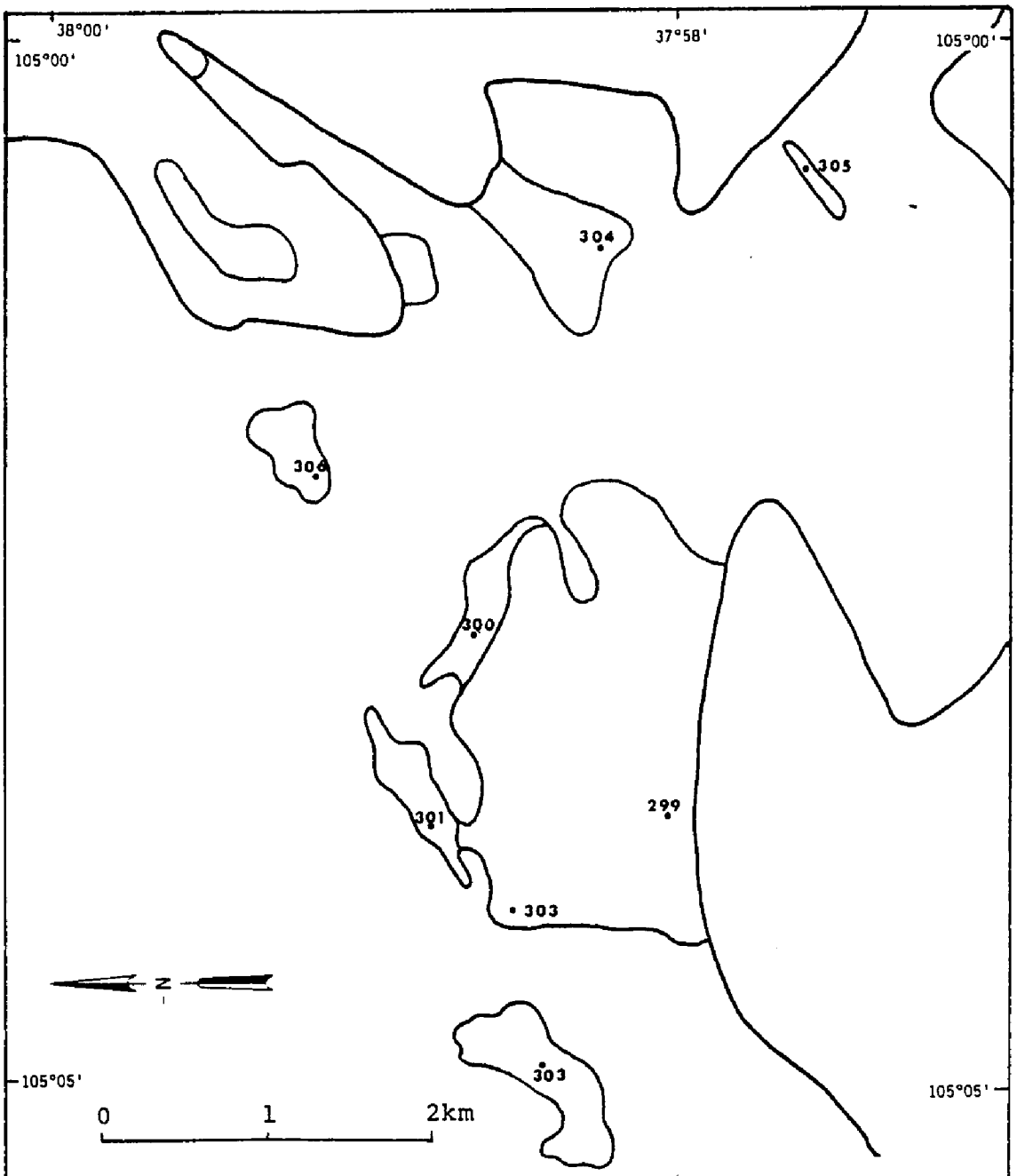

Figure G.1. Index map for sample localities of the Cliff Creek plutons

Table G.2. Modal Data in Volume Percent of the Granites of Cliff Creek Specimen numbers 305 and 306 taken from Murray (1970).

Sample Number	Kspar	Plag	Qtz	Biot	Mag	'Sph	Hbl	Zir	Ap	Ep	Sericite	Chl	Hem	Others	To'al
299	44.5	16.6	37.4	1.2	0.3	---	---	---	---	---	---	---	---	---	100.0
300	39.2	20.2	38.9	1.3	0.2	---	---	---	---	0.2	---	---	---	---	100.0
301	48.4	14.8	33.4	2.3	1.1	---	---	---	---	---	---	---	---	---	100.0
302	40.7	10.8	47.2	0.7	0.1	0.5	---	---	---	---	---	---	---	---	100.0
303	58.9	17.5	23.0	0.6	0.3	---	---	---	---	---	---	---	---	---	100.3
304	34.7	21.6	36.0	1.5	1.9	---	---	0.1	---	0.3	---	---	---	White Mica 3.9	100.0
305	52.4	6.1	34.1	3.5	2.2	0.1	---	0.1	---	---	---	---	---	---	98.5
306	44.3	23.5	25.5	4.9	1.1	0.2	---	0.3	---	---	---	---	---	---	99.8

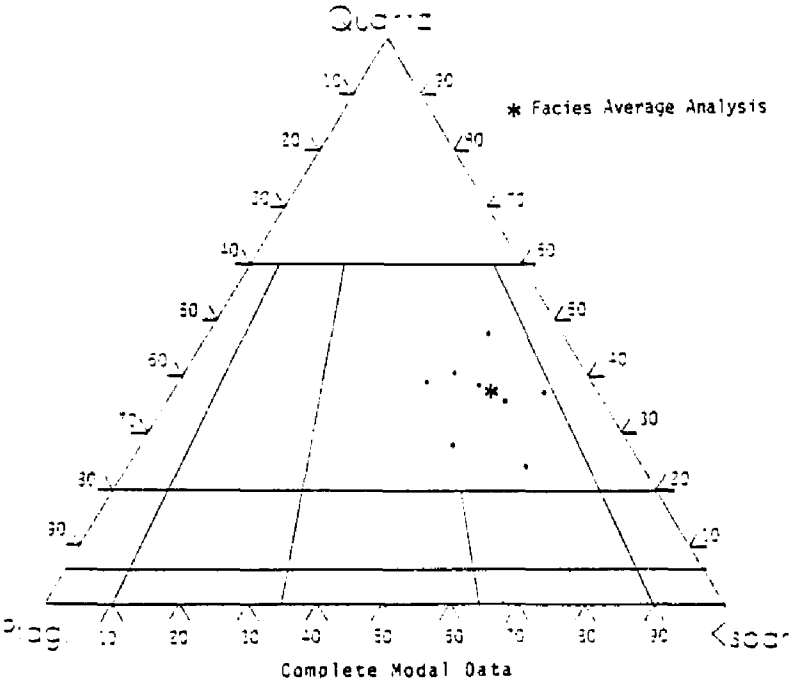

Figure G.3. Modal distributions of quartz, Kspar, and plagioclase in 8 samples of the Cliff Creek granite

Table G.4. Chemical analysis and CIPW norms of the granites of Cliff Creek (percent weight)

Sample #	300	302
Chemical #	92	93
SiO_2	76.84	77.36
Al_2O_3	12.97	13.23
Fe_2O_3	0.20	0.18
FeO	0.06	0.02
MnO	0.00	0.00
MgO	0.00	0.00
CaO	0.55	0.96
Na_2O	2.32	1.79
K_2O	5.76	5.60
TiO_2	0.28	0.11
	98.98	99.25
Qtz	40.32	43.62
Or	33.96	32.84
Ab	19.40	15.21
An	2.78	4.73
C	1.43	2.55
Hm	0.16	0.16
Il	0.15	
Rt	0.24	0.08

VITA

Russell Berryman Bender, Jr. was born in Collingswood, New Jersey, on August 20, 1946, the son of Mary Cole Bender and Russell Berryman Bender, Sr. After completing high school at Bastrop High School, Bastrop, Louisiana in 1964, he entered Northeast Louisiana University in Monroe, Louisiana, during the summer of 1964. He received the degree of Bachelor of Science with a major in geology and a minor in chemistry from Northeast Louisiana University in May 1968. In September 1968, he entered the Graduate School at Northeast Louisiana University with a teaching assistantship. During the academic year 1969-70 he was president of the Northeast Geological Society, and in March 1970, he was installed a charter member of Gamma Iota Chapter of Sigma Gamma Epsilon. He was awarded the degree of Master of Science in August, 1971. In September, 1971 he accepted the position as instructor of Geology at Nicholls State University in Thibodaux, Louisiana. He married

Catherine Fate Voisin on May 26, 1972 and fathered Nichole Marie Bender on December 27, 1975. In September 1972, he entered the Graduate School of Louisiana State University to persue a major in geology and a minor in geochemistry. During the fall semester of 1977, he was tenured and appointed Assistant Professor of Geology at Nicholls State University. He was awarded a Doctor of Philosophy at Louisiana State University on May 19, 1983. He is presently an Associate Professor of Geology at Nicholls State University.

Present address:

212 Belle Meade Blvd.
Thibodaux, Louisiana 70301

EXAMINATION AND THESIS REPORT

Candidate: Russell B. Bender, Jr.

Major Field: Geology

Title of Thesis: Petrology and Geochemistry of the Silver Plume-Age Plutons of the Southern and Central Wet Mountains, Colorado

Approved:

Gary Byerly
Major Professor and Chairman

William Payne
Dean of the Graduate School

EXAMINING COMMITTEE:

Date of Examination:

March 3, 1983